Doctoral Dissertation

Metabolic profiling of *Drosophila melanogaster*: a new insight into the central metabolic pathways

PHAN NGUYEN THUY AN

June, 2017

International Program of Frontier Biotechnology,
Division of Advanced Science and Biotechnology,
Graduate School of Engineering,
Osaka University

Table of contents

List of Abbreviations

(*in alphabetical order*)

2OG	2-Oxoglutarate
3PGA	3-Phosphoglycerate
ADP	Adenosine Diphosphate
AEL	After Egg Laying
a-GP	Alpha-Glycerophosphate
AMP	Adenosine Monophosphate
ANDI	Analytical Data Interchange Protocol
ANOVA	Analysis of Variance
APCI	Atmospheric Pressure Chemical Ionization
ATP	Adenosine Triphosphate
AWP	After White Pupae
cAMP	Cyclic Adenosine Monophosphate
CS	Canton S
CBB	Coomassie Brilliant Blue
CE	Capillary Electrophoresis
CMP	Cytosine Monophosphate
DESI	Desorption Electrospray Ionization
EHMN	The Edinburgh Human Metabolic Network
ESI	Electrospray Ionization
F1P	Fructose 1-Phosphate
F6P	Fructose 6-Phosphate
FAA	Free Amino Acids
FAD	Flavin Adenine Dinucleotide
FMN	Flavin Mononucleotide
FQM	Feature Quantification Matrix
FT-ICR	Fourier Transform Ion Cyclotron Resonance
G1P	Glucose 1-Phosphate
G6P	Glucose 6-Phosphate
GC	Gas Chromatography
GC-Q/MS	Gas Chromatography-Quadrupole/Mass Spectrometry
GDP	Guanosine Diphosphate

GMP	Guanosine Monophosphate
GTP	Guanosine Triphosphate
HCA	Hierarchical Cluster Analysis
IMP	Inosine Monophosphate
IP-LC-MS/MS	Ion-pair Liquid Chromatography-tandem Mass Spectrometry
IT-TOF	Ion trap Time-of-Flight
KEGG	Kyoto Encyclopedia of Genes and Genomes
LC	Liquid Chromatography
LC/MS	Liquid Chromatography/Mass Spectrometry
MALDI	Matrix-Assisted Laser Desorption/Ionization
Mn6P	Mannose 6-Phosphate
MRM	Multiple Reaction Monitoring
MS	Mass Spectrometry
MSTFA	N-methyl-N-(trimethylsilyl)trifluoroacetamide
MVA	Multivariate Analysis
NAD	Nicotinamide Adenine Dinucleotide
NIST	National Institute of Standards and Technology
NMR	Nuclear Magnetic Resonance
OPLS-DA	Orthogonal Projection to Latent Structures-Discriminant Analysis
OR	Oregon R
p(corr)	Loadings scaled as a correlation coefficient between the model and original data
PC	Principal Component
PCA	Principal Component Analysis
PLS	Projection to Latent Structures
PLS-DA	Projection to Latent Structures-Discriminant Analysis
QC/QA	Quality Control/Quality Assurance
QTOF	Quadrupole Time-of-Flight
R1P	Ribose 1-Phosphate
R5P	Ribose 5-Phosphate
RMSEE	Root Mean Squared Error of Estimation
RMSEP	Root Mean Squared Error of Prediction
RP-LC-MS/MS	Reversed Phase Liquid Chromatography-tandem Mass Spectrometry
Ru5P	Ribulose 5-Phosphate
S7P	Sedoheptulose 7-Phosphate
SDS-PAGE	Sodium Dodecyl Sulfate- Polyacrylamide Gel Electrophoresis

SMPDB	Small Molecule Pathway Database
SOMs	Self-Organizing Maps
TAG	Triacylglycerol
TCA cycle	Tricarboxylic Acid cycle
TMP	Thymidine Monophosphate
TOCSY	Total Correlation Spectroscopy
UDP-Glc	UDP-Glucose
UHPLC	Ultra High Performance Liquid Chromatography
UMP	Uridine Monophosphate
UNV	Univariate Analysis
UTP	Uridine Triphosphate
VIP	Variable Importance in Projection
XMP	Xanthosine Monophosphate

Chapter 1

General Introduction

1.1. Drosophila melanogaster-The model organism of choice

Drosophila melanogaster was firstly used in 1904 by Dr. Thomas Hunt Morgan for investigating the chromosome theory of inheritance [1]. Even the starting points for using *Drosophila* were due to its convenience, Dr. Morgan soon realized that it has several advantages for genetic analyses. From this early beginning, many generations of scientists have succeeded to develop ever-increasing genetic screen techniques that made *Drosophila* one of the most tractable multicellular organisms [2] (Table 1-1).

The advantages of *Drosophila* as a model organism are summarized as follows:

- *Drosophila* has short life cycle and high reproductive capacity. It takes around 10 days from fertilization to eclosion of the adult fly at 25 ˚C. A female fly can produce around 100 eggs per day and around 2000 progeny in a lifetime [3]. With the average size 3mm, *Drosophila* is easy to rear and keep large amount in the laboratory, which provide the amenability to high throughput screening. They also require simple diet consisting of simple sources of carbohydrates and proteins (cornmeal, yeast extract, grape juice, banana, etc.). In order to keep *Drosophila* strains, transfer of flies to the new food is required every 10-14 days at 25 ˚C or 5-6 weeks at 18 ˚C.

- *Drosophila* has no meiotic recombination in males and small genome size of 120 megabase [4]. Four chromosomes of *Drosophila* can be directly visualized in the giant salivary gland chromosomes of the larval salivary gland. Moreover, the exoskeleton provides a wealth of external features. The mutant phenotypes appearing at different organs (bristles, wing veins, compound eyes, etc.) are easily observed under microscope. All of these advantages made *Drosophila* become the major organism in the studies of

transmission genetics during the first half of twentieth century. Nowadays, by combining modern molecular biotechnologies with the rich legacy of genetic techniques originally developed for *Drosophila,* researchers have made stunning progress in understanding how genes control the development and behavior of higher organisms.

- The genome was fully sequenced in 2000. From this data, 197 out of 287 known human disease genes were found to match in the genome of *Drosophila* [4,5]. Between fly and mammal, the overall identity at the nucleotide levels or protein sequences between homologs are usually approximately 40% and can reach to 80-90% or higher in conserved functional domains [6]. It is estimated that there are around 14000 genes in *Drosophila* [4], which is fewer than in *Caenorhabditis elegans* but twice as many of these have clear homologues in humans (*E*-value < 10^{-50}) [7]. The sequence and annotation of the *Drosophila* genome is freely available to all and can be accessed via "Flybase", the biggest online database for *Drosophila* [8]. From this database, we can find the detail information of each gene in *Drosophila* including links to practically everything known about that gene including nucleotide sequence, gene product amino acid sequence, mutations, expression pattern during development and related literature.
- As an invertebrate, no ethical approval is required for using *Drosophila* in most countries. With these advantages, the central research paradigm using mutation in *Drosophila* to investigate gene functions and then follow by study of homologs in mammals and humans is likely to remain at the forefront of biological researches.

Table 1-1: Comparison of commonly used model organisms. (Adapted from IHGSC [9] and Allard J.B. et al.[10])

	Mouse	Fly	Zebra fish	Nematode
Transcriptome size	> 30000	14400	26206	18300
% genes similar to human disease genes *E*-value < 0.001	> 90%	75%	84%	65%
Chromosome number (2n)	40	8	50	12
Generation time	12 weeks	10days	10-12 weeks	3 days
Brood size	6-12 pups/month	~120eggs/day	~200eggs/week	~140 eggs/day
Price to obtain mutant strain	~$200	$14~$300	$200-$900	<$100
Advantages	Mammal, high similarity with human genome, many genetic tools available	Short lifespan, easy to work with, genetically tractable, has a wide range of tissue types, has adult stem cells	Vertebrate, genetically tractable, small size, cheap to maintain	Short lifespan, easy to work with, genetically tractable
Disadvantages	Expensive and long lifecycle	Distant from humans	Longer lifespan than mice	Lacks distinct endocrine tissues and various other tissue types, very distant from humans

1.2. Metabolomics

1.2.1. What is metabolomics?

Metabolomics is the latest "omics" field concerned with the high throughput identification and quantification of the small molecule metabolites (Figure 1-1). They become a particularly good reporter of an organism's phenotype or physiology, because metabolites are the end products of cellular processes in a living cell or living organism [11]. The changes in the metabolism can be the direct or indirect answer of an organism to genetic alterations, diseases,

or environmental influences. Together with genomics, transcriptomics and proteomics, metabolomics can give more complete picture of living organisms.

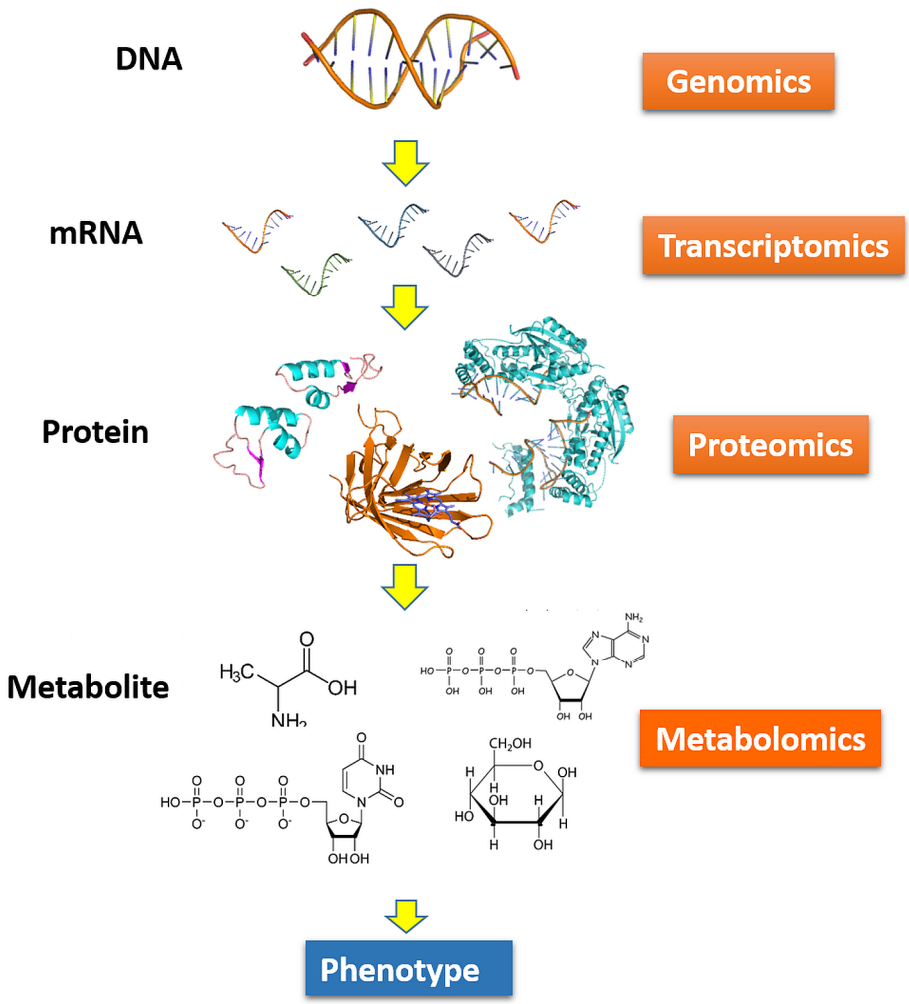

Figure 1-1: The central dogma of biology showing the flow of information from genome to the phenotype. Associated with each cellular level is the corresponding "omics" field. First, genes are transcribed to mRNA and translated into proteins. Proteins can acts as the biological catalysts to give rise to metabolites. As the final product, metabolites can provide important information on all aspect of cell activities.

There are two main strategies that can be applied, including targeted and non-targeted metabolomics. Targeted metabolomics is the method focusing on a specific group of metabolites related to the pathways of interest. The strategy for targeted metabolomics commonly based on a specific biochemical question or hypothesis that motivates the investigation of a particular pathway. This approach can be applied on pharmacokinetic studies

of drug metabolism as well as for measuring the influence of therapeutics or genetic modifications on a specific enzyme. On the other hand, non-targeted metabolomics is a method with global scope measuring as many metabolites as possible from biological samples without preference. This method will provide a broader coverage which has great potential to provide insights into fundamental biological processes; however, a great number of metabolites remain uncharacterized with respect to their structure and function of health or diseases. These strategies have been used either separately or together for the following approaches:

- Metabolomics: focus on the complete set of metabolites within a cell, tissue or biological sample under a certain condition. Due to the connection of metabolic pathways, any factors that cause the changes in the metabolism are usually not limited to only one pathway. Therefore, it is necessary to have a biological system that can cover the identification and quantification of metabolites in all branches of an organism's metabolism.[12]
- Metabolic profiling: analysis of set of metabolites in a pre-defined biochemical pathway or a specific class of compounds. In this method, it is not necessary to cover all metabolic pathways of an organism. Instead, it focuses on the identification and quantification of the selected metabolites in biological samples.[12]
- Metabolic fingerprinting: a sufficient approach to classify samples based on the distinction of metabolic states due to their biological relevance or origins but does not necessarily give specific metabolite information.[12]
- Metabolic foot printing (exometabolomics): focus on extracellular metabolites in cell culture media. By comparing the metabolic profiles of media before and after culturing, this method provides a reflection of metabolite excretion or uptake by cells.[13]

The field of metabolomics has made remarkable progress within the past decade and has

implemented new tools that have offered mechanistic insights by allowing the correlation of biochemical changes with phenotype. Recent advances in metabolomics technologies are leading to a growing number of mainstream applications such as drug discovery, human disease research, system biology, plant study and food industry.

1.2.2 General work flow for metabolomics studies

Unlike other cellular products, each metabolite has different characteristics that hampers the identification and quantification of all detected metabolites. Thus, as a high throughput approach, metabolomics study required the combination of analytical chemistry, biology, mathematics and informatics. A general workflow for metabolomics study includes the following steps:

- **Experimental design**

The design of a metabolomics experiment is the crucial step and depends on the scientific question under consideration. Researchers can choose a metabolomics approach which is best suited for their sample types and study objectives.

- **Sample preparation**

Because metabolomics capture the instant snapshot of the metabolic profile under a certain condition, the sample collection, quenching, extraction and storage methods should be developed prior to study to guarantee the qualities of samples. The most important point that cause the variation among samples is the duration of time that a sample sits at room temperature before storage or analysis [14]. In animal studies, the differences in anesthesia or euthanasia methods can also be the reason for variations [15]. It is highly recommended to use the pooled quality control/quality assurance (QC/QA) samples periodically throughout the analysis to evaluate the stability and reproducibility of the analytical system [16].

- **Metabolomic analysis**

The two commonly used analytical platforms for metabolomics studies are nuclear magnetic resonance (NMR) and mass spectrometry (MS) [17]. NMR is a spectroscopic technique that is based on the energy absorption and re-emission of the atom nuclei due to variations in an external magnetic field [18]. Depending on the purpose of each study, different atom nucleus can be targeted by the applied magnetic field such as ^{1}H-NMR (hydrogen), ^{13}C-NMR (carbon) or ^{31}P NMR (phosphorus) [19]. This method is highly reproducible and the revealed data from NMR are able to provide the information of not only concentrations but also structures of metabolites. On the other hand, MS generates metabolite spectral data as mass-to-charge (*m/z*) ratios and relative intensities of compounds [17]. The extracts from samples first need to undergo a separation step (LC, GC or CE) prior to ionization (ESI, APCI, MALDI, etc.) and analysis by MS (IT-TOF, triple quadrupole, FT-ICR, obitrap, etc.) [20]. MS is a highly sensitive method and quantitative analysis can be achieved with the use of compound standards.

Each method has its own advantages and disadvantages (Table 1-2), which make not any single method can capture all classes of metabolites present in the metabolome. The characteristic of sample and target pathways can influence the choice of analytical technique.

Table 1-2: The comparison between NMR and MS as analytical platforms for metabolomics studies. (Adapted from Emwas AH.M., et al.[21])

	NMR	Mass spectrometry
Sensitivity	Low but can be improved with higher field strength, cryo and microprobes and dynamic nuclear polarization	High, but can suffer from ion suppression in complex and salty mixtures
Selectivity	Even though few selective experiments are available such as selective TOCSY, it is in general used for nonselective analysis	Can be used for both selective and nonselective (targeted and nontargeted) analyses
Sample measurement	All metabolites that have appropriate concentration for NMR can be detected in one measurement	Usually need different chromatography techniques for different classes of metabolites

Sample recovery	Nondestructive; sample can be recovered and stored for a long time, several analyses can be carried out on the same sample	Destructive technique but need a small amount of sample
Reproducibility	Very high	Moderate
Sample preparation	Need minimal sample preparation	More demanding; needs different LC columns and optimization of ionization conditions
Number of detectable metabolites in urine sample	40–100 depending on spectral resolution	Could be more than 500 using different MS technique
***In vivo* studies**	Yes—widely used for ^{1}H magnetic resonance spectroscopy (and to a lesser degree ^{31}P and ^{13}C)	No—although suggestion that DESI may be a useful way to sample tissues minimally invasively during surgery
Molecular dynamic, molecular diffusion	NMR can be used to probe the molecular diffusion and dynamics	No

- **Data acquisition**

The sample spectra of a metabolomics study have to be processed in order to archive accurate identification and quantification. Data acquisition usually includes baseline correction, noise filtering, peak detection, peak alignment, and normalization [17]. The methodologies applied for each step depend on the selected analytical technique. The use of appropriate methods should be considered when connecting the dataset from different batches or analytical platforms to avoid experimental errors. The obtained data is generally arranged in a feature quantification matrix (FQM) that contains the information of all detected metabolites in the samples and will be used for subsequent statistical analysis.

- **Statistical analysis**

Statistical analysis is a critical part in any high-throughput studies. Multiple univariate and multivariate analyses, commonly known as chemometric methods, provide practical way

to deal with large amount of data [22]. Multivariate analysis (MVA) can be used first to have a general view of the dataset. The non-supervised (ex: HCA, PCA and SOMs) and supervised methods (ex: PLS, PLS-DA and OPLS-DA) take all the metabolomic features to identify relationship patterns simultaneously into account. The metabolites that are important for the differences among samples are revealed. Consequently, the metabolites that are important for the differences among samples are revealed. Next, the univariate analysis (UVA) (ex: Student's *t*-test and ANOVA) will be utilized for the validation of candidate metabolite credentials.

- **Metabolite identification**

This is one of the major challenges of high throughput metabolomic analysis. The metabolite spectra databases have been developed to support the identification in metabolomic study. The number of metabolite reference spectra of many organisms obtained from different analytical techniques is growing continuously (Table 1-3). Since the differences in spectra comparing to structural isomers can be very small or not present at all, it is necessary to compare the library search results with a reference spectrum of the standard and desirably by chromatographic retention of the standard [23].

- **Data interpretation**

In the last decade, scientists put a lot of effort to develop many informative databases on metabolites and metabolic pathways such as Kyoto Encyclopedia of Genes and Genomes (KEGG) [24], Small Molecule Pathway Database (SMPDB) [25], The Edinburgh human metabolic network **(**EHMN) [26], WikiPathways [27], and MetaCyc [28]. The information from pathway and network analysis approaches will help characterize the complex relationships in the set of measured metabolites. Recently, many researchers tend to combine metabolomics with other "omics" studies in order to gain the fundamental knowledge from the multiple aspects of biology.

Table 1-3: Available spectral database. (Adapted and modified from Alonso A., et al.[17])

Database	Spectral data	Website	Information	Reference
HMDB	MS/NMR	http://www.hmdb.ca	41,806 metabolite entries and 1,579 metabolites with spectra (^{1}H-NMR, LC-MS, GC-MS …)	29
LMSD	MS	http://www.lipidmaps.org	37,500 lipid structures with MS/MS spectra	30
METLIN	MS	http://metlin.scripps.edu	240,516 metabolite entries and 12,057 metabolites with MS/MS spectra	31
NIST	MS/NMR	http://chemdata.nist.gov/	Reference mass spectra for GC/MS (by electron ionization) and LC-MS/MS (by tandem mass spectrometry), NMR as well as gas phase retention indices for GC	32,33
TOCCATA COLMAR	NMR	http://spin.ccic.ohio-state.edu	Multiple spectral NMR datasets: ^{1}H- and ^{13}C-NMR, 2D ^{13}C–^{13}C TOCSY (n = 463), 2D ^{1}H–^{1}H TOCSY and ^{13}C–^{1}H HSQC-TOCSY (n = 475), and 2D ^{13}C–^{1}H HSQC (n = 555)	34-37
MassBank	MS	http://www.massbank.jp	2,337 metabolites and 40,889 spectra (LC-MS, GC-MS …)	38
Golm metabolome	GC-MS	http://gmd.mpimp-golm.mpg.de	2,019 metabolites with GC-MS spectra	39
BMRB	NMR	http://www.bmrb.wisc.edu	9,841 biomolecules with ^{1}H, ^{13}C, or ^{15}N spectra	40
Madison	NMR	http://mmcd.nmrfam.wisc.edu	794 compounds with spectra including ^{1}H, ^{13}C, ^{1}H–^{1}H, ^{1}H–^{13}C …	41
NMRShiftDB	NMR	http://nmrshiftdb.nmr.uni-koeln.de	42,840 structures and 50,897 measured spectra	42
RIKEN	MS/NMR	http://prime.psc.riken.jp	1,589 metabolites (*Arabidopsis*)	43,44
Birmingham Metabolite Library	NMR	http://www.bml-nmr.org	208 metabolites and 3,328 1D- and 2D-NMR spectra	45

1.3. Metabolomics can serve as a key technology to apply on studies using *Drosophila melanogaster*

1.3.1. Previous metabolomics studies on Drosophila

As in other areas of biology, the use of model organisms in metabolomics can provide easy sample preparation for methods development, which will become possible to expand the applications of metabolomics. After the full genome successfully sequenced, the modENCODE high-throughput RNA-sequence data showing the mRNA expression levels throughout the life cycle and in different organs of adult flies were published in 2011 and 2014, respectively[46,47]. In the context of system biology, metabolome analysis in biological samples is now regarded as a viable counterpart to proteome, transcriptome and genome. With an attempt to fulfill the knowledge on this model organism, many metabolomics studies have been established (Table 1-4).

In fact, several metabolomics studies have been conducted using *Drosophila* that focused on the effect of heat tolerance [48-53], hypoxia tolerance [54], oxidative stress [55], longevity [56] and obesity [57]. Furthermore, metabolomics using *Drosophila* as a model organism has been applied for the study of *Listeria monocytogenes* infection [58] and drug efficacy test [59]. In these studies, several techniques have been applied for metabolic profiling of *Drosophila* larvae or adults, such as GC-MS, LC-MS and NMR. Of note, most of the current reports on the metabolome of *Drosophila* just performed at a limited developmental stage and each study focused on different biological issues. The target metabolic pathways were also not consistent among those researches, which makes the information of *Drosophila* metabolome is still limited.

Therefore, it is essential to achieve better knowledge on *Drosophila* metabolic profiles, which will greatly enhance the understanding of regulation and biochemical interactions in *Drosophila* metabolism at a systems level.

Table 1-4: The application of metabolomics on studies using *Drosophila*

Application field		Analytical platform	Sample type	Important metabolites/pathways	Reference
Cold tolerance		GC-MS LC-MS NMR	Adult fly	Increase in gluconeogenesis, amino acid synthesis, and cryoprotective polyol synthesis	48,49,53,60-65
Heat stress		NMR	Adult fly	Alterations in the levels of free amino acids, maltose, a galactoside and 3-hydroxykynurenine	50,52,66
Hypoxia tolerance		NMR	Adult fly	Flexibility in energy metabolism supports hypoxia tolerance in *Drosophila* flight muscle and in correlation with aging	67,68
Oxidative stress		LC-MS	Adult fly	The metabolic response to lack of superoxide dismutase activity and to paraquat induced oxidative stress, and the metabolic profiles of four different *Drosophila* species	55,69
Infection	Infected with *Staphylococcus aureus* and treated with oral linezolid	NMR	Adult fly	Sepsis survivors had a metabolic signature characterized with decreased glucose, tyrosine, beta-alanine, and succinate	70
	Listeria monocytogenes infection	GC-MS LC-MS	Adult fly	Lose both of energy stores, triglycerides and glycogen, and show decreases in both intermediate metabolites and enzyme message for the two main energy pathways, beta-oxidation and glycolysis	58
Environment	Insecticidal activity (BowmanBirk inhibitors (BBIs))	GC-MS	Adult fly	Increase in F6P, and decrease in citric acid/isocitric acid levels	71
	Effects of CO_2 anaesthesia	GC-MS	Adult fly	The most important metabolic changes were the accumulation of succinate and G6P	72
System	Embryogenesis	GC-MS	Embryo	Over all metabolic transitions during *Drosophila* embryogenesis	73

biology	Tissue-specific metabolomes	LC-MS	Adult fly	A baseline tissue map of *Drosophila* for both polar metabolites and for a range of lipids	74
	The influence of daily cycles of light and temperature	NMR	Adult fly	Alterations in the levels of free amino acids	75
	rosy, *y* mutation	FT-MS	Adult fly	Metabolomic profiling of *Drosophila*	76,77
	Effect of storage temperature of quiescent larvae	GC-FID LC-MS	Larvae	Over all metabolic transitions	78
	Different in among wild type strains	FT-MS	Adult fly	Different in genotype caused the different in metabolome	79,80
	Estrogen-related receptor	GC-MS	Larvae	Abnormally high levels of circulating sugar and diminished concentrations of ATP and triacylglycerides	78
Aging	Effect of diet, age, sex, and genotype on aging	LC-MS	Adult fly	Numerous metabolic pathways that were affected including pathways involving sugar and glycerophospholipid metabolism, neurotransmitters, amino acids, and the carnitine shuttle.	56,81-83
Diseases	Charcot-Marie-Tooth disease (gene GDAP1)	NMR	Adult fly	Alterations in the levels of free amino acids and carbohydrate metabolism	84
	Obesity	GC-MS LC-MS	Larvae	CoA is required to support fatty acid esterification and to protect against the toxicity of high sugar diets. The overall metabolic rate of flies on a high fat diet was significantly increased	57,85
	m-aconitase deficiency	LC-MS	Adult fly	Reduced triacylglyceride and increased acetyl-CoA	86
	Alzheimer's disease	NMR	Adult fly	Metabolomic changes may lead to the age-related toxicity of the amyloid beta (Aβ) peptide	87
	Parkinson-like model (Paraquat exposure)	GC-MS	Adult fly	Alteration in 24 metabolites, including amino acids, carbohydrates, as well as fatty acids	88

	Drug efficacy test	LC-MS	Adult fly	The alterations in these metabolites were associated with perturbations in amino acid and fatty acid metabolism, in response to insomnia through immune and nervous system.	[59]
Nutrient	Transient receptor potential TRPA1	GC-MS	Adult fly	Down-regulation of intermediates in the methionine salvation pathway, in contrast to the synchronized up-regulation of a range of free fatty acids	[89]
	Effects of diet and development	LTQ Orbitrap XL	Larvae, pupae	The overall changes of lipidome	[90]

1.3.2. Metabolomics approaches using in this study

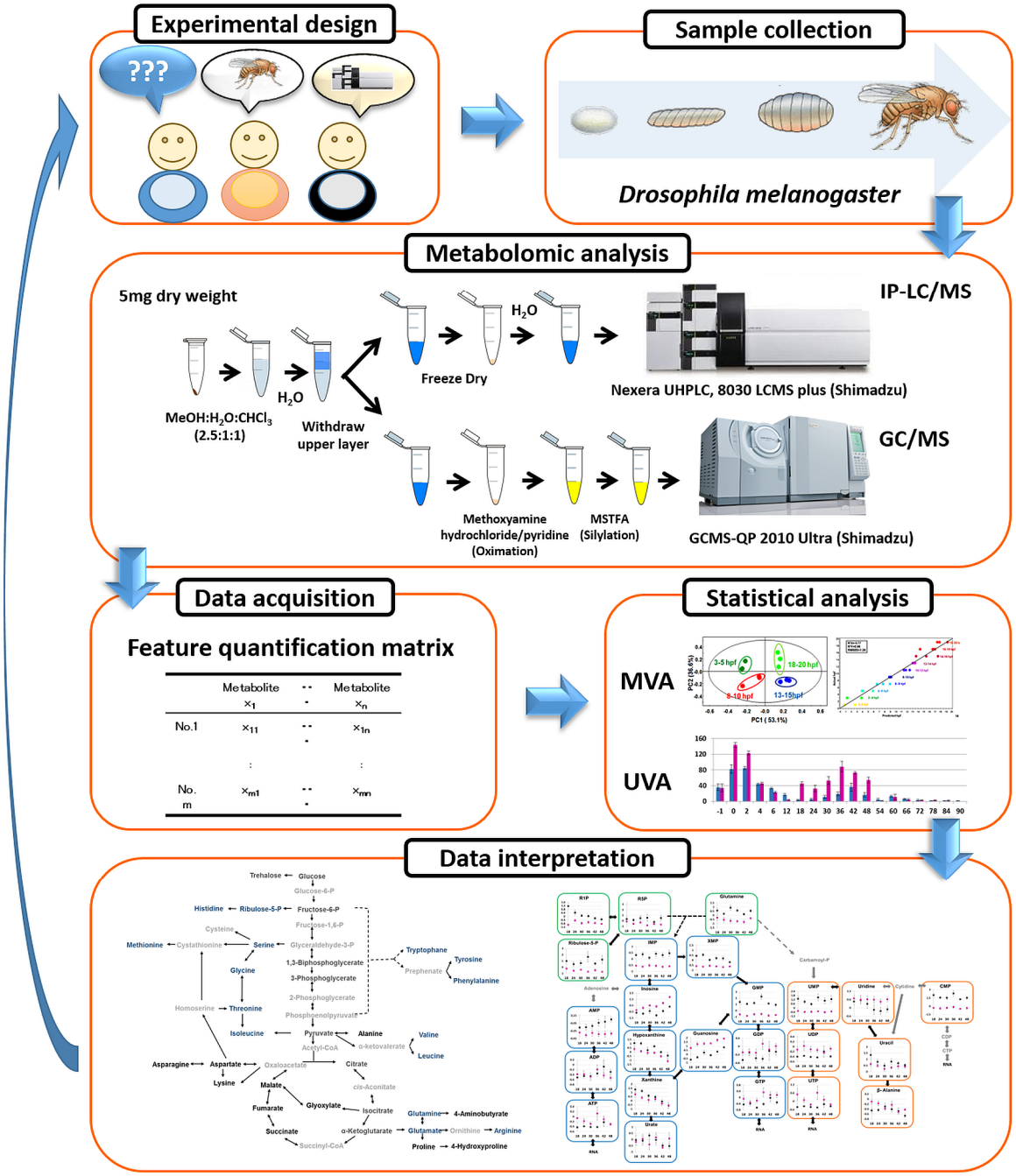

Figure 1-2: Metabolomic approaches using in this study

In this study, metabolomic technologies were presented as effective methods to access the changes of central metabolic pathways in *Drosophila*. Metabolites have diverse chemical properties such as molecular weight, polarity, hydrophobicity, volatility, and chemical structures. Therefore, no single technology is capable of covering a complete identification and quantification of the metabolome[91]. In previous study, GC-MS has been proving to be an

effective tool to analyze a wide range of low molecular weight hydrophilic compounds such as sugars, amino acids and organic acids[92,93]. On the other hand, a targeted method using IP-LC-MS/MS was conducted to cover a wide range of metabolites especially the highly polar intermediates from central metabolism, such as sugar phosphates and nucleotide triphosphates[94,95]. Therefore, in this study, these two methods were combined to observe the central metabolic pathways together with their intermediates focusing on glycolysis, TCA cycle, amino acid metabolism as well as purine and pyrimidine metabolism. The mega-data sets will be analyzed using MVA (HCA, PCA, PLS, PLS-DA and OPLS-DA) to thoroughly screen and isolate significant metabolites in each experiment. Then, these results were validated using UVA (Student's *t*-test and ANOVA). Additional bioassays were used particularly to validate the hypothesis raised from metabolic profiles. (Figure 1-2)

1.4. Research objectives

The availability of the genome sequence and genetic tools in *Drosophila* has made this tiny insect a model organism for comparative genomics, transcriptomics, and proteomics. With an attempt to deepen the knowledge on this model organism, many metabolomics studies have been established. However, most of the current reports on the metabolome of *Drosophila* just performed at a limited developmental stage such as larvae or adult. Each study was focused on different biological issues so that the target metabolic pathways were not consistent among those researches. Therefore, this study aimed to elucidate global changes in the central metabolic pathways in *Drosophila* by using metabolomics approaches.

- First, non-targeted GC/MS-based and targeted LC/MS-based metabolic profiling methods were conducted to obtain a general view on the changes of central metabolic pathways throughout *Drosophila* lifecycle.
- The effects of temperature and origin on metabolic profiles were examined

to optimize the experimental design for metabolomics study using *Drosophila*.

- Finally, these approaches were applied to study the role of *Drosophila* histone methyltransferase G9a.

1.5. Thesis outline

This thesis includes five chapters that provides the importance of central metabolic pathways in studies using *Drosophila*. The developed methods focused on the central metabolic pathways, whose information throughout *Drosophila* lifecycle was explored and further proven to be effective to study gene functions. Chapter 1 provides the general introduction concerning the importance of *Drosophila* as a model organism and how metabolomics can be an effective tool for researches using *Drosophila*. In Chapter 2, non-targeted GC/MS-based and targeted LC/MS-based metabolic profiling methods were employed to cover a wide range of metabolites in the central metabolic pathways of detailed time-course *Drosophila* samples throughout its life cycle. In Chapter 3, in order to investigate the appropriate experimental design for metabolomics study using *Drosophila*, the effects of origins and temperature within non-stressed conditions (22–29 $^{\circ}$C) on the metabolic profiles were examined. In these experiments, all samples were screened only during metamorphosis because the developmental stages can be easily defined based on the morphology. In Chapter 4, the developed metabolomic approaches were applied to investigate the roles of *Drosophila* histone methyltransferase G9a (dG9a) in starvation stress tolerance. Finally in Chapter 5, the conclusions revealed from this study were summarized and the future perspectives were proposed.

Chapter 2

Metabolic profiling of *Drosophila melanogaster* throughout its lifecycle

2.1. Introduction

Developmental biology is one of the most challenging fields for biologists since the mechanism governing the development of an organism from a single cell still remains unclear. This process involves many pathways such as cell proliferation, differentiation and apoptosis. A large array of cell types will be organized with an intricate architecture to create a functioning adult [96,97]. The same mechanisms that control development are also critical in human disease so that a better knowledge in this field is required for dealing with human health issues. However, even the genomes of several organisms have been sequenced and many genes related to developmental processes have been investigated [98-100], it is hard to have a comprehensive view if we just focus on the effects of an individual gene or protein on the development of an organism especially in animal.

Among many model organisms, *Drosophila* has been widely utilized as an ideal model for genetics and developmental biology due to its small size, short generation time and large brood size. Especially, the Nobel Prized in in Physiology or Medicine in 1995 was awarded to Lewis et al. for their discovery concerning the genetic control of embryonic development. The authors found that there is a high conservation of genomic organization and expression patterns between *Drosophila* and human embryogenesis. Moreover, *Drosophila* lifecycle has four stages including embryo, larvae, pupae and adult flies (Figure 2-1). The embryo also grows outside the body so that *Drosophila* can easily be studied at every stage of development, which lets scientists bypass some of the ethical issues of developmental research involving human

subjects. Thus, *Drosophila* have been commonly applied to study the function of genes related to biological pathways occurring during its development such as cell proliferation, differentiation and apoptosis [101].

At 25 °C, a *Drosophila* complete its life cycle from egg to emergence of adult fly in 10 days. After fertilization, *Drosophila* embryo undergoes thirteen cycles of rapid, highly synchronized nuclear division to form a syncytium in the absence of cytokinesis. Following these nuclear division cycles, each nucleus at the cortex surface is simultaneously packaged into individual cells in a process known as cellularization. Then, the single-layered cellular blastoderm is then rearranged during gastrulation to produce an embryo composed of three primordial tissue layers [102]. The whole process of *Drosophila* embryogenesis takes around 24h. During larval stages, the instar larvae transition from foraging to wandering behavior occurs in feeding and non-feeding stage, respectively. After three days of development from 1st to 2nd and 3rd instar larva, a fly increases 200-fold in mass and acquire enough nutrients for energy source to enter metamorphosis [103]. Additionally, the body size of adult flies also depends on how fast the larvae grow and how big they are before they stop eating. Throughout metamorphic processes, the adult progenitor cells such as imaginal discs undergo cell proliferation, differentiation and organogenesis to give rise to the adult structures, while most larval tissues undergo autophagy and cell death [104]. Cells undergo one or more of these processes in response to the hormone 20-hydroxyecdysone (ecdysone), which initiates larval-prepupal and prepupal-pupal transitions [105]. Consequently, the flies go through significant morphological changes that require the tight regulation and interaction of various biological networks and pathways. *Drosophila* metamorphosis lasts for 4 days and an adult emerges from the pupal case. Male and female *Drosophila* differ in many aspects of development and physiology such as body size [106] or lipid storage[107] due to the compositions of genes on X and Y chromosomes [108]. Although many genes related to developmental processes have been

identified and the gene expression database throughout *Drosophila* cycle is now available [46], it is still not clear how the gene products participate in various cellular processes.

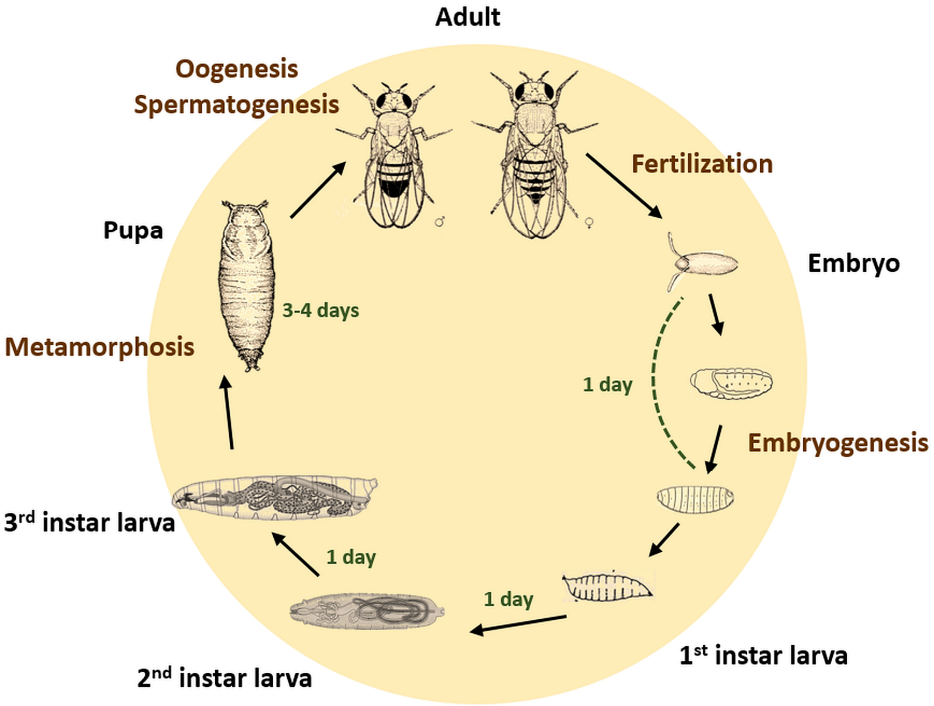

Figure 2-1: *Drosophila* lifecycle. At 25 °C, it takes around 10 days for a fertilized eggs to undergo embryogenesis, molting, metamorphosis and finally eclose into adult fly.

On the other hand, metabolites, the end products of various cellular processes in a living cell or living organism are particularly good indicators for an organism's physiology [11]. Moreover, comparing to the huge database that we have from genomics and proteomics studies, applications of metabolomics on developmental biology were just limited in a few models such as yeast, zebra fish or frog [109-111]. Thus, metabolomics, one of the latest "omics" technology concerned with the high throughput identification and quantification of metabolites, is indispensable in elucidating the mechanism underlying *Drosophila* development.

This present study aimed to discover the changes in the central metabolic pathways including glycolysis, TCA cycle, amino acid metabolisms as well as purine and pyrimidine metabolisms of *Drosophila* throughout its life cycle by using the metabolomics approach. For the first time, a metabolic profile focusing on the central metabolism during *Drosophila*

development were established by employing GC-MS and LC-MS. The data showed that substantial fluctuations in metabolite abundance were highly correlated with actual developmental stages, which was validated by multivariate analyses. Since these pathways provide the precursor metabolites to almost all the other pathways in the body, the obtained data on the metabolic profiles could be useful to understand *Drosophila melanogaster* physiology throughout its life cycle.

2.1. Materials and methods

2.1.1. Fly strain and sample collection.

Canton S, a wild type strain of *Drosophila melanogaster* (Bloomington stock center, USA), was reared at 25 °C on standard food (0.7% agar, 10% glucose, 4% dry yeast, 5% cornmeal, 3% rice bran). First, the virgin flies of each gender were collected and then kept separately for three days until they become mature enough. Each sample set was derived from independent mating of 100 females and 100 males. Mating was subsequently done overnight in egg collecting cages on agar plates containing standard food with freshly prepared yeast paste. The following day, the plates were exchanged every two h and plates from the first two h were discarded to clear the eggs laid by flies overnight.

- Embryos were incubated at 25 °C in which samples were collected every 2 h from 0-24 h AEL (h After Egg Laying). The collecting embryo step was done by using the method as described previously [112,113].
- 1st, 2nd and 3rd instar larvae were collected based on the morphology [114].
- For pupal stage, the time course sampling started when the animals reached white pupal stage. The samples were collected from 0-90 h AWP (h after white pupae). The developmental stages were defined based on morphology [114].
- For adult stage, after emerging, the 5-day-old virgin files of each genders were collected.

Of note, flies with the different genders were only split at adult stage. After collection, the samples were washed with NaCl-Triton (0.7% NaCl; 0.03% Triton X-100) five times and subsequently washed three times with H_2O. Samples were then frozen in liquid N_2 immediately and freeze-dried overnight. Finally, all samples were stored at -80 °C before extraction.

Three to five biological replicates were used for each condition.

2.1.2. Sample preparation

5 mg freeze-dried of each sample was crushed using a ball mill for 5 min at 20 Hz before extraction to increase the extraction efficiency. Afterwards, sample was extracted with 1 mL extraction solvent, which consisted of methanol/water/chloroform (2.5:1:1). 60 µL ribitol (0.2 mg/mL) was added subsequently as internal standard. After centrifugation at 16,000 x g for 3 min at 4 °C, 900 µL of the supernatant was transferred to a 1.5 mL micro tube and mixed with 400 µL distilled water (Wako, Japan). After repeating centrifugation, 400 µL of the polar phase was transferred into a fresh 1.5 mL microfuge tube with a screw cap. Then, the solvent was removed using a centrifugal concentrator (VCe36S, Taitec Co., Japan) for 2 h and sample was subsequently freeze-dried overnight.

For GC-MS analysis, 400 µL of the extract were used. Derivatization of the samples was done by oximation using methoxyamine hydrochloride (Sigma Aldrich, USA) in pyridine (50 µL, 10 mg/mL) at 30 °C for 90 min, followed by silylation using 25 μL of N-methyl-N-(trimethylsilyl) trifluoroacetamide (MSTFA) (GL Sciences, Japan) at 37 °C for 30 min.

For LC-MS analysis, 400 µL were dried out and diluted in 30 µL of ultra-pure water for IP-LC-MS analysis.

All samples were analyzed within 24h after extraction.

2.1.3. GC-MS analysis

GC-Q/MS analysis was performed on GCMS- QP 2010 Ultra (Shimadzu, Japan) with a with a InertCap™ 5MS/NP ultra low bleed column (0.25 mm × 30 m, 0.25 µm, GL Sciences Inc., Japan) and an AOC-20i/s autosampler (Shimadzu, Japan). Tuning and calibration of the mass spectrometer was done prior to analysis. One microliter of derivatized sample was injected in split mode, 25:1 (v/v), with an injection temperature of 230 °C. The carrier gas (He) flow was 1.12 mL/min with a linear velocity of 39 cm/s. The column temperature was held at 80 °C for 2 min, increased by 15 °C/min to 330 °C, and then held for 6 min. The transfer line

and ion source temperatures were 250 and 200 °C, respectively. Ions were generated by electron ionization (EI) at 0.94 kV. Spectra were recorded at 10000 u/s over the mass range m/z 85−500. A standard alkane mixture (C8−C40) was injected at the beginning and end of the analysis for tentative identification.

The raw chromatographic data were converted into ANDI files (Analytical Data Interchange Protocol) using GC-MS Solution software package (Shimadzu, Japan). The data were imported to MetAlign software [115,116] (Wageningen UR, The Netherlands, available for free at the website http://www.pri.wur.nl/UK/products/MetAlign/) for peak selection and alignment. AIoutput2 (version 1.29) was used as annotation software. The retention indices of all detected metabolites were calculated based on the standard alkane mixture and tentative identification of metabolites was done by comparing the retention indices with our in-house library [117] to aid the tentative identification of compounds. Internal standard, ribitol, was used to check experimental errors as well as the stability of analytical systems. On the other hand, the retention time of each metabolite was used to compare with the NIST 2011 Library (NIST11/2011/EPA/NIH).

2.1.4. IP-LC-MS/MS analysis

IP-LC-MS/MS (ion-pairing-liquid chromatography-tandem mass spectrometry) analysis was done using the Shimadzu Nexera UHPLC (Ultra High Performance Liquid Chromatography) system coupled with LCMS 8030 Plus (Shimadzu, Japan). The column used was Mastro C18 HPLC column (150 mm × 2.1 mm, particle size 3 μm, Shimadzu, Japan). The mobile phases were 10 mM tributylamine and 15 mM acetic acid in water (A), and methanol (B) at a flow rate of 0.3 mL/min. Gradient curve: 0% B (0–1 min), 15% B (1.5–3 min), 50% B at 8 min, 100% B at 10–11 min and 0% B at 11.5–17 min. The injection volume was 3 μL, and the column oven temperature was kept at 45 °C. MS parameters: probe position (+1.5 mm), desolvation line temperature (250 °C), drying gas flow (15 L/min), heat block temperature

(400 °C), and nebulizer gas flow (2 L/min). Other MS parameters were determined by auto-tuning. This analysis used the scheduled MRM mode [94,95] (Table S1).

In order to evaluate the stability and reproducibility of the analytical system, standard mixtures of all authentic metabolites were injected periodically throughout the analysis. The peaks of each target metabolite were identified by comparison of its chromatographic shapes and retention times with that of the corresponding standards. The areas were determined by using LabSolutions version 5.60 (Shimadzu, Japan).

2.1.5. Multivariate analysis.

The peaks obtained from each GC-MS and LC-MS analyses were separately normalized to total peak intensity [118] and unit variance scale was applied in order to reduce the variance of analytical methods. Then, the data was integrated and subjected to multivariate analyses. No transformation was performed.

Principle Component Analysis (PCA), Partial Least Square projection to the latent structure (PLS) and Orthogonal Projections to Latent Structures Discriminant Analysis (OPLS-DA) were performed by utilizing SIMCA-P$^+$ version 13 (Umetrics, Sweden) with the default missing data tolerance 50%. All PLS models in this study were validated using permutation test (data not shown). The R^2Y-intercepts ≤ 0.3-0.4 and Q^2-interceps ≤ 0.05 would indicate not overfitting and overprediction, respectively [119]. The OPLS-DA models were validated using CV-ANOVA test.

Hierarchical Cluster Analysis (HCA) was conducted using Multiexperiment View Version 4.9[120] (Dana-Farber Cancer Institute, USA, available for free at the website http://www.tm4.org/mev.html).

The two-way ANOVA test was performed using “Time series Analysis” function of Metabolyst 3.0 [121], a web-based metabolomics data processing tool that is available for free at the website (http://www.metaboanalyst.ca).

2.1.6. Total protein measurement

In Bradford assay, 10 µL of homogenized sample was diluted ten times and 5X Protein Assay Coomassie Brilliant Blue (CBB) G-250 solution (Nacalai, Japan) was diluted five times. Then, 20 µL of sample was mixed with 1 mL 1X CBB solution and incubated at room temperature for 10 mins. The mixture analyzed in a spectrometer at 595 nm and the protein quantification has been done using bovine serum albumin as a standard.

2.2. Results and discussion

2.2.1. The metabolic profiles of Drosophila throughout lifecycle.

Since there was no previous studies covering the central metabolic pathways throughout *Drosophila melanogaster* lifecycle, I decided to combine non-targeted GC-MS-based and targeted LC-MS-based metabolic profiling to provide an instantaneous snapshot of the changes in *Drosophila* metabolic profiles. All flies were reared at 25 °C and the detailed time course sampling has been done for each developmental stage including embryo, larvae, pupae and adult flies. The sample preparation methods were optimized to cover a wide range of low molecular weight hydrophilic compounds. From these platforms, 73 metabolites related to the central metabolic pathways were detected, including amino acids, sugars, and organic acids, as well as intermediates of central metabolism, such as sugar phosphates and cofactors (Table 2-1).

Then, hierarchical clustering analysis was performed to classify metabolites into clusters of different expression trends for each stages of *Drosophila* development (Figure 2-2). Each metabolite showed distinct expression patterns and change drastically from early to late stage of *Drosophila* development. These results will be discussed deeper in the next sections (Sections ***2.2.2-2.2.5***) focusing on each developmental stage.

Table 2-1: Detected metabolites using GC-MS and LC-MS

Primary ID	KEGG ID	Instrument	Primary ID	KEGG ID	Instrument
2-Aminoethanol	C00189	GC-MS	Lysine	C00047	LC-MS
2-Oxoglutarate	C00026	LC-MS	Malate	C00711	LC-MS
3-phosphoglyceric acid	C00597	LC-MS	Methionine	C00073	LC-MS
4-Aminobutyric acid	C00334	GC-MS	NAD	C00003	LC-MS
ADP	C00008	LC-MS	NADP	C00006	LC-MS
Alpha-glycerophosphate	C00093	LC-MS	NADPH	C00005	LC-MS
Alanine	C00041	GC-MS	Nicotinate	C00253	LC-MS
AMP	C00020	LC-MS	Oleic acid	C00712	GC-MS
Asparagine	C00152	GC-MS	*O*-Phosphoethanolamine	C00346	GC-MS

Aspartic acid	C00049	GC-MS	Orotate	C00295	LC-MS
ATP	C00002	LC-MS	Pantothenate	C00864	LC-MS
cAMP	C00575	LC-MS	Phenylalanine	C00079	LC-MS
Citric acid	C00311	GC-MS	Phosphoric acid	C00009	GC-MS
CMP	C00055	LC-MS	Proline	C00148	GC-MS
Cysteine	C00097	LC-MS	Pyroglutamic acid	C01879	GC-MS
Fructose 1-phosphate	C01094	LC-MS	Pyruvate	C00022	LC-MS
Fructose 6-phosphate	C00085	LC-MS	Sedoheptulose 7-phosphate	C05382	LC-MS
Flavin adenine dinucleotide	C00016	LC-MS	Serine	C00065	GC-MS
Flavin mononucleotide	C00061	LC-MS	Succinic acid	C00042	GC-MS
Glucose 1-phosphate	C00103	LC-MS	Threonine	C00188	GC-MS
GDP	C00035	LC-MS	TMP	C01081	LC-MS
Glucose	C00031	GC-MS	Trehalose	C01083	GC-MS
Glutamic acid	C00025	GC-MS	Tryptophan	C00078	GC-MS
Glutamine	C00064	LC-MS	Tyrosine	C00082	GC-MS
Glycine	C00037	GC-MS	UDP	C00015	LC-MS
GMP	C00144	LC-MS	UDP-Glucose	C00029	LC-MS
GTP	C00044	LC-MS	UMP	C00105	LC-MS
Guanosine	C00387	LC-MS	Uracil	C00106	GC-MS
Histidine	C00135	GC-MS	Urate	C00366	LC-MS
Hypoxanthine	C00262	GC-MS	Urea	C00086	GC-MS
IMP	C00130	LC-MS	Uridine	C00299	LC-MS
Inosine	C00294	LC-MS	UTP	C00075	LC-MS
Isocitric acid	C00158	GC-MS	Valine	C00183	GC-MS
Isoleucine	C00407	LC-MS	Xanthine	C00385	GC-MS
Lactate	C00186	LC-MS	XMP	C00655	LC-MS
Lauric acid	C02679	GC-MS	Xylitol	C00379	GC-MS
Leucine	C00123	LC-MS	ß-Alanine	C00099	GC-MS

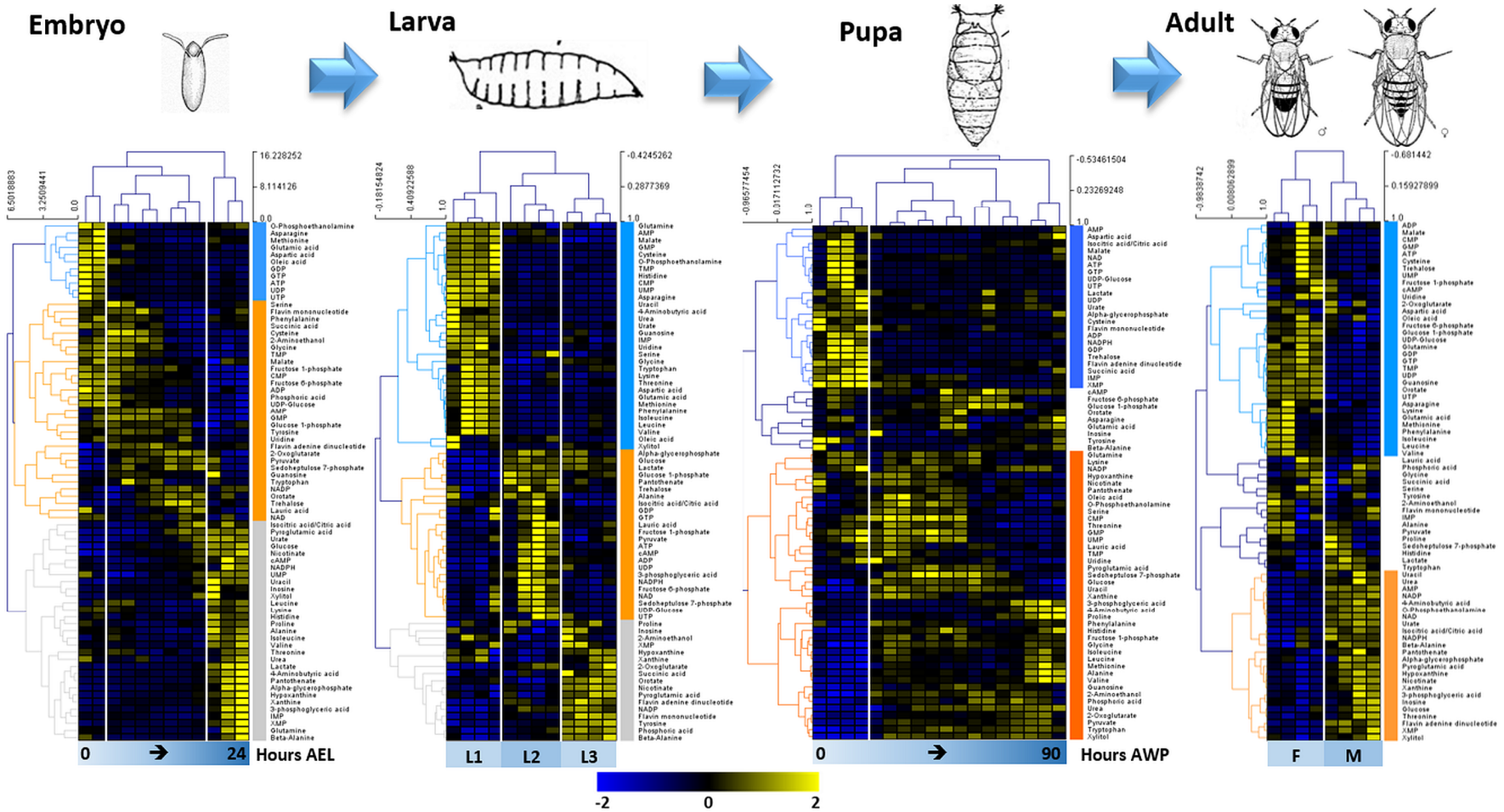

Figure 2-2: Heat maps showing the metabolic profiles of *Drosophila* throughout its lifecycle. Metabolite levels were expressed relative to its average value at each stage separately. The color scale is plotted at the bottom of the figure. Metabolites were discriminated hierarchically into clusters which are correlated with the physiology of *Drosophila* within each stage. L1: first instar larvae; L2: second instar larvae; L3: third instar larvae; F: female adult; M: male adult. The detail of HCA plots for embryos, larvae, pupae and adult flies were show in Figure S2-1, S2-2, S2-3 and S2-4, respectively

2.2.2. Embryogenesis

In order to clearly elucidate the correlation between the metabolome and actual developmental stages of *Drosophila* embryo, the metabolome data matrix was subjected to PCA. The results showed that in the principal component (PC) space formed by PC1 (35.4%) and PC2 (18.5%), the sample data separated into three distinct clusters namely "0-4 h AEL", "4-18 h AEL" and "18-24 h AEL". Specifically, PC1 clearly separates the different developing stages of the embryo. PC2 seems to contribute to the separation of the middle stage "4-18 h AEL" from the other stages ("0-4 h AEL" and “18-24 h AEL”) (Figure 2-3A).

This grouping tendency was in complete agreement with the actual developmental processes occurring during *Drosophila* embryogenesis. Within the first 3 h AEL, the important phenomena include synchronized nuclear divisions, formation of the primary germ cells, pole cells and conversion of syncytium into cellular blastoderm stage of embryo [101,122]. The gastrulation starts from 3h AEL and lasts until 18 h AEL. During gastrulation, the single-layered blastula is reorganized into the gastrula composed of ectoderm, mesoderm, and endoderm. Then, it undergoes organogenesis, segmentation and the segregation of the imaginal discs. During the last stage (18-24 h AEL), the ventral cord continues retracting to complete embryogenesis [101,122]. The metabolites corresponding for this separation can be observed on the metabolite clusters from HCA plot. Metabolites with high expression level during 0-4, 4-18 and 18-24 h AEL were grouped into blue, orange and grey clusters, respectively. Similar trend was also found on the loading plot showing the contributions of each metabolite on the discrimination in score plot according to the distance to the origin (Figure 2-3B).

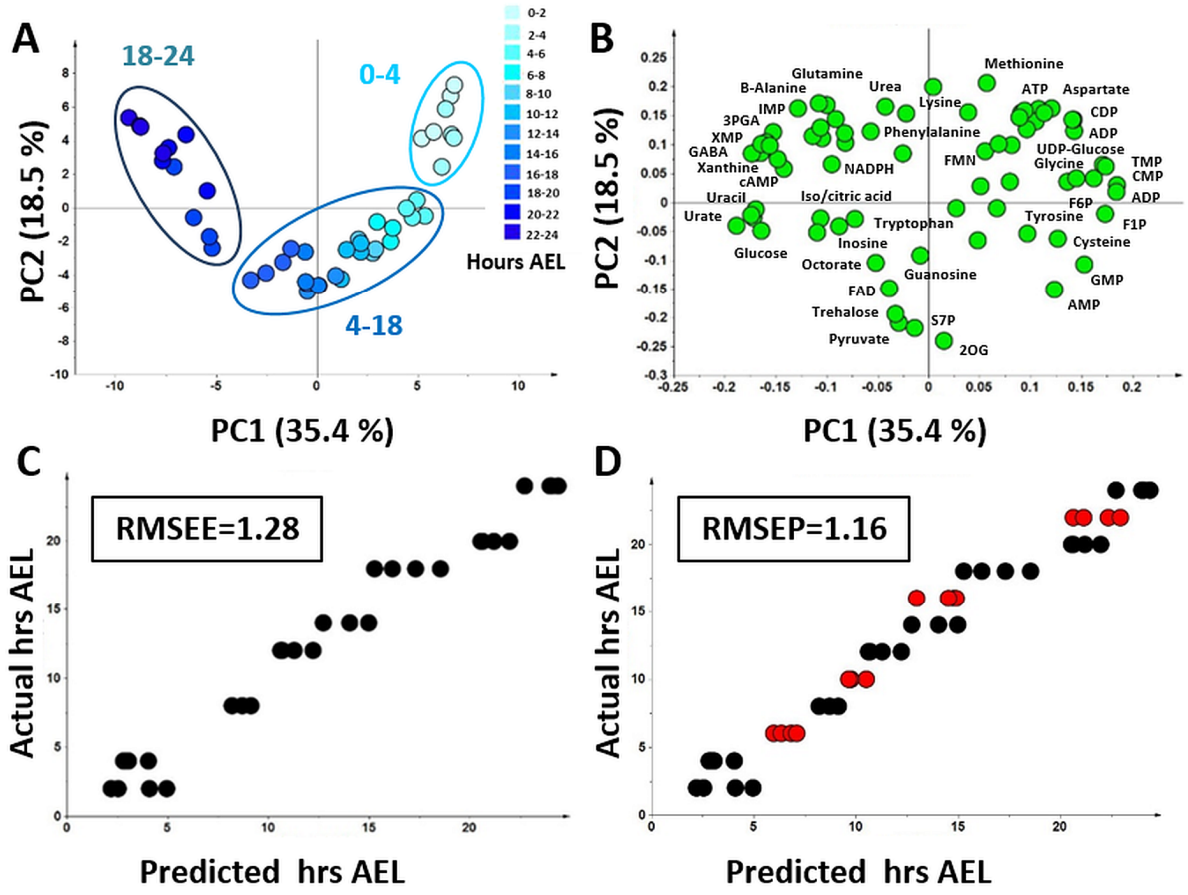

Figure 2-3: There is a high coincidence between the composition of metabolome and actual developmental stages of *Drosophila* embryo. Embryos were collected at 10 time points namely 0-2, 2-4, 4-6, 6-8, 8-10, 10-12, 12-14, 14-16, 16-18, 18-20, 20-22 and 22-24 h AEL. **(A)** PCA score plot shows 3 main clusters namely 0-4, 4-18 and 18-24 h AEL, which is in total agreement with the developmental stages of *Drosophila* embryo. **(B)** The loading plot shows the contributions of each metabolite on the discrimination in score plot according to the distance to the origin. Partial Least Square was performed to construct a robust and accurate prediction model for *Drosophila* embryo developmental stages based on the metabolic data. **(C)** A good correlation between metabolome data and developmental stages could be achieved. R^2 and $Q^2 > 0.9$ indicated an excellent predictive model. **(D)** Cross-validation of the model using the test set (red) were fitted onto the prediction model constructed using the training set (black). RMSEP was not so different from RMSEE, showing that the model was validated.

Since the metabolic profile was found to be correlated with biological activities during *Drosophila* embryogenesis, it is speculated to be possible to construct a prediction model based on metabolite information. In this method, PLS, a regression extension of PCA, was utilized to find the relationship between metabolite abundances and the h after egg laying (h AEL).

Among the 10 time points investigated, 4 time points namely 4-6, 8-10, 14-16 and 20-22 h AEL were selected as the test set, while the rest were used as the training set. PLS regression was first performed with the training set by importing the information of all 73 metabolites to the X-matrix while the actual AEL were imported to the Y-matrix. A good correlation between the metabolite information and developmental stages of *Drosophila* embryogenesis was observed with the goodness-of-fit (R^2) and goodness-of-prediction (Q^2) values of 0.97 and 0.97, respectively. The high R^2 and Q^2 values indicated an excellent predictive model (Figure 2-3C). In order to verify these results, the test set was added into the model wherein they fit perfectly in the predicted regression line (Figure 2-3D). Moreover, the root mean square error was calculated to determine how well the observed h AEL matched the actual h AEL. Results showed that the root mean square error of prediction (RMSEP = 1.16) was not significantly different from the root mean square error of estimation (RMSEE = 1.28), thus indicating that the regression model was valid. In conclusion, a prediction model of *Drosophila* embryogenesis based on metabolome data was successfully developed.

From PLS model, the VIP (Variable Importance in the Projection) scores of a predictor are calculated as the weighted sum of squares of the PLS weights, which indicates the contribution of that variable to the model [123]. Since the average of squared VIP scores equals 1, the “greater than one rule” is generally used as a criterion for variable selection. Any metabolites with VIP scores higher than 1 were considered to have strong impact on the prediction of *Drosophila* development based on the metabolic profiles. On the other hand, the regression coefficient plot was utilized to see the correlation trend (negative or positive) of each metabolite to this model. Within this model, the metabolite which had a negative correlation was deduced as important during early embryogenesis and vice versa. Among the 73 metabolites detected, 33 metabolites were found to have strong correlation with *Drosophila* embryogenesis (Table 2-2).

Table 2-2: Important metabolites showed strong correlation with *Drosophila* embryogenesis

Compound ID	VIP Score	Regression Coefficient	Compound ID	VIP Score	Regression Coefficient
Nicotinate	1.6		Pantothenate	1.3	+
CMP	1.6	-	GABA	1.3	+
F6P	1.5	-	GTP	1.2	-
Glucose	1.5	+	Hypoxanthine	1.2	+
Urate	1.5	+	Aspartic acid	1.2	-
Pyroglutamic acid	1.5	+	Glutamic acid	1.2	-
UDP-Glucose	1.5	-	ATP	1.2	-
TMP	1.5	-	XMP	1.2	+
ADP	1.4	-	2-Aminoethanol	1.2	-
Phosphoric acid	1.4	-	3PGA	1.1	+
GDP	1.4	-	cAMP	1.1	+
F1P	1.4	-	Xanthine	1.1	+
Glycine	1.4	-	UDP	1.1	-
Lactate	1.3	+	UTP	1.0	-
Oleic acid	1.3	-	GMP	1.0	-
Uracil	1.3	+	Xylitol	1.0	+
α-glycerophosphate	1.3	+			

Sugars, especially glucose, showed high VIP score and had positive correlation to the model, which means their levels increased throughout embryogenesis. Previous studies reported that trehalose is present as an energy source in the *Drosophila* hemolymph as early as the larval stage[124,125], however it did not have high VIP score here. From PCA loading plot, trehalose was found to be accumulated in an abundant level during gastrulation (4-18 h AEL) (Figure 2-4). In addition, expression data have also shown that two *Drosophila* trehalose transporters, encoded by the *Tret 1-1* and the *Tret 1-2* genes, are highly expressed during gastrulation while the *Treh* gene, encoding for the enzyme that converts trehalose into glucose, is expressed throughout embryogenesis [126]. Therefore, there was a possibility that from 8 to 16 h AEL trehalose is synthesized and transferred to the tissues that require it as a carbon source.

Although in larval stage glucose in the fat body is utilized to generate trehalose [124,125], trehalose used in embryogenesis must be generated from other sources, properly from the yolk since the level of glucose is quite low in the early stage. Afterwards, the level of trehalose decreases, while the level of glucose increases from 18 to 24 h AEL. Taking account of these observations, trehalose was proposed to be used as the energy source for glycolysis to supply glucose for the cells during late stage of embryogenesis.

On the other hand, aspartic acid and other metabolites in purine and pyrimidine metabolism had negative correlation, which indicated the highest contribution to the separation of the early stage (0-4 h AEL) from the other periods (6-24 h AEL). These data can also found on HCA plot and PCA loading plot (Figure 2-2, Figure 2-3B and Figure 2-4C). In *Drosophila* embryo, the nuclear division cycle consists of S and M phases without any intervening gap phases like G1 or G2 phase. Thus, the initial division cycles proceed rapidly, ranging from 10 to 25 mins, as compared to the typical cell cycle duration of 24 h [127]. These observations indicate that aspartic acid, which is related to purine and pyrimidine synthesis[128], might be a crucial element for supplying substrates for DNA replication during the rapid nuclear division cycles of early *Drosophila* embryogenesis.

In summary, this study showed that different metabolites play distinct roles during the development of the *Drosophila* embryo, which may reflect the biological changes in the cell. Based on the level of metabolites observed, it was possible to extrapolate their implications in the various pathways that may contribute to the overall development of the *Drosophila* embryo.

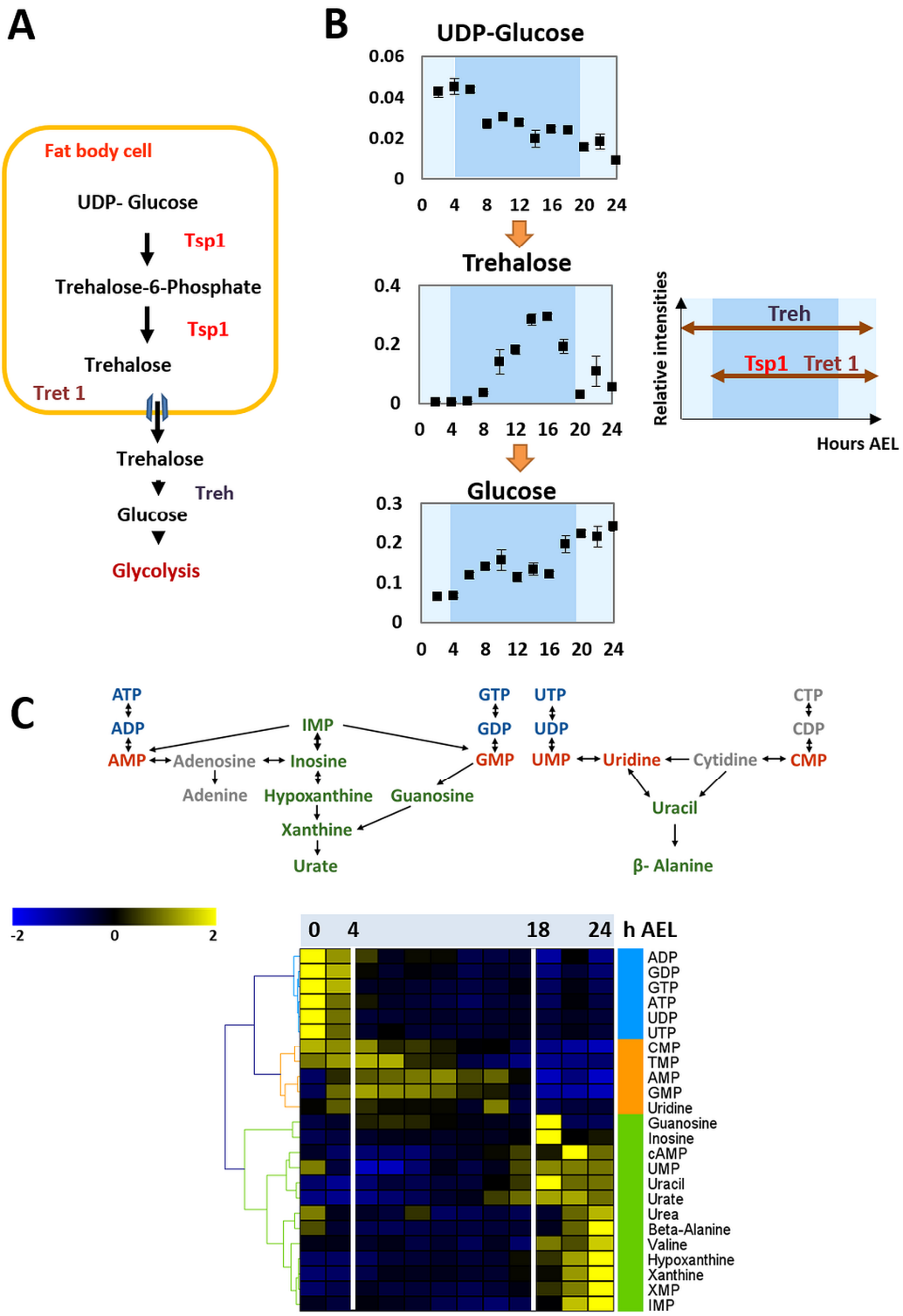

Figure 2-4: Metabolic pathways showed strong correlation with *Drosophila* embryogenesis. (A) Glucose production pathway with important enzymes for each step. Treh: enzyme converts trehalose into glucose; Tsp1: enzyme converts UDP-Glucose into trehalose; Treh 1: trehalose transporter. **(B)** Metabolite expression patterns of glucose production during embryogenesis. (**C**) Purine and pyrimidine metabolism. The metabolic pathways were showed in upper panel. The color of metabolites matched with the color of metabolite clusters in HCA plot (lower panel). The color scale shows the relative levels of each metabolite to its average value.

2.2.3. Larval stage

In HCA plot, the metabolites highly expressed in 1st, 2nd and 3rd instar larvae were clustered into three main groups including blue, orange and grey, respectively (Figure S2-2). Interestingly, a similar trend of discrimination was also observed in PCA results (Figure 2-5). The score plot of PCA showed that it was able to distinguish the developmental stages of larvae based on the metabolic profile (Figure 2-5A). In the principal component space formed by PC1 (48.1%) and PC2 (24.7%), the sample data was separated into three groups representing each stage of instar larvae. Collectively, the clustering of the biological replicates for each sample is clearly observed for each stage and the clear separation of metabolic profiles of all developmental stages indicates that significant metabolic changes occur at each stage of the development.

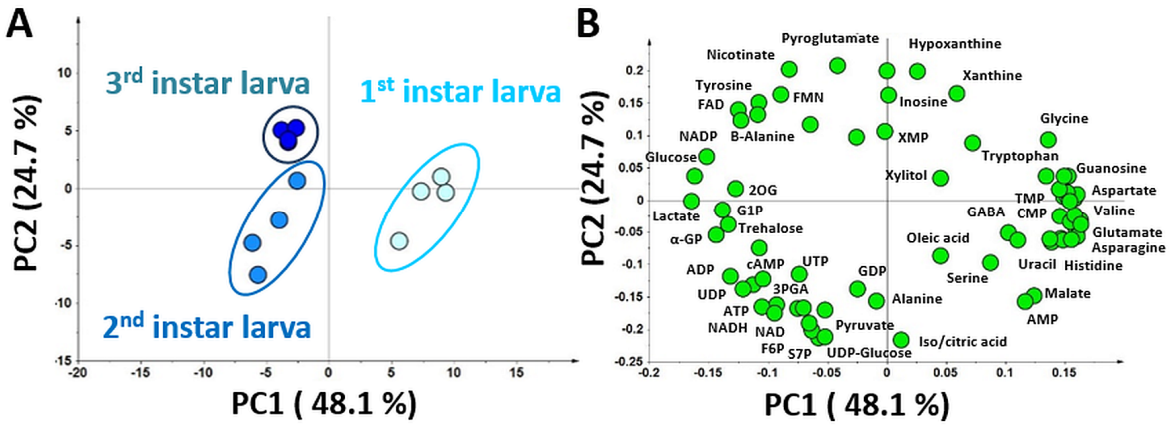

Figure 2-5: Metabolic profile of *Drosophila* during larval stages. PCA showing the discrimination of larval developmental stages based on the metabolic profile. Score plot and loading plot are shown in (**A**) and (**B**), respectively.

During larval stage, the instar larvae transition from foraging to wandering behavior occurs in feeding and non-feeding stage, respectively. After three days of larval development, a fly can increase 200-fold in mass and acquire enough nutrients as the energy source to enter metamorphosis [103]. In the early stage of larval development, the flies can start to uptake food to get enough materials for building their bodies. The high level of free amino acids (FAAs) were detected in first instar larvae, showing in blue cluster of HCA plot (Figure S2-2) and PCA

loading plot (Figure 2-5B), indicated that protein productions were elevated. In second instar larvae, imaginal disc cells are rapidly proliferating to reach an appropriate size and cells of other tissues undergo endoreplication cycles for cell growth. The larvae have to prepare enough material for cell division and cell growth. Therefore, most of the metabolites detected in this stage relate to purine and pyrimidine synthesis pathways, which are shown in the orange cluster of HCA (Figure S2-2) as well as the loading plot of PCA (Figure 2-5B). During the extensive feeding stage, larvae uptake nutrients not only to fuel developmental reorganization but also to survive during metamorphosis and early adult stage. Thus, high levels of some amino acids, sugars and TCA intermediates, which are related to energy metabolism, were detected during the late stage of larval development. Notably, significant amount of sugars accumulated during late larval stages.

2.2.4. Metamorphosis

First, PCA and HCA were performed using all data set to examine how the expression level of metabolites correlated with the metamorphic stages. From the HCA plot, each metabolite had a distinct expression pattern throughout metamorphosis (Figure 2-2). On horizontal axis of HCA results, the samples were grouped into two main group including 0-6 h AWP (stage 1-4) and 12-90 h AWP (stage 5-15), which were matched with the prepupal period marked by pupariation and a subsequent pupal period of *Drosophila,* respectively. Similar discrimination was observed on PCA score plot where PC1 (29.1%) successfully separated prepupal and pupal periods and PC2 (15.7%) can discriminate from the early to late stages of the main pupal period (Figure 2-6A). The HCA and PCA loading plot revealed the high level of metabolites in purine and pyrimidine during prepupal period and high level of amino acids during late stage of metamorphosis (Figure 2-2 and Figure 2-6B).

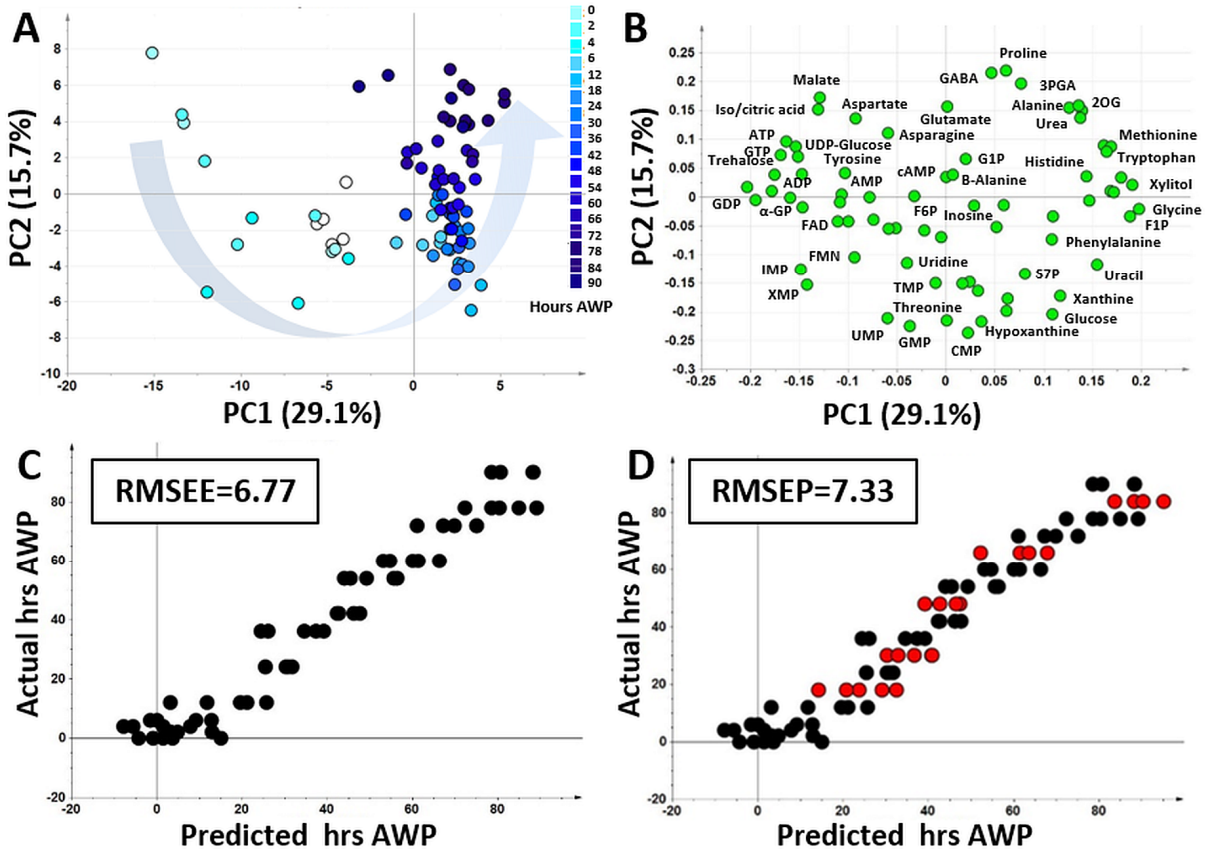

Figure 2-6: Time-Course Metabolic Profiling of *Drosophila* during metamorphosis. (A) PCA score plot showing the high correlation between the metabolic profile and actual developmental stages of *Drosophila* pupae. PC1 (29.1%) successfully separated prepupal and pupal periods while PC2 (15.7%) can discriminate from the early to late stages of each period. The color scale showed the h AWP. **(B)** The corresponding loading plot (lower panel) illustrates the metabolites that contributed to the separation on PC1 and PC2. PLS regression was first performed by importing all compounds to the X-matrix while actual the developmental time were imported to the Y-matrix. **(C)** A good correlation between metabolic profile and developmental stages was achieved with R^2 and $Q^2 > 0.9$. (**D**) Cross-validation of the model using the test set was fitted onto the prediction model constructed using the training set since the RMSEP was not so different from RMSEE.

PLS models were constructed to find the correlations of metabolic profiles with *Drosophila* metamorphic process. Here, a Leave-Group-Out cross-validation was performed, the data were split into a training set (13 time points) to build the models and a test set (5 time points) randomly to estimate the predictability (Figure 2-6C, D). The results from training sets demonstrated accurate model ($R^2 > 0.9$) with adequate robustness ($Q^2 > 0.9$). When the test sets were added into the models, RMSEE values were similar to RMSEP values in each model,

which indicated a good fit and accuracy of prediction models. Altogether, the results demonstrated that the methodologies applied in this study were valid and sensitive enough to distinguish the developmental times as well as the metamorphic stages of *Drosophila* based on the metabolic data. Furthermore, there was a tight coordination of the metabolic profile and the development of *Drosophila,* which made metabolomics a potential tool for studies using the *Drosophila melanogaster* model.

Table 2-3: Important metabolites showed strong correlation with *Drosophila* metamorphosis

Compound ID	VIP Score	Regression Coefficient	Compound ID	VIP Score	Regression Coefficient
Urea	1.9	+	Guanosine	1.2	+
GABA	1.8	+	Leucine	1.2	+
Tryptophan	1.5	+	GDP	1.2	-
Valine	1.5	+	Phosphoric acid	1.2	+
3PGA	1.5	+	NADPH	1.2	-
XMP	1.5	-	CMP	1.2	-
Xylitol	1.5	+	GMP	1.2	-
Proline	1.4	+	FMN	1.1	-
2-Oxoglutarate	1.4	+	UMP	1.1	-
Pyruvate	1.4	+	2-Aminoethanol	1.1	+
Alanine	1.4	+	Isoleucine	1.1	-
Methionine	1.3	+	Succinic acid	1.0	+
Histidine	1.3	+	Threonine	1.0	-
Hypoxanthine	1.3	-	Uridine	1.0	-
Glycine	1.3	+	FAD	1.0	-
Trehalose	1.3	-	ADP	1.0	-
IMP	1.3	-			

Among the important metabolites revealed from PLS models (Table 2-3), the amino acids had the positive correlation to the PLS model, which indicated that the level of these amino acids increased throughout metamorphosis. Therefore, the abundances of FAAs were examined to check how they actually changed during metamorphosis (Figure 2-7A). The level of almost

all amino acids (VIP > 1) significantly increased from prepupal to pupal stage and then either kept constant level from 48 h until 72 h AWP. Finally, FAA abundances increased again up to the end of metamorphosis. Since most insects obtain amino acids from their food by ingesting protein [129] and pupal body is a closed system, the increasing of FAAs is likely caused by the degradation of proteins by autophagy and apoptosis. Moreover, the increase of FAAs during the transition stage between prepupal and pupal periods matched with the timing of increase of urea level. These results suggested that the cells broke down proteins intensively to recycle the amino acids as material to construct proteins or to produce energy via gluconeogenesis. Especially at the late stage of metamorphosis, the unnecessary proteins might be recycled again as reserves for energy, since the fly cannot eat food until 8 h after eclosion [130].

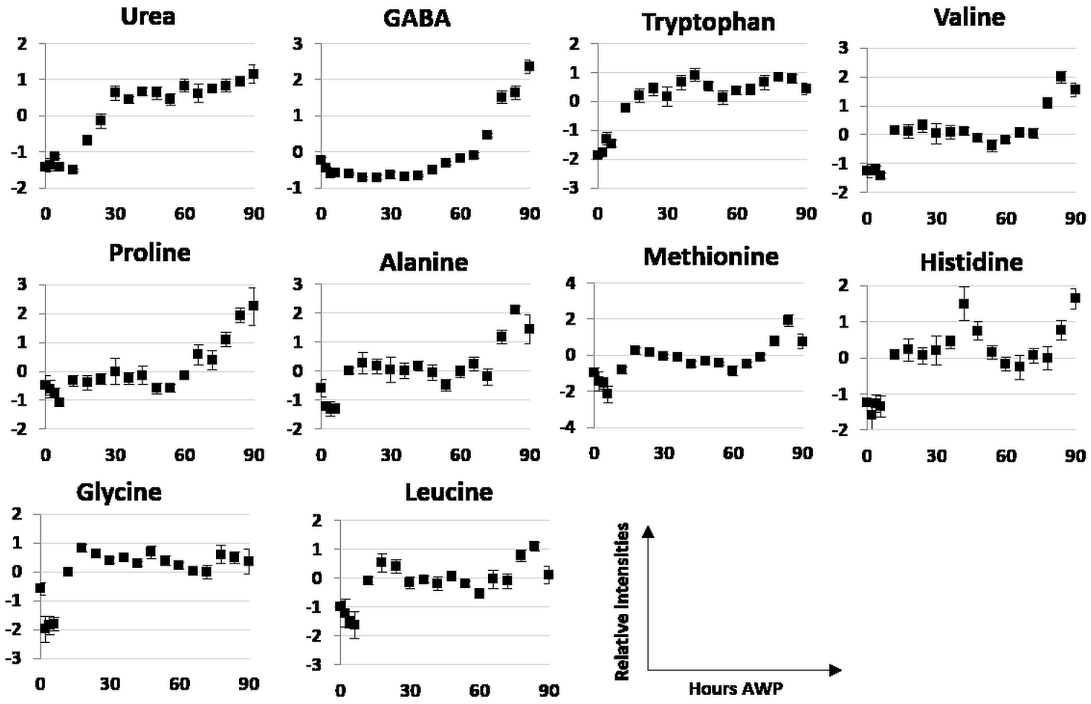

Figure 2-7: Amino acid metabolism of *Drosophila* metamorphosis based on metabolic profiles of CS. The plots showed the expression patterns of metabolites in amino acid metabolism with VIP score > 1.

Compared to human and most of vertebrates, the hemolymph of insects have higher concentration of FAAs. Specifically, the level of FAAs in the blood of most vertebrates is 0.5 mg/ml while it is 2.9-23.4 mg/ml in insect hemolymph and 1 mg/ml in most of invertebrate

hemolymph other than insects [131,132]. A previous metabolomics study on ten different tissues of *Drosophila* has also shown that the most abundant metabolites are amino acids [74]. Thus, the flies appear to regulate the FAA levels not only to maintain the normal development of *Drosophila* pupae but also have to keep a high abundant level of FAAs in the body of adult flies at the end of development.

2.2.5. Adult flies

The PCA score plot showed significant differences between male and female *Drosophila* based on the metabolic profiles (Fig 2-8A). The metabolites highly expressed in female and male *Drosophila* were shown respectively in blue and orange clusters on HCA plot of adult stage (Figure S2-4). In order to figure out the statistically significant metabolites that made these differences, OPLS-DA, a discriminant analysis, was performed to maximize the variations between two genders.

In cooperation with the data from PCA, the score plot from the OPLS-DA models showed a clear separation between the two strains with $R^2 > 0.9$, $Q^2 > 0.9$ and p(CV-ANOVA) < 0.05 (Figure 2-8B). Hence, these OPLS-DA models can be used to investigate the metabolites accounted for the separation between the two strains based on the combination of VIP score and p(corr) (loadings scaled as a correlation coefficient between the model and original data). The criteria for cutoff point were VIP > 1.0 and |p(corr)| > 0.5 [133](Figure 2-8C).

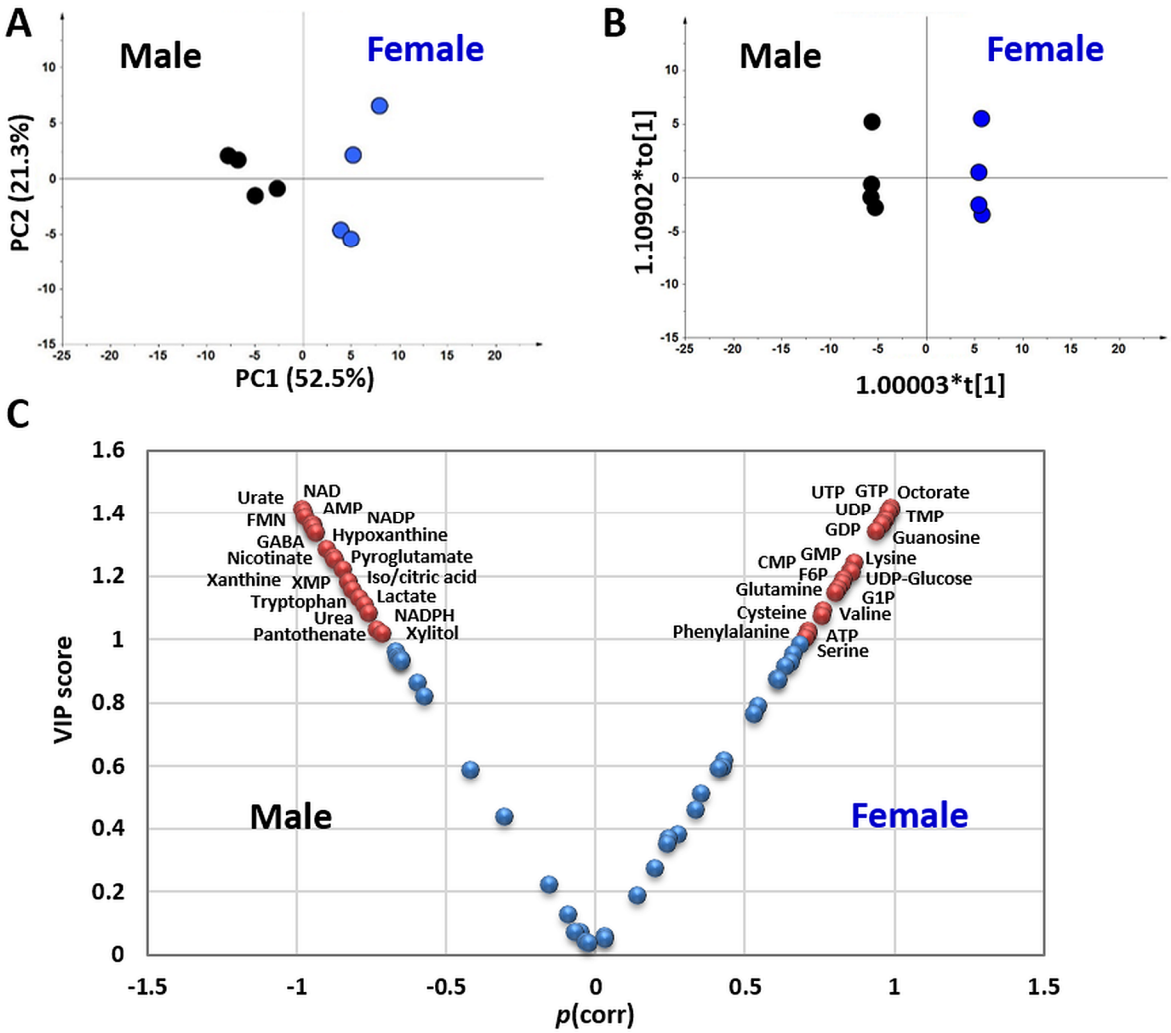

Figure 2-8: The variances between female and male adult flies. (A) PCA score plots showed a clear separation between female and male metabolic profiles on PC1 (52.5%). **(B)** OPLS-DA models were constructed in order to maximize the differences between two genders. $R^2Y > 0.9$, $Q^2 > 0.9$ and p(CV-ANOVA) = 0.006. **(C)** The criteria VIP $\geq$ 1.0 and |p(corr)| $>$ 0.5 were used to select potential metabolites (red).

Previous reports on lipidome showed that 18% of detected lipids had big differences in concentration [134]; however, the lipids in non-gonadal soma did not show much difference between male and female flies [107]. On the other hand, the global analysis of transcription activities between the sexes has been established and found the majority of cases of sex differential gene expression are attributable to the germ cells [135]. Therefore, the differences in the metabolic profiles discovered in this study might also due to the reproductive systems.

Higher level metabolites in sugar metabolism including UDP-Glucose, G1P and F6P were found in female flies. Since adult flies can uptake nutrients directly from food, these results indicated that female *Drosophila* had higher energy demand. This finding matched with previous data suggested that female flies had relatively bigger fat body and more storage lipid to maintain the reservoirs the reproductive organs and eggs [134].

In addition, the metabolites in purine and pyrimidine metabolism were also elevated in female flies. This result was similar with previous study suggesting the additional requirements for DNA biosynthesis and RNA transcription to produce eggs from germ cells in the females [136]. Some metabolites in purine metabolism had higher abundance in male flies including AMP, XMP, hypoxanthine and xanthine. At the meantime, the level of uric acid and urea, the final product of purine and pyrimidine catabolism, were also higher, suggesting that male flies increased the turnover of these metabolites. Even though the mechanism was not clearly understood, these data proposed that the activities of purine and pyrimidine metabolism are sex-biased.

Since male and female flies also differ in body size, stress responses, immunity, physiology, and lifespan [137-139], *Drosophila* present an excellent model to investigate the mechanisms of sex differences in diverse aspects of development and physiology. The obtained data in this study support the idea of a link between sexes and the metabolism in *Drosophila*. Thus, it is highly recommended to notice the changes in the metabolic profiles in order to fully understand the underlying mechanisms.

2.3. Conclusion

Comparing to the huge database on genomics, transcriptomics and proteomics related to developmental biology, information from metabolomics studies are still very limited. This study is the first report demonstrated comprehensive methods using non-targeted GC/MS-based and targeted LC/MS-based metabolic profiling to investigate the changes of central metabolic pathways throughout *Drosophila* development. With these platforms, 73 metabolites were detected. As a high throughput method, the developed methods were possible to focus on a wide range of metabolites in the samples at various time points and determined the similarities or differences among data sets. This provided a better view and higher precision of the metabolic state during the development of an organism. The metabolite abundances changed drastically and had tight connection with the biological activities within each stage of the development. The results from this study can be used as the database of central metabolic pathways throughout *Drosophila* life cycle.

Here, from this study, the strength of metabolomics in developmental biology was emphasized. The approaches established in this study can be an effective tool for any further investigations using the *Drosophila* model, where the observations of metabolites in central metabolic pathways are required to underpin genetic and other pathophysiological manipulations.

Chapter 3

Metabolomics-based analysis for the effects of temperatures and origins on the central metabolic pathways during *Drosophila* metamorphosis

3.1. Introduction

In metabolomics study using *Drosophila*, the effects of temperature and origin on metabolic profiles should be considered carefully. Powerful genetic tools have been developed for *Drosophila*, which makes it an important model organism for human diseases as well as basic research [2]. Among these, many methods allow the control of gene expression levels by switching temperature from permissive condition (18–22 ˚C) to restrictive condition (28–30 ˚C) such as temperature-conditional mutations, GAL4/GAL80^{ts}/UAS system and FLP/FRT system [140,141]. Even the GAL4/UAS system, one of the most commonly used tools for targeted gene expression in *Drosophila,* also achieves the maximal GAL4 activity at 29 ˚C [141]. However, as a poikilothermic animal, changes in temperature directly affect the development of *Drosophila*, including life cycle and aging processes [142]. For instance, a temperature difference of only 2–3 ˚C could affect the synchronization of circadian rhythms in *Drosophila* [143], and changes in rearing temperature during the larval stage had a dramatic effect on the metabolomic network structure measured in adult flies [64]. Therefore, the current study aimed to determine if the metabolic profiles of *Drosophila* were affected by the temperature even in non-stressed conditions (22–29 ˚C) throughout metamorphosis.

On the other hand, the selection of wild type strain as control is also very important for every study. Since *Drosophila* has a long history as a model organism, many wild type strains are available and selected depending on the experience of scientists. Among them, CS and

Oregon R (OR), both obtained from the wild in North America [144], are the most commonly used wild-type strains and selected depending on the experience of scientists studying *Drosophila*. Various studies have shown that CS and OR have differences in their reproduction in stress condition [145], cold tolerance [146], life span [147], and toxin resistance [148]. Previous studies also showed that differences in genotype could affect the metabolic profiles of *Drosophila* [80,149,150]. In particular, recent studies revealed that the lipid composition at the larval stage and metabolic profiles at the adult stage differed between these two strains [79,151]. In order to obtain a general perspective on the differences between CS and OR during metamorphosis, metabolic profiling of OR was performed in exactly same conditions at 25 °C to compare with the profile of CS.

Together, by using the developed metabolomics approaches further experiments were conducted to compare changes in central metabolism among commonly used temperatures as well as between *Drosophila melanogaster* strains CS and OR. These results provide a fundamental basis for future metabolomics studies using *Drosophila melanogaster*.

3.2. Materials and methods

3.2.1. Fly strain and sample collection

D. melanogaster CS was obtained from Bloomington Stock Center (USA). *D. melanogaster* OR was kindly provided by Prof. Mi-Ae Yoo (Pusan National University, Korea). All the fly stocks were reared at 25 °C on standard food (0.7% agar, 10% glucose, 4% dry yeast, 5% cornmeal, 3% rice bran). First, virgin flies of each gender were collected and kept separately for 3 days until they were mature enough for mating. Each sample set was derived from independent mating of 100 females and 100 males. After mating overnight, the flies were transferred to new vials and eggs were collected every 2 h. The time-course sampling started when the animals reached the white pupal stage. After collecting, the samples were washed with H_2O three times and then quenched in liquid N_2 immediately. Finally, all samples were freeze-dried for 16 h and stored at –80 °C.

For experiments at different temperatures, all flies were reared at 25 °C to collect white pupae and then the samples were incubated at 22 °C, 25 °C, and 29 °C until hatching. The details of all experiment are shown in Figure 3-1.

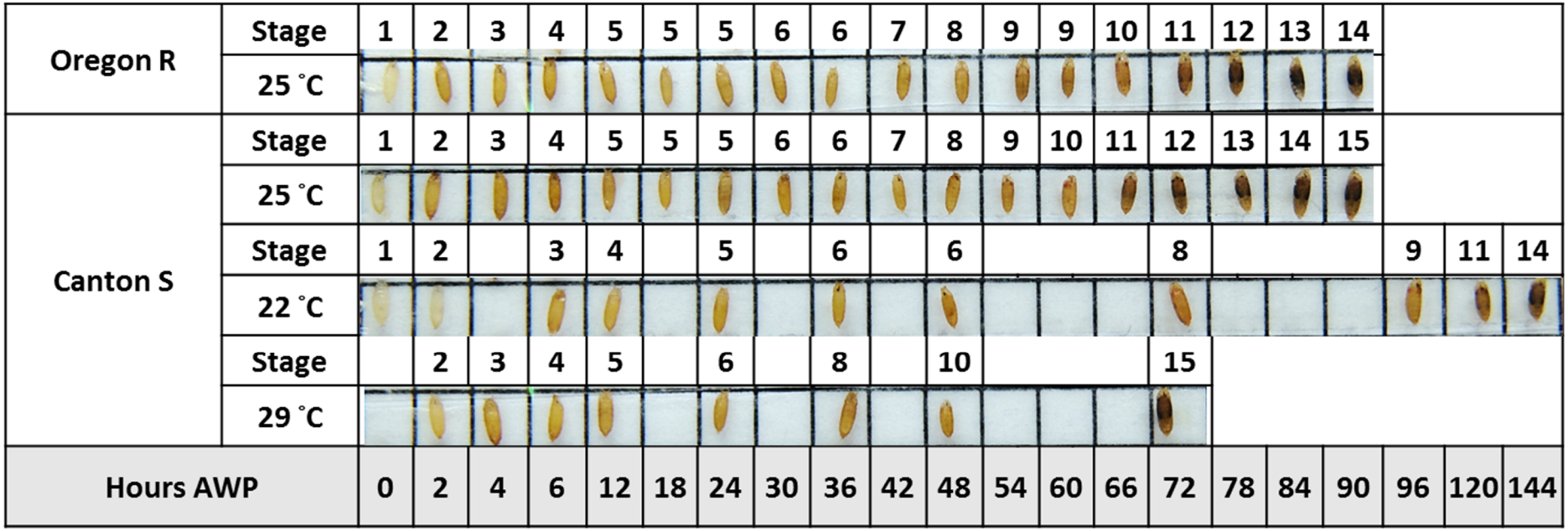

Figure 3-1: Summary of the sampling time points at each condition for metabolic profiling. *Drosophila* metamorphosis includes 15 stages, which can be defined by the morphology. The whole metamorphic process can be divided into two main periods including Stage the samples were grouped into two main group including prepupal period (stage 1-4) and pupal period (stage 5-15). The average developmental times at 22 ˚C, 25 ˚C, and 29 ˚C were 72, 90, and 144 h, respectively.

3.2.2. *Sample preparation for GC-MS and LC-MS*

Each sample contained 10 animals, and 3–5 biological replicates were used per condition. First, the samples were homogenized using ball mills (5 min, 20 Hz). In this chapter, methanol was used as extract solvent instead of the mixed solvent used in chapter 1 in order to cover not only the metabolites in the central metabolic pathways but also the three ecdysteroids in the same extract. Extraction was performed with 2 mL of methanol per sample using a ball mill (15 min, 20 Hz). Centrifugation was performed at 16,000 × g for 3 min, then the supernatant was filtered (0.2 µm PTFE, Millipore).

For GC-MS analysis, 400 µL of each extract was used. The solvent was removed by centrifugal concentration (VCe36S, Taitec Co., Japan) for 2 h and subsequently freeze-dried for 16 h. Then, the samples underwent oximation using methoxyamine hydrochloride (Sigma Aldrich, USA) in pyridine (50 µL, 10 mg/mL) at 30 °C for 90 min, and then silylation with 50 µL N-methyl-N-(trimethylsilyl) trifluoroacetamide (MSTFA) (GL Sciences, Japan) at 37 °C for 30 min.

Four hundred µL and 1 mL of the extracts were dried and diluted in 30 µL ultra-pure water for IP-LC-MS/MS analysis and 30 µL methanol for RP-LC-MS/MS, respectively.

All samples were analyzed within 24 h after extraction.

3.2.3. *GC-MS and IP-LC-MS/MS analysis.*

Same as in section 2.1.3. and 2.1.4.

3.2.4. *RP-LC-MS/MS analysis.*

Reversed phase liquid chromatography-tandem mass spectrometry (RP-LC-MS/MS) analysis was done using a Shimadzu Nexera UHPLC system coupled with LCMS 8050 Plus (Shimadzu, Japan). Three microliters of each sample was loaded onto a Mastro C18 HPLC column (150 mm × 2.1 mm, particle size 3 µm, Shimadzu, Japan) with a 0.2 mL/min flow rate

of 0.1% aqueous acetic acid (A) and acetonitrile containing 0.1% acetic acid (B) at 30 °C. Absolute quantification of ecdysteroids was performed using multiple reaction monitoring (MRM) mode and based on calibration curves of standards.

3.2.5. Data analysis for metabolic profiling

Same as in section 2.1.5.

3.2.6. Measurement of total protein, glycogen and triacylglycerol (TAG)

The total protein measurement is same as in section 2.1.6.

The measurement of glycogen and TAG was carried out based on that described previously [152-155]. For glycogen assay, 5 flies were homogenized in 200 µL of a solution containing 2% sodium sulfate and then 800 µL of chloroform/methanol (1:1) mixture was added to the homogenate. After centrifugation at 6,000 x g for 3 min, pellet was dissolved in 1 mL of anthrone reagent (1.4 g of anthrone in 1 L of 72% H_2SO_4). The solution was heated at 100 °C for 17 min and analyzed in a spectrometer at 625 nm. For TAG assay, 10 adult flies were homogenized in 200 µL of a solution containing 0.1% Tween 20 and the homogenate was heated at 70 °C for 5 min. After centrifugation at 15,000 x g for 5 min, 200 µl of TAG reagent (Sigma Aldrich, USA) was added to the 50 µL supernatant and incubated at 37 °C for 30 min. Incubated solution was analyzed in a spectrophotometer at 540 nm. The remaining homogenate was used for protein quantification by Bradford assay using bovine serum albumin as a standard. The amount of TAG was normalized to the sample weight.

3.3. Results and discussion

3.3.1. *The effects of temperature on Drosophila metabolic profile*

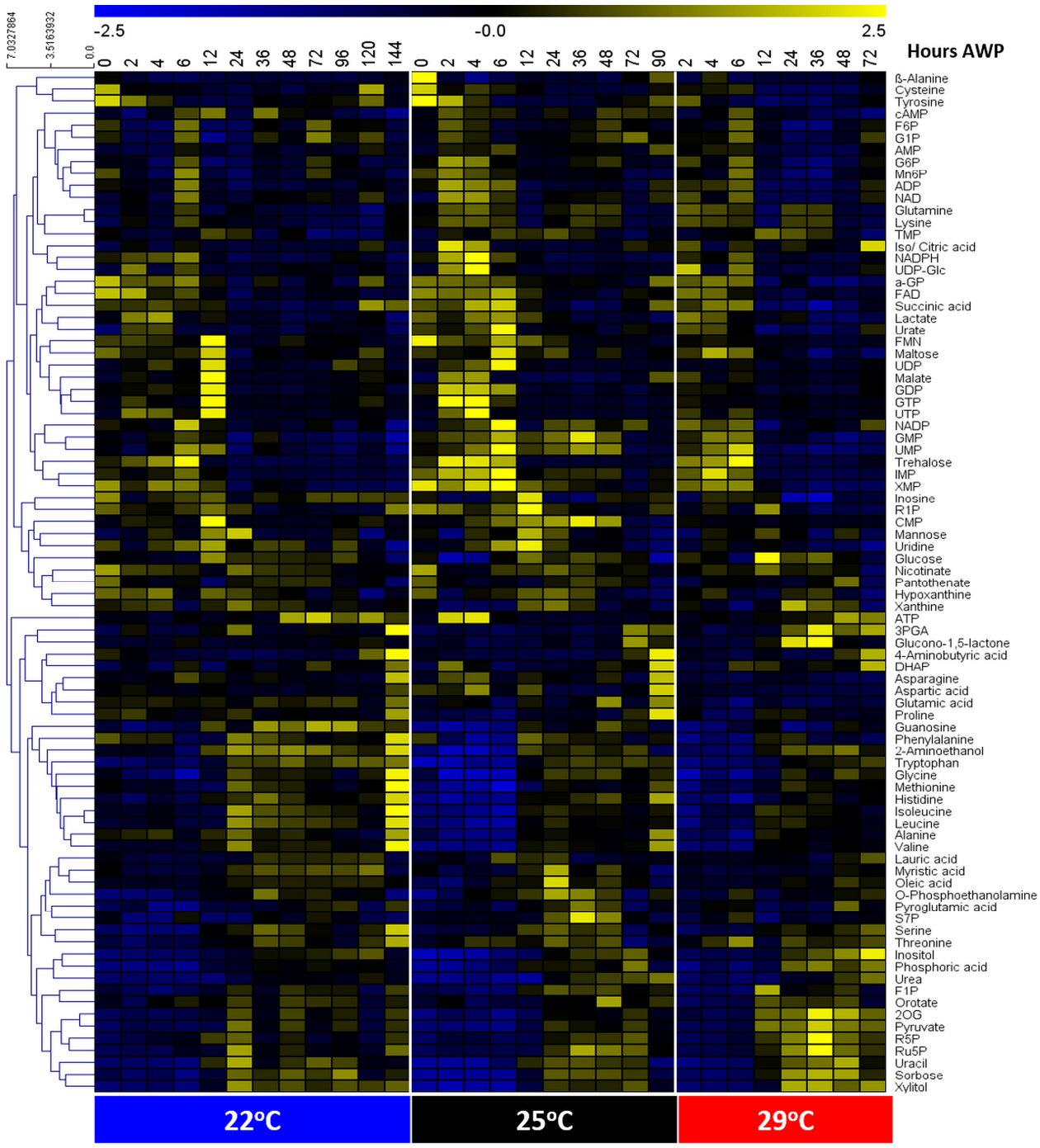

Figure 3-2: Metabolic profiles of CS during metamorphosis at different temperatures. (A) The HCA plot provides the global view of metabolite changes at various temperatures during metamorphosis. Among the flies reared at 22 ˚C, 25 ˚C, and 29 ˚C, similar expression patterns of metabolites were observed. The color scale, showing the relative levels of each metabolite to its average value, is plotted at the top of the figure.

All flies were reared at 25 ˚C to maintain standard conditions for development during embryogenesis and larval stages. Then, the white pupae were collected and screened at different temperatures to compare the metabolic profiles of CS at 25 ˚C with 22 ˚C and 29 ˚C. (Figure 3-2).

From the HCA plot, a similar expression pattern among these three conditions was observed (Figure 3-2), suggesting that the temperature just affected the duration of metamorphosis but not the metabolic profile within developmental stages of *Drosophila*. Next, PLS models were constructed using the data set at 25 ˚C as the training set and the rest as the test set. If this hypothesis is correct, the data at 22 ˚C and 29 ˚C would match to the training set. Strikingly, the test sets fitted well with the training set in the PLS model for actual metamorphic stages (Figure 3-3B). However, this was not in the case with the prediction model for the h AWP (Figure 3-3A). These results indicated that the metabolism of *Drosophila* is directly proportional to the temperature but the metabolic state of CS at a certain metamorphic stage was similar regardless of temperature.

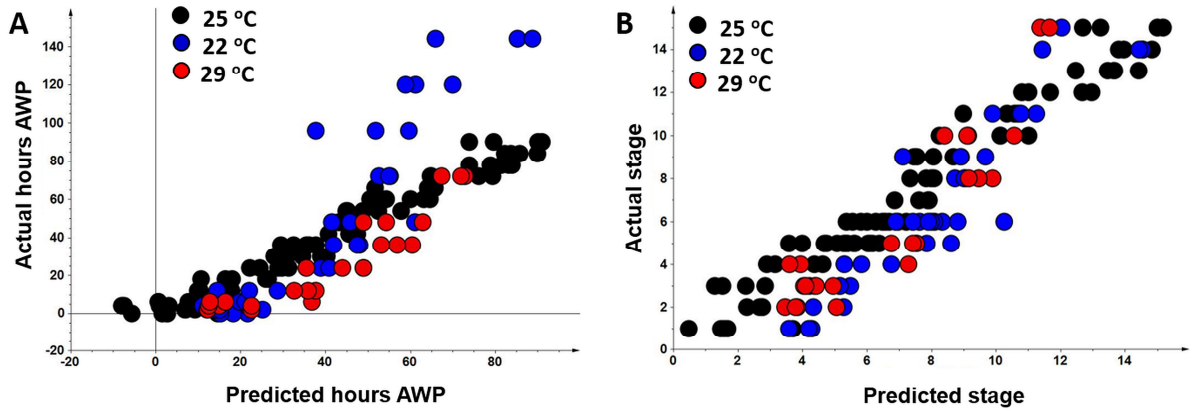

Figure 3-3: PLS regression model at different temperature. First, PLS analyses were performed for the developmental time **(B)** or metamorphic stages **(C).** The data set at 25 ˚C (black) was utilized as the training set. Data from 22 ˚C (blue) and 29 ˚C (red) were used as the test set. **(B)** R^2Y = 0.96, Q^2 = 0.93, RMSEE = 5.91, RMSEP = 26.38**. (C)** R^2Y = 0.95, Q^2 = 0.9, RMSEE = 1.25, RMSEP = 2.1.

As an insect, the developmental time for *Drosophila* during metamorphosis increases gradually due to the rise in temperature. Specifically, the average developmental times at 22 ˚C,

25 °C, and 29 °C were 72, 90, and 144 h, respectively. However, these results demonstrated that within the non-stress range of temperatures, the metabolic profile of CS was stable at each developmental stage. These data also identified a notable point for future metabolomics studies using *Drosophila*, in that all experiments should be performed at exactly the same temperature. If the flies are reared at different temperatures, even within non-stress conditions, differences in metabolic profiles at the same time point maybe caused by the effect of temperature.

3.3.2. *CS and OR showed similar global metabolic pools during metamorphosis*

When comparing the metabolic profiles between CS and OR, the distribution of different time points during metamorphosis of OR matched with CS on the PCA score plot (PC1 of 27.8%; PC2 of 11.8%) (Figure 3-4A). Because PCA is an unsupervised method, these results indicated that CS and OR shared similar metabolic profiles. The details of metabolite expression patterns can be observed on the HCA plot (Figure S3-1). The similarities in the metabolic profiles were further confirmed using the PLS model. If this interpretation was correct, there would be a possibility to predict the developmental times of OR based on the metabolic profile of CS and vice versa. Indeed, when either the data set from CS or OR was utilized as the training set to construct the PLS model, it was successful in predicting the h AWP as well as the actual metamorphic stages of another strain (Figure 3-4B, C, D, E).

Altogether, the obtained results further emphasized the overall similarities in the metabolic profiles of CS and OR during metamorphosis. Because metabolites are the intermediates and products of metabolism, these data indicated that the activities of the central metabolic pathways were also relatively similar between these two strains during metamorphosis.

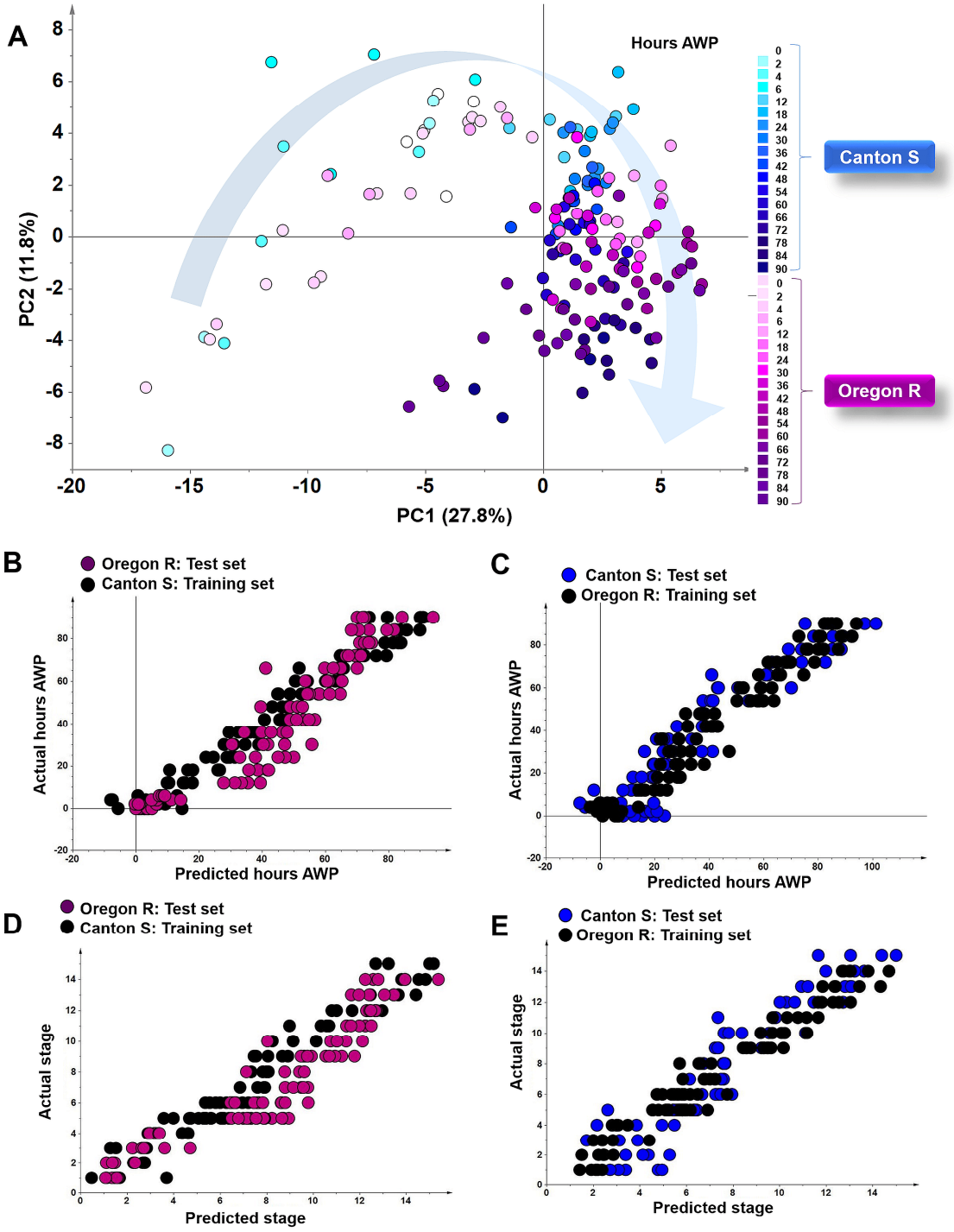

Figure 3-4: Comparing the metabolic profiles of CS and OR during metamorphosis. (A) PCA score plot showing the relatively identical distribution of developmental time based on the metabolic profiles between CS and OR. PC1 (27.8%) successfully separated the prepupal and pupal periods, whereas PC2 (11.8%) can discriminate from the early to late stages of each period. The color scale shows the h AWP. PLS models were constructed for h AWP **(B, C)** and for metamorphic stages **(D, E).** The whole data set from CS was used as the training set and OR was used as the test set (**B, D**) and vice versa in **(C, D). (B)** $R^2Y = 0.96$, $Q^2 = 0.92$, RMSEE = 5.91, RMSEP = 11.66**. (C)** $R^2Y = 0.94$, $Q^2 = 0.9$, RMSEE = 7.17, RMSEP = 9.98. **(D)** $R^2Y = 0.95$, $Q^2 = 0.91$, RMSEE = 0.93, RMSEP = 1.73. (**E**) $R^2Y = 0.95$, $Q^2 = 0.91$, RMSEE = 0.87, RMSEP = 1.51.

3.3.3. *Purine and pyrimidine metabolism was altered between CS and OR during the early stage of the main pupal period*

Because many studies have reported the differences between CS and OR, there was a possibility that there are differences in the metabolic profiles only at some specific time points during metamorphosis. To check this possibility, the data set was separated into prepupal and pupal stages. Of note, the data from CS and OR could be partially discriminated by PC3 of 8.32% and 9.15% in the PCA model for prepupal and pupal periods, respectively (Figure 3-5A, B). The analysis suggested that there was a minor difference in the metabolic profiles of CS and OR during metamorphosis.

Next, OPLS-DA, a supervised method, was conducted to maximize the differences between CS and OR in the prepupal and pupal periods. As predicted, each score plot from the OPLS-DA models showed a clear separation between the two strains with $R^2 > 0.9$, $Q^2 > 0.8$ and the p(CV-ANOVA) value for each model was far lower than 0.001 (Figure 3-5C, D). Hence, these OPLS-DA models can be used to investigate the metabolites accounted for the separation between the two strains based on the combination of VIP score and p(corr). The criteria for cutoff point were VIP > 1.0 and |p(corr)| > 0.4 [133].

Many metabolites related to purine and pyrimidine metabolism showed significantly higher levels in CS compared with OR, especially during the early stage of the pupal period at 18–48 h AWP (Figure 3-5E, F). The data was then confirmed using an ANOVA test (Table 3-1). Therefore, the metabolic pathway map based on the KEGG database was built using all detected metabolites related to this pathway (Figure 3-6). The levels of sugar phosphates, glutamine, and all nucleoside monophosphates in CS were significantly higher than in OR. Conversely, the levels of ribonucleosides and nucleoside triphosphates in OR were higher than in CS.

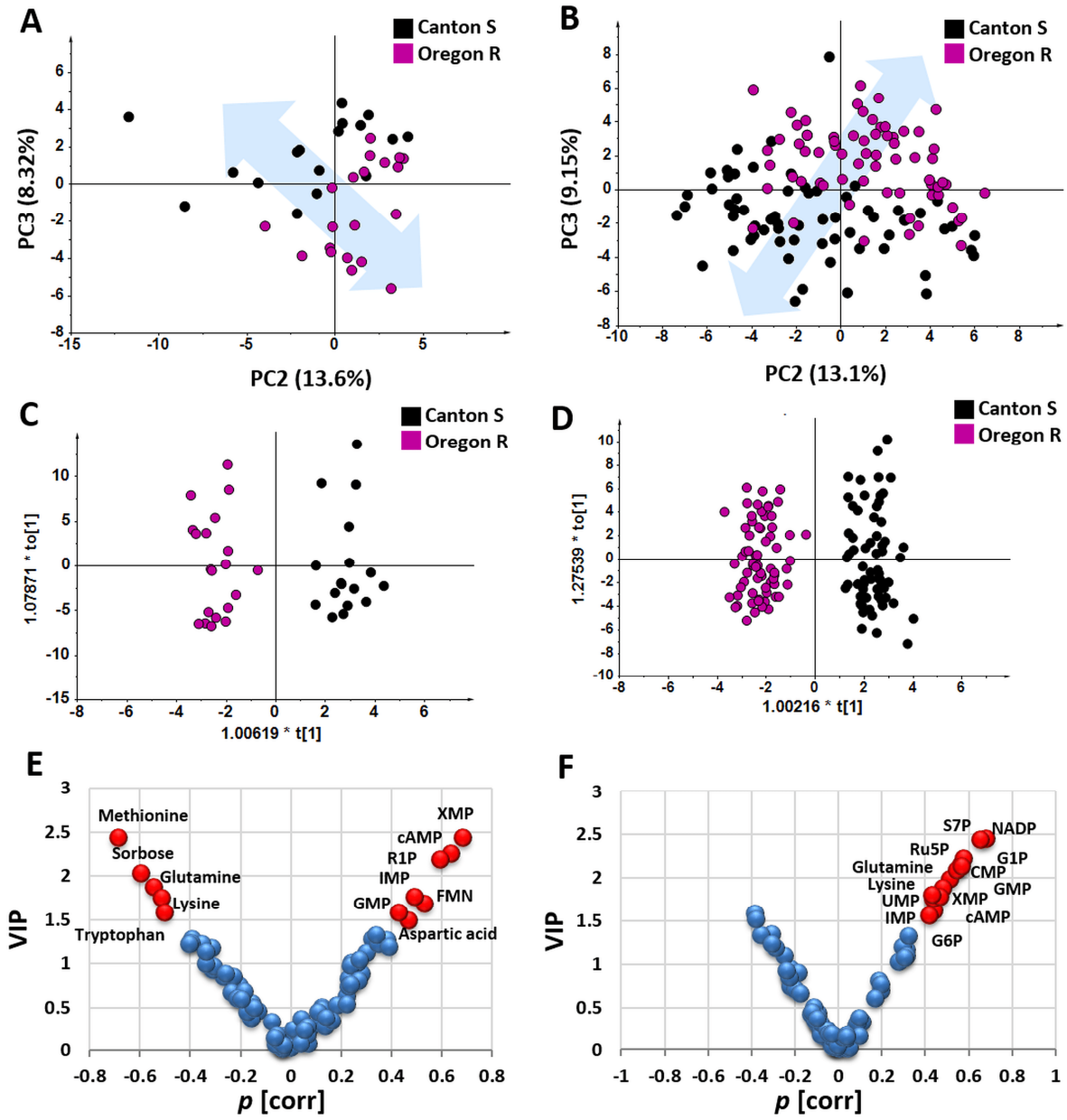

Figure 3-5: The variances between CS and OR in the prepupal and pupal periods. PCA score plots for prepupal **(A)** and pupal periods **(B).** PC3 of 8.32% and 9.15% successfully separated the prepupal and pupal periods. OPLS-DA models were constructed in order to maximize the differences between CS an OR in the prepupal **(C)** and pupal periods **(D). (C)** $R^2Y = 0.94$, $Q^2 = 0.85$, p(CV-ANOVA) = 7.07e-11**. (D)** $R^2Y = 0.94$, $Q^2 = 0.85$, p(CV-ANOVA) = 3.72e-37. The criteria VIP $\geq$ 1.0 and |p(corr)| $>$ 0.4 were used to select potential metabolites (red) with large changes between CS and OR. Plot formed by VIP score and p(corr) from OPLS-DA are shown for the prepupal **(E)** and pupal periods **(F).**

Table 3-1: Metabolites showed the significant different between CS and OR during 18-48 hours AWP

Compound ID	P-value	FDR	Bonferroni	Compound ID	P-value	FDR	Bonferroni
XMP	2.11E-07	1.82E-05	1.82E-05	**G1P**	1.68E-04	1.60E-03	1.44E-02
Guanosine	8.77E-07	3.77E-05	7.55E-05	**IMP**	1.93E-04	1.66E-03	1.66E-02
GMP	4.74E-06	1.36E-04	4.08E-04	**R1P**	2.26E-04	1.77E-03	1.94E-02
NADP	7.91E-06	1.46E-04	6.81E-04	**cAMP**	2.73E-04	1.94E-03	2.34E-02
S7P	8.51E-06	1.46E-04	7.32E-04	**UMP**	3.09E-04	1.94E-03	2.66E-02
Inosine	2.66E-05	3.78E-04	2.29E-03	**Lysine**	3.15E-04	1.94E-03	2.71E-02
CMP	3.08E-05	3.78E-04	2.65E-03	**Malate**	4.03E-04	2.31E-03	3.47E-02
AMP	6.32E-05	6.80E-04	5.44E-03	**Glutamine**	4.39E-04	2.36E-03	3.77E-02

FDR: false discovery rate

In *Drosophila*, ecdysteroids are the molting hormones which trigger the major developmental transitions in *Drosophila* during metamorphosis [156-158]. When the tissues were triggered to undergo cell death together or cell proliferation by ecdysteroids, the abundance of metabolites in purine and pyrimidine metabolism may also be affected. To check this possibility, the level of three essential ecdysteroids in *Drosophila*, namely 20-hydroxyecdysone, α-ecdysone, and Makisterone A in CS and OR were examined (Figure 3-6). Of note, the levels of ecdysteroids in OR were significantly higher than in CS, especially during the early stage of the pupal period.

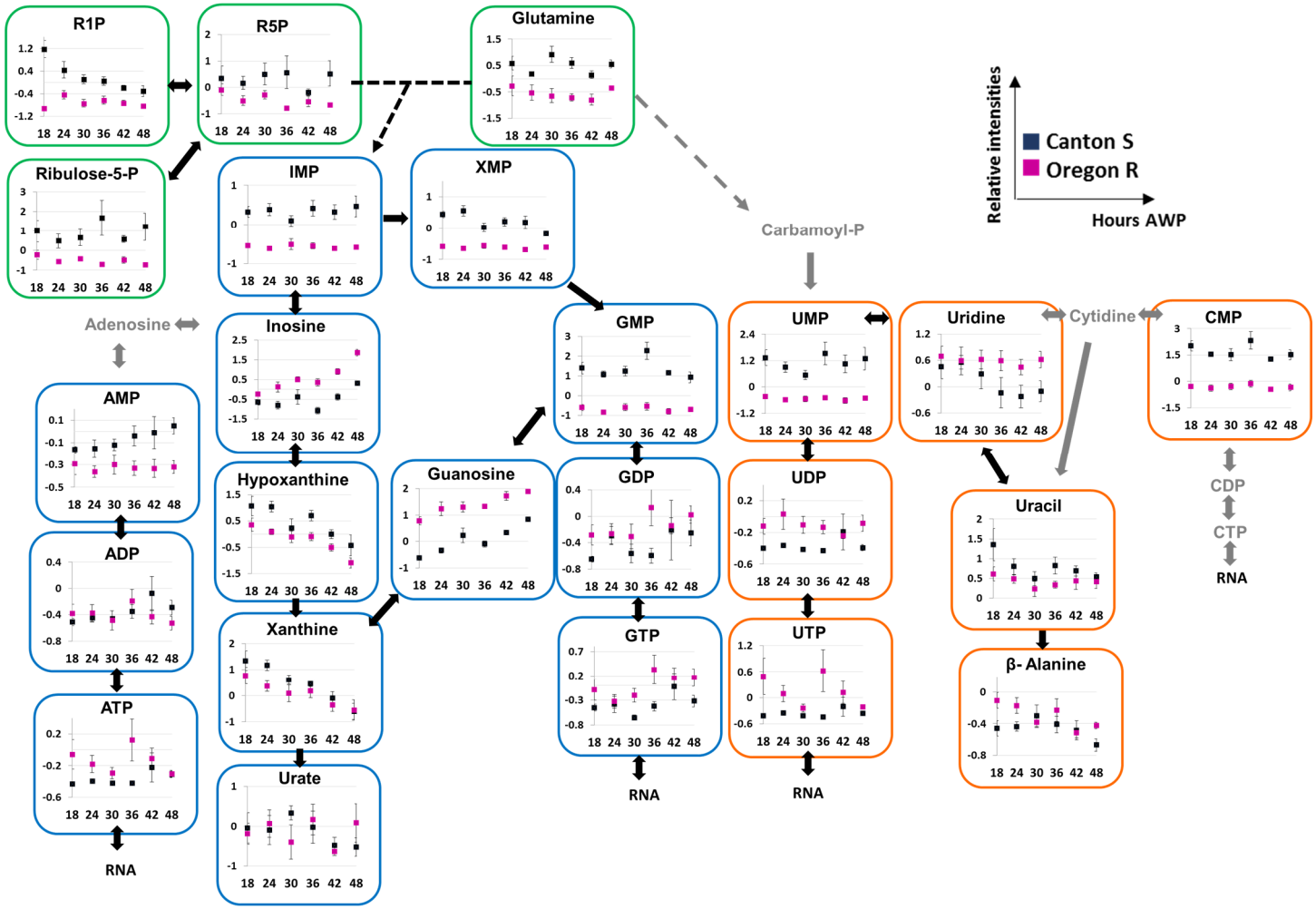

Figure 3-6: Purine and pyrimidine metabolism in CS and OR. Pathway overview for the data from 18 to 48 h AWP. The x-axis represents the relative intensity of the metabolites. The y-axis represents the h AWP. Blue box: metabolites in purine metabolism. Yellow box: metabolites in pyrimidine metabolism. Green box: metabolites related to both pathways.

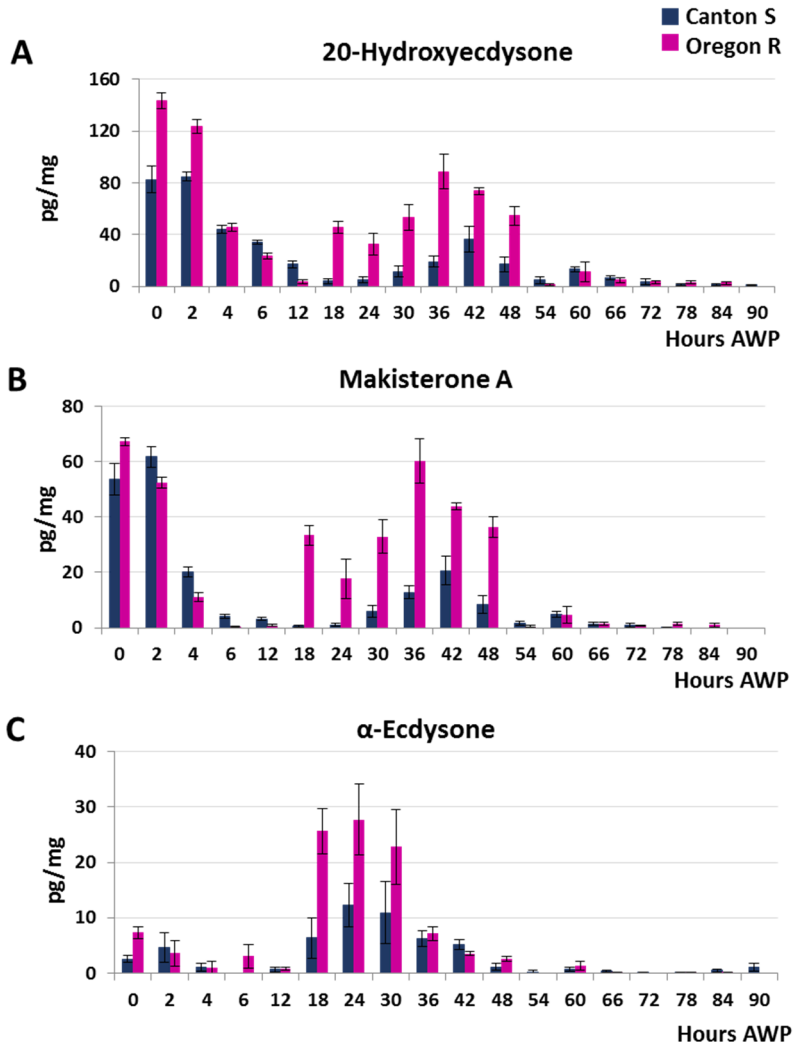

Figure 3-7: Purine and pyrimidine metabolism in CS and OR. The levels of three ecdysteroids in CS and OR during metamorphosis. **(A)** 20-hydroxyecdysone, **(B)** α-ecdysone, and **(C)** Makisterone A

Next, the levels of the important energy sources in *Drosophila* (total proteins, triacylglycerol, and trehalose) and the final products of purine and pyrimidine catabolism (urea, uric acids, and β-alanine) between CS and OR were examined (Figure 3-8). Because no significant differences in their abundances has been found between these two strains throughout metamorphosis, the variances in purine and pyrimidine metabolism were probably not due to degradation process of to generate energy. At the point of metamorphosis, besides the tissues triggered to undergo cell death, many tissues undergo cell proliferation, differentiation, and organogenesis to give rise to the adult structures. Thus, one possibility for

the difference in the observed metabolites in purine and pyrimidine metabolism was that CS and OR had different RNA transcriptional rates.

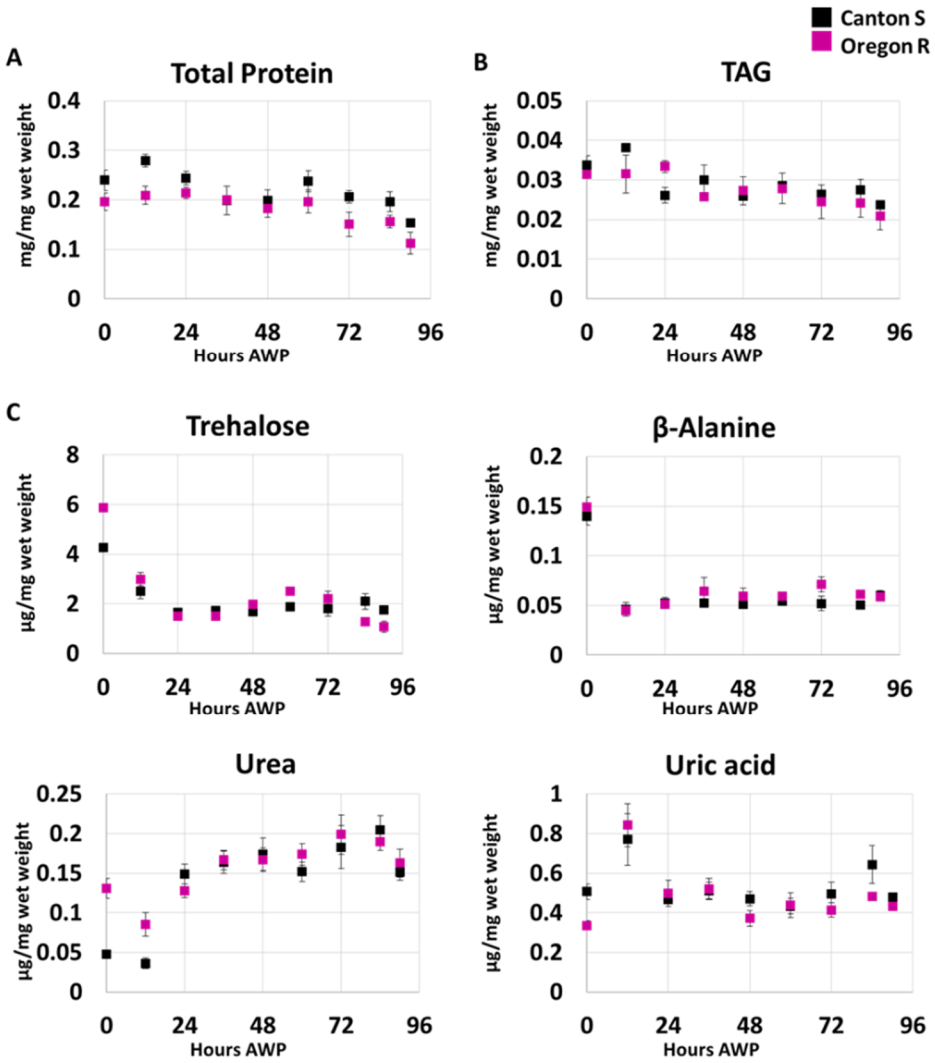

Figure 3-8: Quantification data. The total level of **(A)** protein and **(B)** TAG were examined using bioassay. **(C)** The abundances of trehalose, β-alanine, urea and uric acid were measured using GC-MS. No significant differences was detected between CS and OR especially from 18 to 48 h AWP in all cases.

In summary, even though the overall metabolic profiles were very similar in CS and OR, there were still differences in purine and pyrimidine metabolism at the early pupal stage, which could be the result of differences in ecdysteroid levels at the same time points but were not likely to be related to metabolite catabolism to generate energy. Ecdysteroids control both the programmed cell death and cell reconstruction during metamorphosis, so it would be interesting to investigate further the mechanism of this phenomenon.

3.4. Conclusion

In the current study, non-targeted GC/MS-based and targeted LC/MS-based metabolic profiling methods were used to investigate the effect of genetic backgrounds and temperatures on the metabolism of *Drosophila* during metamorphosis. With these platforms, a strong correlation between metabolic profiles and the development of *Drosophila* pupae was discovered. This tight connection was observed in the consistent metabolic profiles at each metamorphic stage among different wild-type strains or temperatures. On the other hand, the coincidence of changes in pyrimidine/purine metabolism and ecdysteroid levels draw new attention to the way insect hormones maintain metabolism during metamorphosis. The findings in this study also supported the experimental design for further metabolomics studies, where the temperature and genetic background of transgenic strains might directly affect the experimental results.

Chapter 4

Applying metabolome analysis to elucidate the role of *Drosophila* histone methyltransferase G9a

4.1. Introduction

Appropriate responses to stressful conditions are crucial for the adaptation of an organism to the environmental challenges. There are potential connections between gene regulation, nutrition and metabolism since a lot of enzymes involved in stress tolerance needs co-substrates generated by cellular metabolism [159,160]. Likewise, stress responses might cause the changes in the metabolism of an organism to support the adaptations or stress tolerances[161,162]. In essence, metabolomics study can be used as the fundamental method to assess the changes in metabolic pathways of an organism and provide the dynamics of cellular function to help an organism survive in their natural habitat [11].

In terms of a starvation stress, it was firstly reported that prenatal starvation altered the DNA methylation marks on imprinted gene *IGF2* and the change persisted throughout human life-span [163]. Other studies also suggested that Sirtuin 1, a histone deacetylase, plays a role in response to starvation stress in both yeast [164] and *Drosophila* [165]. However, except for Sirtuin 1, it has not been fully studied yet which epigenetic factors are critical in response to starvation stress. Recently, histone methyltransferase G9a was reported to mediate autophagy by regulating the expression of autophagy related genes including *LC3B*, *WIPI* and *DOR* in starved human pancreatic cancer cells [92]. Since autophagy is an intracellular degradation system that responds to starvation, the signaling pathways mediating starvation-induced autophagy have been identified in detail [166]. However, the gene regulation of the components in these signaling pathways has not been fully studied *in vivo*.

G9a was first reported in 2001 as a mammalian histone lysine methyltransferase accounted for the methylation at lysine K9 and K27 of histone H3 *in vitro*[167]. In the last decade, the epigenetic regulation of gene expression via post-translational modifications of G9a in diverse biological processes has been a rapidly growing research subject. G9a can specifically associate with euchromatin and catalyze mono-, di-, and trimethylation reactions on H3K9; thus, involves in the transcriptional gene silencing [168-171]. This function of G9a has been proven to be important for early embryogenesis [172-175], cell survival under hypoxic stress [176], the propagation of imprints [177] and control of DNA methylation [178,179]. Besides the regulation of gene expression via histone, G9a has also been found to be able to methylate many proteins including automethylation [180] not at histone residues. Even the full mechanism of these processes are not fully understood, the non-histone methylation of G9a can either activate or inhibit the gene expression [181-185].

Nowadays, G9a has attracted more attention due to its role in the promotion of tumorigenesis. High expression level of G9a has been observed in variety of human cancer cells such as prostate [186], leukemia [183], lung [187], breast [188] and aggressive ovarian carcinoma [189]. Pharmaceutically or genetically inhibition of G9a in cancer cells can significantly affect the cell proliferation by triggering cell cycle arrest, inducing apoptosis or activating autophagic cell death [92,190-193]. Thus, a better understanding on the functions of G9a is very important to develop potential cancer treatment especially for the aggressive metastatic subtypes for which no current treatments is efficient. However, most of G9a studies were established on cell lines rather than on model organisms. The common G9a models are rodent and *Drosophila melanogaster*. As the loss of G9a causes the embryonic lethal phenotype in mouse, rodent model is usually used to study the role of G9a locally while most of the G9a whole body knockdown or null mutant studies were performed using *Drosophila*. Moreover, even when the G9a knockdown or null mutant were used, most of the experiments were screen under

laboratory optimum condition [194,195], which prevent the stress responses of G9a. Therefore, the experiments performed under different environmental conditions will play a central role in assessing the functions of G9a.

Here, in order to achieve a better understanding on the roles of G9a, the flies lack of dG9a, a homolog of G9a in *Drosophila,* were exposed to various stress conditions. The dG9a-depleted *Drosophila* were only sensitive to the starvation but not heat stress or oxidative stress. To explain this phenomena, the global metabolic profiling of fasted wild type and dG9a-depleted flies has been constructed to explore the metabolic changes occur when dG9a is removed. The major changes in cellular metabolites account for the energy generation under nutrient stress was observed in dG9a-depleted flies. Interestingly, further investigation showed that the loss of dG9a leads to the inactivation of autophagy during starvation, which is totally opposite with the behavior of G9a in cancer cells.

4.2. Materials and methods

4.2.1. Fly stocks

All the fly stocks were reared at 25°C on standard food (0.7% agar, 10% glucose, 4% dry yeast, 5% cornmeal, 3% rice bran). CS, obtained from Bloomington Drosophila Stock Center (USA), was used as wild type were. $dG9a^{RG5}$ flies were kindly provided by Dr. P. Spierer (University of Geneva, Switzerland). $dG9a^{RG5}$ flies were backcrossed 10 times with CS to adjust the genetic background to CS.

4.2.2. Starvation assay

For starvation assay, 3-5 days old adult flies were placed into vials with a piece of paper soaked 1.0 mL phosphate-buffered saline (PBS) and the number of living flies were monitored until all had died. All the assays were performed under non-crowded conditions (20 flies per vial). Median life spans were calculated and graphs were generated with GraphPad Prism 6 (Graphpad Software).

In rescue assay with glucose, 1% and 10% glucose was resolved into PBS in vials.

4.2.3. Stress assays

In oxidative stress assay, newly eclosed adult flies were transferred on instant food Formula 4-24® (Carolina, USA) with 10mM paraquat (Nacalai, Japan). Every 3 days, they were transferred to new vials containing the fresh instant food and the number of living flies was monitored until all were dead. In heat stress assay, 3-5 days old adult flies in vials containing the fresh instant food were placed into the temperature controlled incubator at 36°C and the number of living flies were monitored until all were dead. All the assays were performed under non-crowded conditions (20 flies per vial).

4.2.4. GC-MS and LC-MS analysis

Same as in section 2.1.3. and 2.1.4.

4.2.5. Data analysis for metabolic profiling

Same as in section 2.1.5.

4.2.6. Measurement of glycogen and TAG

Same as in section 3.2.6.

4.2.7. Western immunoblot analysis

Fifteen adult flies were homogenized in 100 μL 2x sodium dodecyl sulfate (SDS) sample buffer (2% SDS, 10% glycerol, 0.002% bromophenol blue, 0.063 M Tris-HCl) and heated at 95 ˚C for 2 mins and centrifuged at 15,000 x g for 10 mins at 4 ˚C. 5 μL of supernatants were fractionated by 15% Sodium Dodecyl Sulfate- Polyacrylamide Gel Electrophoresis (SDS-PAGE) and transferred to polyvinylidene difluoride (PVDF) membranes (Biorad, Japan). The membranes were blocked with 0.3% dry milk in Tris-buffered saline containing Tween 20 (TBS-T) (137 mM NaCl, 2.7 mM KCl, 25 mM Tris-HCl, 0.1% Tween 20, pH 7.6) and incubated with anti-Atg8a antibody (1:1000, Cell Signaling, USA) or anti-α-tubulin antibody (1:10000, DSHB, USA) at 4 ˚C for 16 h. Membranes were washed with TBS-T and incubated with HRP-conjugated anti-rabbit or mouse IgGs (Thermo Scientific, USA) for 60 min. After washing membranes with TBS-T, visualization was performed with ECL-select (GE Healthcare, Japan). Signal intensity measurement was performed with CS analyzer (ATTO, Japan).

4.2.8. Reverse transcription-quantitative PCR (RT-qPCR)

RNAs were isolated using Trizol® reagent (Invitrogen, USA) from adult whole bodies. cDNA was synthesized using PrimeScript RT reagent kit (TaKaRa, Japan) according to the manufacturer's instructions. qPCR was carried out with SYBR® Premix Ex Taq™ II (TaKaRa, Japan) using CFX96 touch™ Real-time PCR Detection System (Biorad, Japan), and the data were analyzed with ΔΔCt method. *β-tubulin* is used for internal control. Primer sequences of

examined genes are listed below.

β-tubulin forward 5’-ATACGGTGACCTGAACCATC-3’
β-tubulin reverse 5’-TACTCGGACACCAGATCG-3’
CG6262 forward 5’-GGATCGGGTACACAGCTATTC-3’
CG6262 reverse 5’-CGGGAACGAGAAGGTGAAA-3’
G6P forward 5’-CTGGGAAGTTACCTGGGAATTAG-3’
G6P reverse 5’-AAACAGCTGAGACCGCATAG-3’
HEXA forward 5’-GGATCGGGTACACAGCTATTC-3’
HEXA reverse 5’-CGGGAACGAGAAGGTGAAA-3’
Pgi forward 5’-TCGAGAAGAATGCTCCTGTTATC-3’
Pgi reverse 5’-GCAAGTACTGATCGTAGGGAAG-3’
fbp forward 5’-GCCGGAGAAGGGAAAGATATAC-3’
fbp reverse 5’- TCTTGGCCGCAATGTAGTT-3’
Gapdh1 forward 5’-ATGTCTCCGTTGTGGATCTTAC-3’
Gapdh1 reverse 5’-CCTCGACCTTAGCCTTGATTT-3’
Pgk forward 5’-GCTGAACAAGGAGCTGAAGTA-3’
Pgk reverse 5’-TCTCAATCAGCTGGATCTTGTC-3’
Atg8a forward 5’-TACCAGGAACATCACGAGGA-3’
Atg8a reverse 5’-CGACCGGAGCAAAGTTAGTTA-3’

4.3. Results

4.3.1. dG9a^{RG5} null mutant flies are sensitive to starvation

In previous studies, knockdown dG9a using RNA interference (RNAi) showed lethal phenotype at *Drosophila* larvae and pupae[194,196], which was consistent with previous studies on mammalian about the importance of G9a. However, other studies using dG9a null mutant strain (*dG9a^{RG5}*) showed that dG9a was not essential for *Drosophila* viability or fertility [195]. Therefore, in order to investigate the roles of dG9a, the adult CS and *dG9a^{RG5}* null mutant strain were examined under several challenging environmental conditions including heat exposure, oxidative stress and starvation.

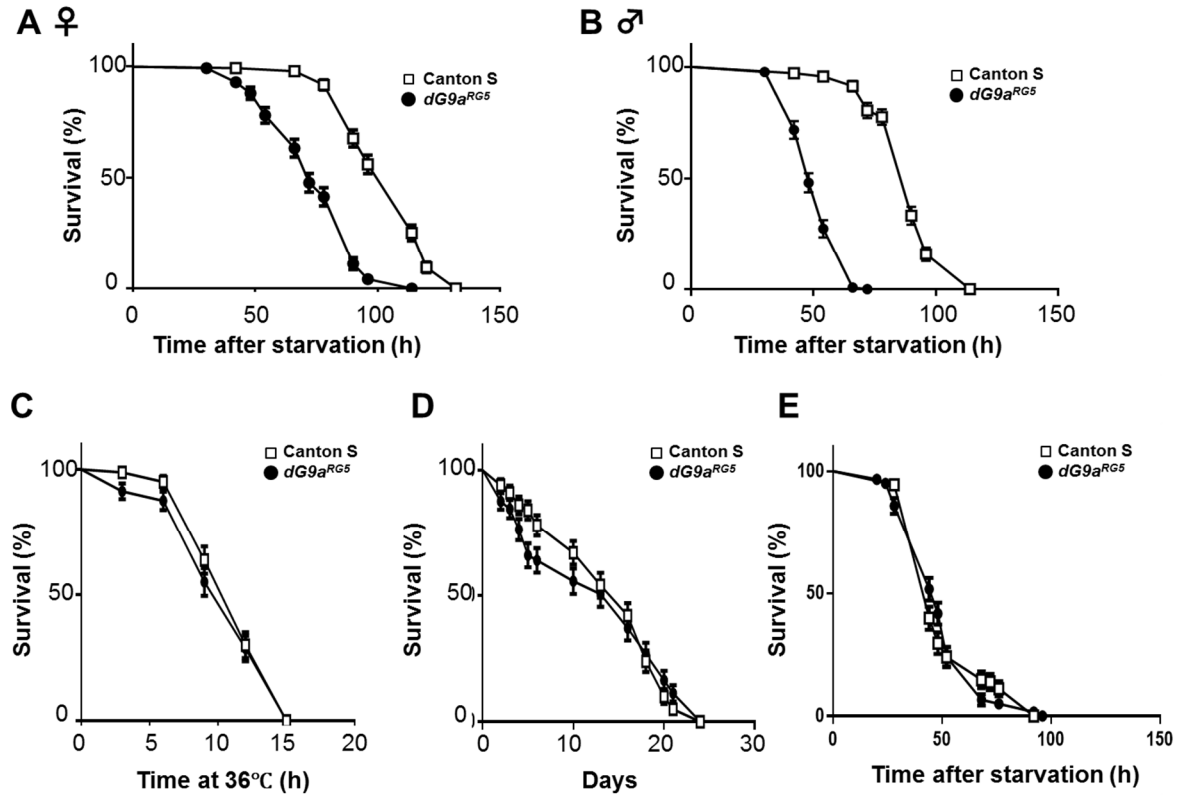

Figure 4-1. dG9a is critical for survival under starvation stress. (A) The result of viability assay under starvation condition using females of wild type (CS) (n=153) and dG9a null mutant (*dG9a^{RG5}*) (n=135). P <0.0001**. (B)** The result of viability assay under starvation condition using males of wild type (n=131) and dG9a null mutant (*dG9a^{RG5}*) (n=138). P <0.0001. **(C)** The result of viability assay under heat stress using males of wild type (n=80) and dG9a null mutant (*dG9a^{RG5}*) (n=80). P =0.41. **(D)** The result of viability assay under oxidative stress using males of wild type (n=100) and dG9a null mutant (*dG9a^{RG5}*) (n=97). P =0.80. **(E)** The result of viability assay under starvation conditions using larvae of wild type and *dG9a^{RG5}* mutant (n=120). *P* >0.05.

Interestingly, *dG9a*^{RG5} mutant flies were exclusively sensitive to the fasting condition but not heat stress or oxidative stress (Figure 4-1A-D). For starving assay, the flies were kept on standard food for 48 h after hatching and then placed on a diet consisting only of PBS in order to maintain hydration. After 24 h of fasting, a statistically significant decrease in animal viability in *dG9a*^{RG5} null mutant strain and a severer effect was observed in male than in female flies carrying *dG9a*^{RG5} null mutant (Figure 4-1A, B). The starving assay was also performed at larval stages; however, no significant decreases in animal viability was observed (Figure 4-1E). These results suggest that dG9a played an important role in maintaining the persistence of adult fly during nutrient stress condition.

4.3.2. *The differences between CS and dG9a*^{RG5} *flies under starvation can be explained by the composition of metabolome*

To obtain a general perspective on the changes due to the reduction of dG9a, metabolic profiling of fasted CS and *dG9a*^{RG5} was performed by employing the developed metabolomics approaches to focus on the central metabolic pathways. Only unmated male flies were used and the samples were collected after 0, 12, 24, 36 and 48 h of fasting.

First, HCA was constructed to provide the global view of the metabolic state of both fasted control and *dG9a* null mutant flies (Figure 4-2A). In this study, the similarity between two objects was obtained without losing the generality based on the Euclidean distance. From the horizontal axis of HCA result, two strains shared similar metabolic profiles before starvation (at 0 h); they therefore were grouped in the same grey cluster. However, during starvation, the expression patterns of metabolites were varied between two strains resulting in the separation of CS and *dG9a*^{RG5} into two different clusters, blue and orange, respectively (Figure 4-2A). This separation could be explained by the two main clusters of metabolites where the levels of metabolites in upper cluster (yellow) were lower in *dG9a*^{RG5} than in CS and vice versa for the lower cluster (green).

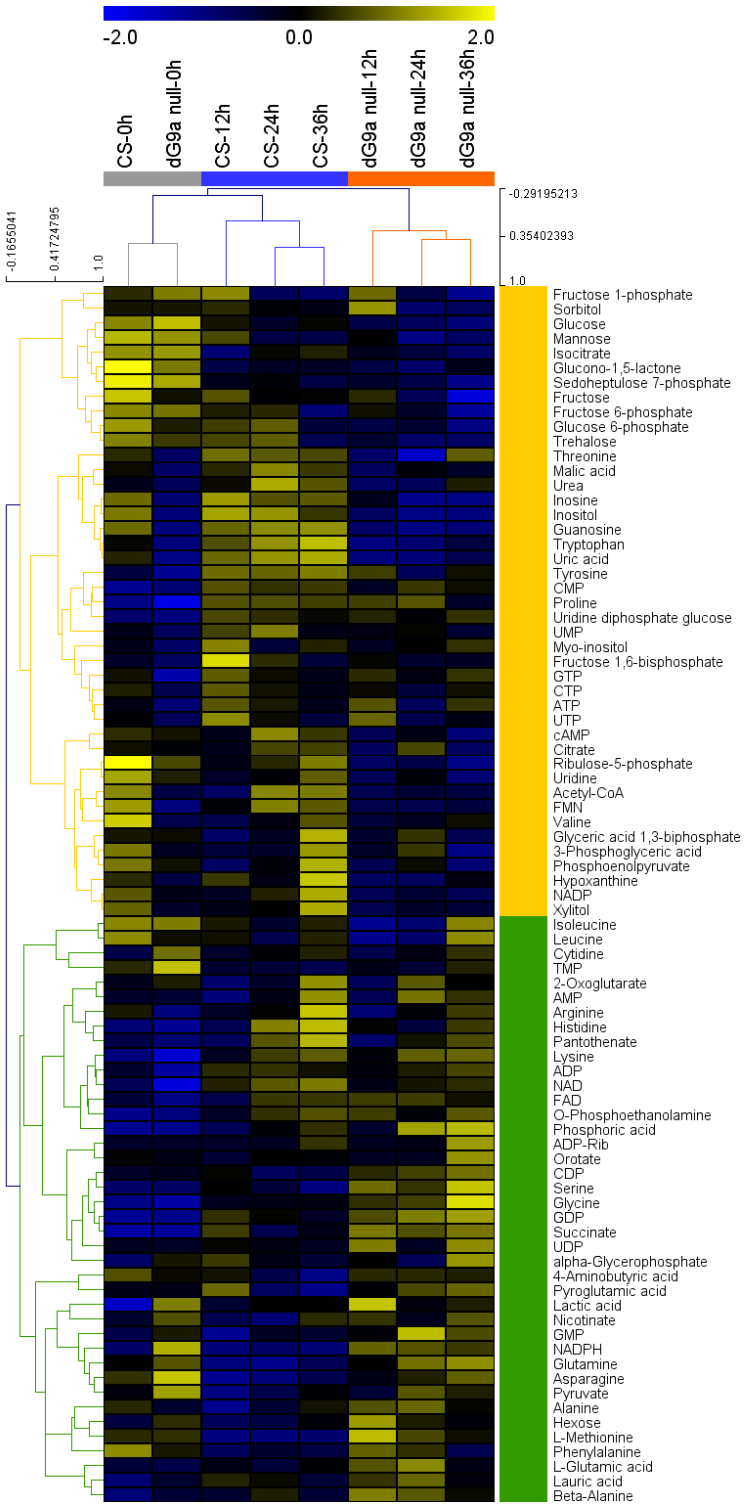

Figure 4-2: Comparison of the metabolic profiles between wild type and *dG9a^{RG5}* mutant flies under starvation using HCA. HCA data showing the changes in cellular metabolites of both wild type and *dG9a^{RG5}* mutant flies under starvation; the color scale is plotted on the top of the figure. Before starvation, both genotypes shared similar profiles and were grouped into one cluster (grey). During starvation, fly with each genotype showed different profiles and were discriminated hierarchically into two clusters, wild type (blue) and *dG9a^{RG5}* mutant (red).

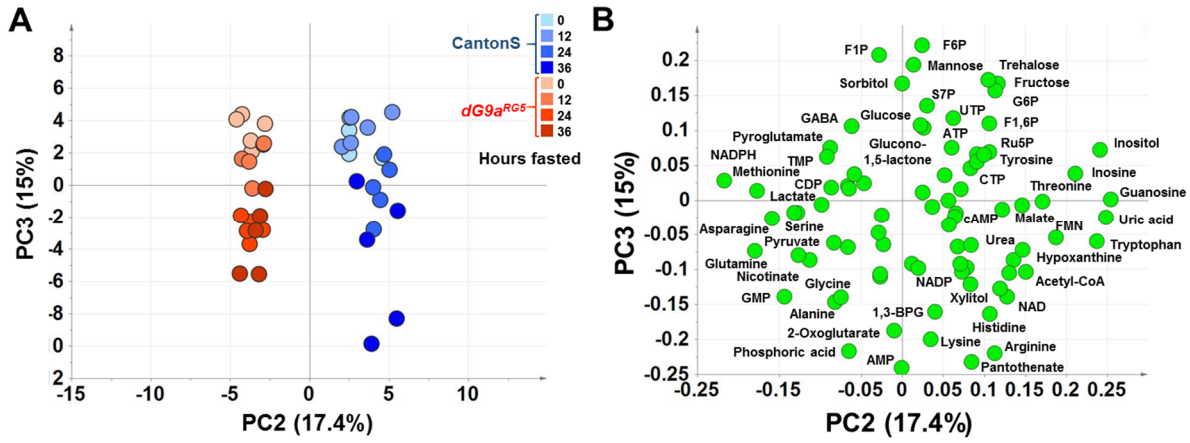

Figure 4-3: Comparison of the metabolic profiles between wild type and *dG9a*^{RG5} mutant flies under starvation using PCA. PCA score plot **(A)** constructed by PC2 (17.4%) and PC3 (15%) shows the discriminations in genotypes and in various time points under starvation. This discrimination is explained by the composition of metabolites on loading plot **(B).** 4-5 replications for each time point.

Then, the whole data set was utilized to perform PCA, an unsupervised analysis, to explore the data based on sample variance. The clustering of the biological replicates for each sample was clearly observed, suggesting overall good quality of the IP-LC-MS/MS and GC-MS analysis (Figure 4-3). Moreover, the differences in genotypes and in various time points under starvation were explained by 17.4% and 15% variances in PC2 and PC3, respectively. The PCA score plot formed by PC1 and PC2 is showed in Figure S4-1. Together, these results suggested that significant metabolic changes were observed and genetic diversity more strongly influenced the data separation than time perturbation under starvation.

In summary, the high agreement from HCA and PCA results shows that the composition of metabolome can be used to explore the metabolic changes occur when dG9a is depleted.

4.3.3. *Fasted dG9a*^{RG5} *mutant flies have altered level of cellular metabolites*

In order to obtain the detail information regarding compounds contributing to the data separation between fasted CS and *dG9a*^{RG5}, the data was then subjected to a supervised discriminant analyses. From PLS-DA model with the eight different groups (CS and *dG9a*^{RG5} at four different time point), we found that the separation on the score plot showed similar

trends as HCA results (Figure 4-4A). PLS-DA model was considered valid after permutation since the R^2Y-intercepts and Q^2-interceps did not exceed 0.3-0.4 and 0.05, respectively (Figure 4-4B) [119]. These data strongly indicated that the fasted $dG9a^{RG5}$flies had altered level of cellular metabolites.

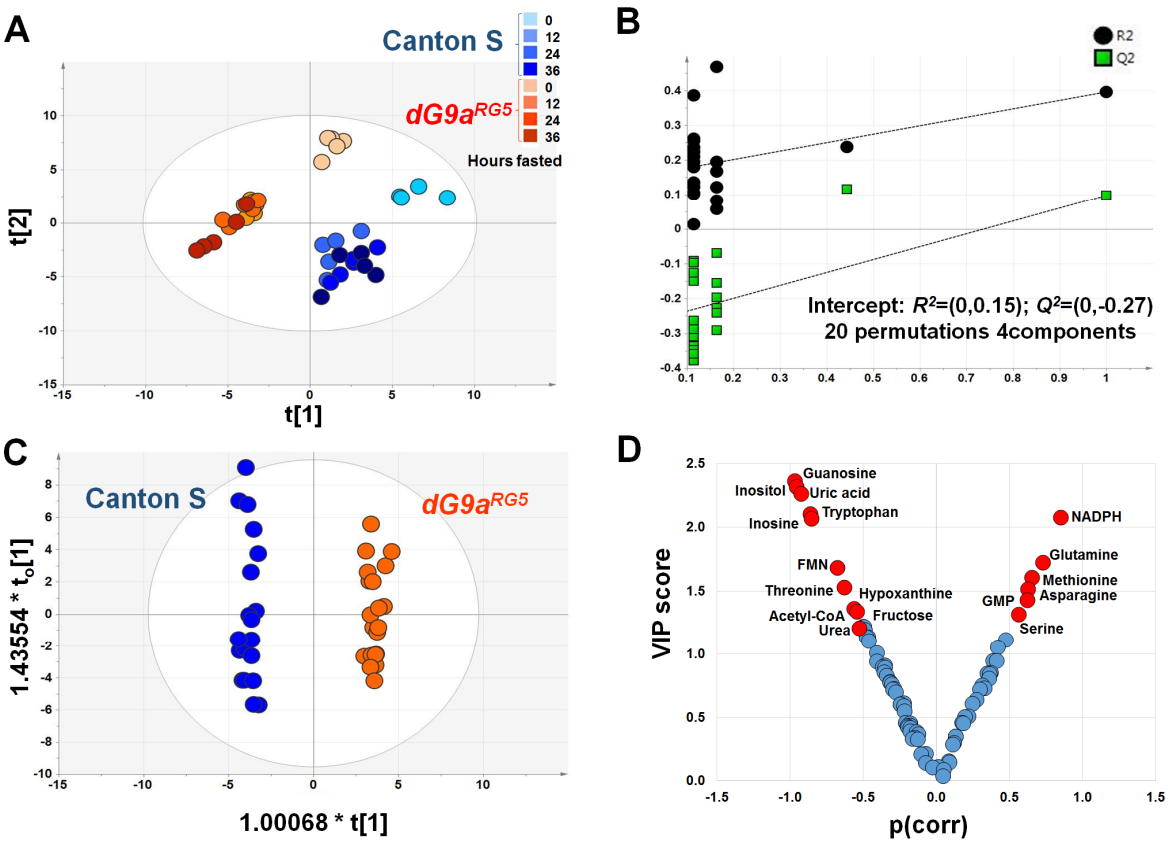

Figure 4-4: Fasted $dG9a^{RG5}$ mutant flies shows distinct metabolic profile. (A) The score plot of supervised analysis PLS-DA clustered the samples based on the genotypes. For each genotype, the samples collected before fasting clearly separated from samples collected during fasting. **(B)** Statistical validation by permutation test with 20 permutations of PLS-DA (R^2Y-intercepts = (0, 0.15); Q^2-interceps = (0,-0.27)). **(C)** OPLS-DA score plot showed the clear separation between two genotype with p(CV-ANOVA) = 1.99925E-23**. (D)** A plot formed by VIP score and p(corr) revealed from OPLS-DA. The criteria VIP > 1.0 and |p(corr)| >0.5 was used to select the potential metabolites (red) showing big changes due to the loss of dG9a.

Therefore, with the intension of maximizing the difference between two genotype and figure out the important metabolites, OPLS-DA was generated. The model was constructed with one predictive and two orthogonal components, which showed a clear separation between the groups along the predictive component (Figure 4-4C). This OPLS-DA model was then

validated with p(CV-ANOVA) far lower than 0.001. Moreover, the good quality of OPLS-DA model was designated by the R^2 and Q^2 values of 0.99 and 0.97, respectively. Together, this OPLS-DA model showed good separation between two genotype and can be used to propose the important metabolites related to the function of dG9a under fasting condition.

The criteria for cutoff point to select important metabolites were VIP > 1.0 and |p(corr)| > 0.5 from OPLS-DA model (Figure 4-4D)[133]. An independent two way ANOVA test was used to determine whether the candidates obtained from OPLS-DA were significantly different or not.

4.3.4. *The loss of dG9a causes major changes in amino acid metabolism*

From the revealed candidates, many metabolites showing big changes due to the loss of dG9a belonged to amino acid metabolism. Consistent to mammalian, 20 amino acids found in protein of *Drosophila* can also be classified into essential and non-essential amino acids [197]. Interestingly, the level of many essential amino acids in dG9a-depleted flies were lower than in wild type during the whole 36 h of fasting (Figure 4-4D and Figure 4-5).

The expression levels of tryptophan, threonine, arginine, histidine and valine showed significant differences between fasted CS and $dG9a^{RG5}$ with *p*-value for genotype less than 0.05 in two-way ANOVA test (Figure 4-5A). As there was no nutrient supplement during fasting, the only source for free essential amino acids is from protein degradation process. The level of non-essential amino acids do not reflect the actual rate of proteolysis, since they can be synthesized or derived from essential amino acids. Moreover, the expression level of uric acid and urea, the waste product of amino acid and nitrogen metabolisms, increased overtime and significantly higher in CS than in $dG9a^{RG5}$ (Figure 4-5C). Thus, these results suggested that comparing to wild type strain, dG9a-depleted flies could not maintain an appropriate protein degradation rate, an essential process to recycle amino acids for translation or energy

generation under fasting. On the other hand, the levels of asparagine, glutamine and methionine were significantly higher in dG9a-depleted flies (Figure 4-5A,B). These amino acids were reported to be the inhibitors of the autophagic pathway of protein degradation in isolated hepatocytes [198]. Especially, the high level of L-glutamine was described to be important for the activation of the target of rapamycin (TOR) pathway, which suppressed autophagy [199].

Altogether, these data raise a hypothesis that the loss of dG9a affects the ability to recycle amino acids via protein degradation in starvation-induced autophagic pathways, which could be the reason why they had lower viability than wild type strain throughout starvation.

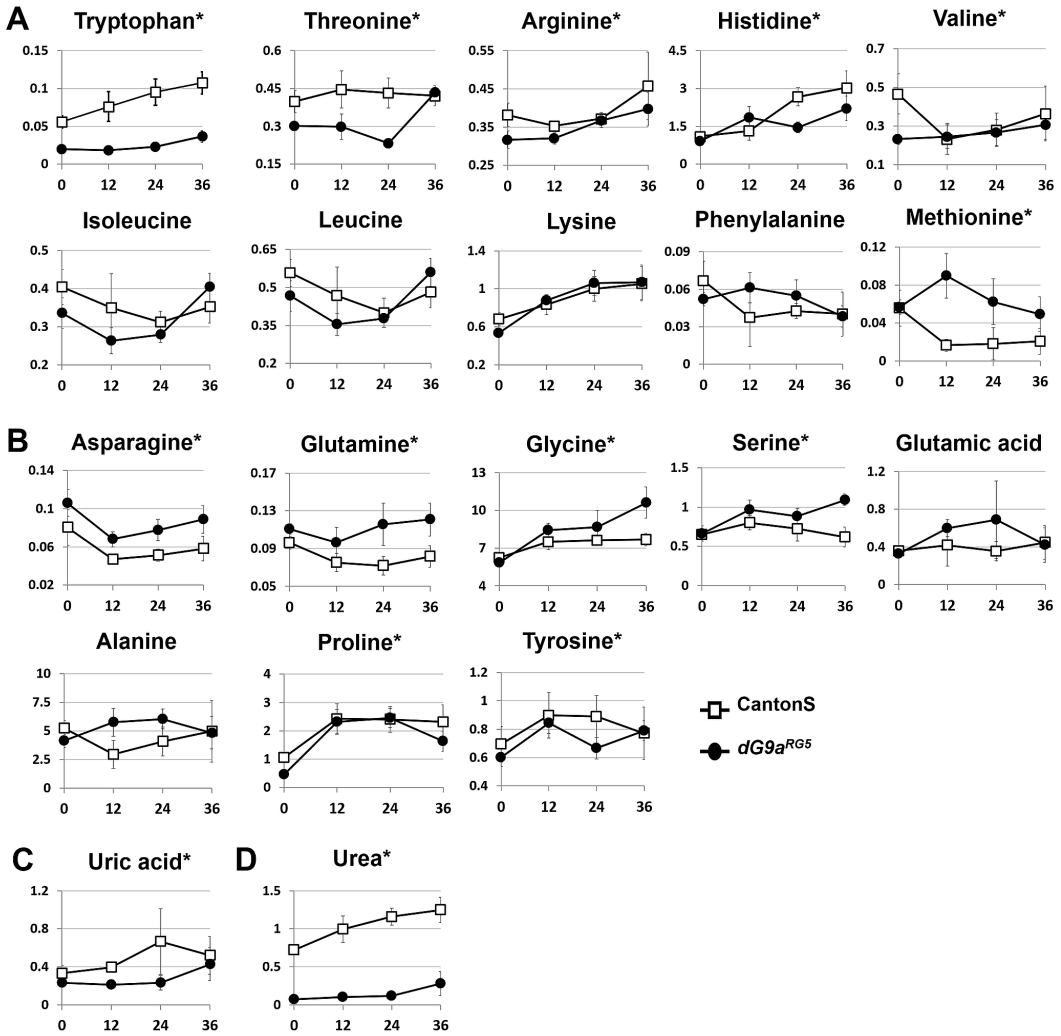

Figure 4-5: Amino acid metabolism. The general view of the detected metabolites belong to amino acid including: **(A)** Essential amino acids **(B)** Non-essential amino acids **(C)** Uric acid **(D)** Urea. 4-5 replications for each time point. *The metabolites show significantly different between wild type and dG9a^{RG5} mutant in two-way ANOVA test with P <0.05.

4.3.5. *dG9a has an important role in maintaining the energy reservoirs by controlling the starvation-induced autophagy*

The responses of cells to nutrient deprivation via autophagy is a nonselective process of bulk cytoplasmic degradation [200,201]. Hence, if this hypothesis is correct, the changes will also appear in the metabolites related to lipid and carbohydrate sources. In *Drosophila*, TAG and glycogen are the main primary forms of energy sources stored in the fat body, analogous to the mammalian liver and white adipose tissue. In response to energy needs of the body, trehalose will be synthesized in the fat body, excreted to hemolymph and utilized to produce glucose [202].

As predicted, the amount of TAG and glycogen in dG9a-depleted flies were significantly lower from 12 fasted hour (Figure 4-6A, B). From the GC-MS data, trehalose also showed a significantly lower level in $dG9a^{RG5}$ ($p = 0.01$); however, it was not in the case of glucose (Figure 4-6C, D). Additionally, when the level metabolites together with the mRNA levels of enzymes related to glycolysis were checked, not a big difference was observed between two genotypes (Figure 4-7). Taken together, these results suggested that the loss of dG9a did not affect the ability to generate energy via glycolysis but the capability to conserve the energy sources, which lead to the weak tolerance under nutrient stress.

To validate this hypothesis, the glucose supplement was utilized to rescue the viability of dG9a-depleted flies. After hatching, adult flies of both CS and $dG9a^{RG5}$ were kept on standard food for 48h and then shifted to either PBS or 1% and 10% glucose in PBS. As predicted, the additional of glucose completely rescued the sensitivity of dG9a-depleted flies and helped them achieve the similar viability as the wild type CS (Figure 4-6E). This result confirmed that dG9a had an important role in maintaining not only amino acid catabolism but also the overall energy reservoirs, which would be use to generate glucose for the body during starvation.

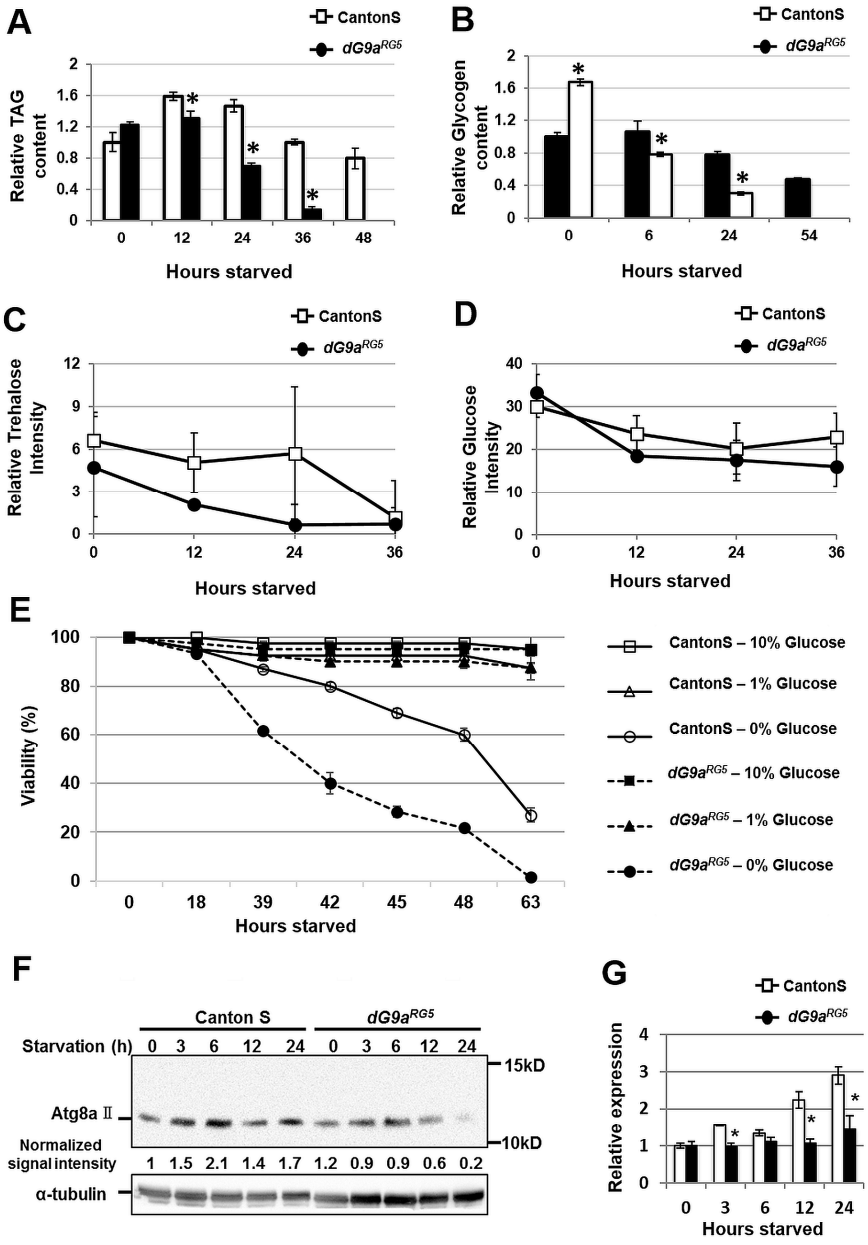

Figure 4-6: The loss of dG9a affect the energy homeostasis in *Drosophila* during fasting. (A) Relative level of TAG in wild type and $dG9a^{RG5}$ mutant under starvation stress. n=3. *P <0.05. **(B)** Relative level of glycogen in wild type and $dG9a^{RG5}$ mutant under starvation stress. n=5. *P <0.05. The level of trehalose **(C)** and glucose **(D)** from GC-MS analysis. Only the level of trehalose showed significantly "genotype" between wild type and $dG9a^{RG5}$ mutant in two-way ANOVA test with p = 9.17E-03. **(E)** The results of viability assay with glucose supply (n=40). When the $dG9a^{RG5}$ mutant was fed with 1% and 10% glucose in PBS, they recovered their sensitivity and had similar viability as wild type. **(F)** Western blot analysis of extracts from starved wild type and $dG9a^{RG5}$ mutant. The blots were probed with anti-Atg8a and anti-α-tubulin antibodies. The signal intensity normalized with that of α-tubulin is shown. **(G)** Quantification of mRNA levels by RT-qPCR analysis of *Atg8a* in starved wild type and $dG9a^{RG5}$ mutant. Results were normalized to α-tubulin and are displayed as relative values for that of 0 h starved wild type. n=3. *P < 0.05.

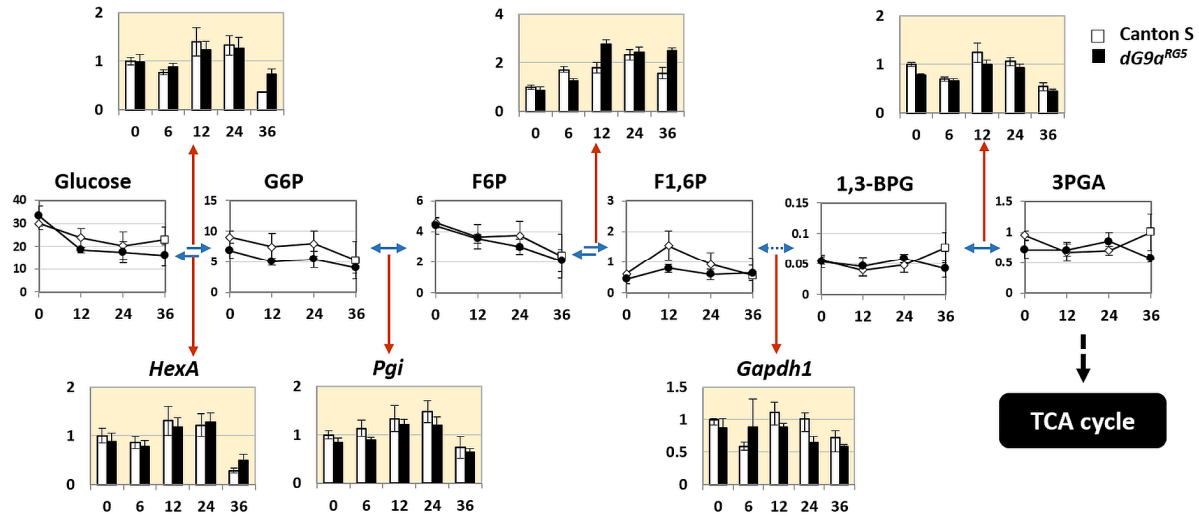

Figure 4-7: Glycolysis pathway of wild type and *dG9a*^{RG5} mutant flies during fasting. The line graphs showing the changes of metabolites. 4-5 replications for each time point. The bar graphs showing the mRNA level of enzymes related to glycolysis.

For further understanding in the mechanism underlying the role of dG9a in nutrient stress tolerance, the level of Atg8a-II, belong to Atg8 family were examined and can be used as a marker for autophagy [203]. Western immunoblot analysis were performed with protein extracts from the whole bodies of CS and *dG9a*^{RG5} at 0, 3, 6, 12 and 24 starved h. The blots were probed with anti- Atg8a-II antibody and anti-α-tubulin antibody as a loading control. After checking the intensity of detected bands, Atg8a signal in each sample was normalized to α-tubulin of the same sample to exclude the sample variances. In consistent with the results achieved from immunostaining, the level of Atg8a-II in the whole bodies of dG9a-depleted flies is lower than in CS (Figure 4-6F). Interestingly, the mRNA level of Atg8a was significantly decreased after 3, 12 and 24 h of starvation in the *dG9a*^{RG5} mutant compared with that of wild type (Figure 4-6G). These results proposed that Atg8a was under the regulation of dG9a to trigger autophagy in *Drosophila* under the nutrient stress condition.

In summary, the revealed data showed that the regulation of dG9a on gene expression was necessary for the survival of *Drosophila* under fasting by controlling the activities of autophagy to maintain the energy homeostasis.

4.4. Discussion

Previous studies revealed that G9a is important for early embryogenesis and essential for viability in mouse [172-175]. G9a is also highly conserved among various metazoans including *Drosophila*, frog (*Xenopus tropicalis*), fish (*Danio rerio*, *Tetraodon nigroviridis*, and *Takifugu rubripes*) and mammals. In *Drosophila*, although G9a is not essential for viability, the findings in this study suggest that G9a can be conserved from fly to mammals because of its importance for starvation stress tolerance to which organisms are often exposed in the wild. This is also the first indication that G9a plays an essential role in acquisition of starvation tolerance in an organism.

In order to clarify the underlying mechanism why *dG9a* null mutant is more susceptible to starvation stress, the "bottom up" approaches has been used. First, non-targeted GC-MS-based and targeted LC-MS/MS-based metabolic profiling was performed to investigate changes in metabolomes due to the loss of dG9a. Interestingly, the results from metabolic profiles showed that dG9a played important roles in maintaining the energy homeostasis, the key factor for nutrient stress tolerance. Via the autophagic process, dG9a modulated the energy reservoirs including amino acids, trehalose, glycogen and TAG levels during starvation.

The present study also indicated that dG9a controlled the starvation-induced autophagy by activation of the expression level of Atg8a. In previous studies, both histone and non-histone protein methylation by G9a have been found to be able to either activate or inhibit the gene expression [180-185]. G9a is also reported to activate gene expression as a molecular scaffold for assembly of transcriptional coactivators [204]. Therefore, additional examinations will be required to understand how dG9a regulates the expression level of Atg8a. During the development of *Drosophila*, metamorphosis is also a process that flies have to suffer starvation stress. Even though this study proves that dG9a is important for starvation stress tolerance, the viability of $dG9a^{RG5}$ mutant is not significantly decreased compared to wild type during pupal stage [195,205]. Together with these results showing that the viability of $dG9a^{RG5}$ mutant at larval

stage was not affected by fasting conditions, the function of dG9a for starvation stress is likely specific to adult stage. Since the programmed autophagy during the 3rd instar larval and pupal stage is well known to be regulated by ecdysone through PI3K pathway [206], the starvation-induced autophagy by dG9a in adult stage might be operated by other pathways.

Currently, G9a is suggested to play a positive role in the promotion of tumorigenesis of a variety of human cancer cells such as prostate [186], leukemia [183], lung [187], breast [188] and aggressive ovarian carcinoma [189]. Inhibition of G9a activity in cancer cells significantly inhibited the cell proliferation by triggering cell cycle arrest, inducing apoptosis or activating autophagic cell death [92,190-193]. Novel finding obtained by the present study on role of dG9a to acquire starvation tolerance can also make it possible to explain the positive role of G9a in the promotion of tumorigenesis. It is well known that cells inside of tumor mass are under starved conditions, since nutrients are not fully supplied to these cell [207,208]. In order to overcome the starvation stress, autophagy is induced in these inside cells [207,208]. G9a therefore very likely plays a role in acquisition of starvation tolerance for cells in tumor mass. Notably, in the present study, the loss of dG9a led to the inactivation of starvation-induced autophagy due to the decrease of Atg8a level. In contrast, previous study in cancer cells showed that the loss of G9a during starvation activated the transcription of LC3B (Atg8a ortholog in mammal) and triggered autophagy [92]. Together, these results suggest that the gene regulation of G9a depends on the cell/tissue types.

Chapter 5

Conclusions and perspectives

This is the first report demonstrated comprehensive methods using non-targeted GC/MS-based and targeted LC/MS-based metabolic profiling to investigate the changes of central metabolic pathways throughout *Drosophila* lifecycle. The combination between these high throughput approaches and detailed time course sampling methods provided a deeper insight and higher precision of the metabolic state during the development of *Drosophila*. Each metabolite has a distinct expression pattern during the development of the *Drosophila*, which may reflect the biological changes in the cell. The data obtained from this study serves as the database for the central metabolic pathways of *Drosophila melanogaster*.

A strong correlation between metabolic profiles and the development of *Drosophila* was discovered. This tight connection was further observed in the consistent metabolic profiles at each metamorphic stage among different wild-type strains or temperatures. The coincidence of changes in pyrimidine/purine metabolism and ecdysteroid levels draws new attention to the way insect hormones maintain metabolism. The findings in this study supported the experimental design for further metabolomics study, where the temperature and genetic background of transgenic strains might directly affect the experimental results.

The developed metabolomic approaches were successfully applied to investigate the roles of *Drosophila* histone methyltransferase G9a (dG9a). In face of adverse environmental conditions, the dG9a-depleted flies were only sensitive to starvation stress. Metabolome analysis revealed that dG9a played a critical role in maintaining the important energy reservoirs related to the central metabolic pathways. Further investigations on the mechanism showed that the depletion of dG9a repressed starvation-induced autophagy, the important progress to supply energy for the survival of an organism under fasting condition.

The data obtained from this study emphasize the strength of metabolomics to study *Drosophila*. Since the central metabolic pathways provide the precursor metabolites to all other pathways in an organism, the changes in these pathways can directly or indirectly reflex all aspects of the cells. Thus, the approaches established in this study are effective for any further investigations using the *Drosophila* model to underpin genetic and other pathophysiological manipulations. Future studies should focus on enlarging the analytical capacity in order to cover wider range of metabolic pathways in *Drosophila*. The development of metabolome libraries with sufficient resolution is therefore expected to promote the applications of metabolomics in various research fields using *Drosophila*. To fully unravel the biological networks, it is important to develop appropriate techniques that allow metabolomics data to be integrated, interpreted, and verified alongside with proteomics and transcriptomics strategies.

References

1 Kohler, R. E. *Lords of the Fly: Drosophila Genetics and the Experimental Life*. (University of Chicago Press, 1994).

2 St Johnston, D. The art and design of genetic screens: *Drosophila melanogaster*. *Nat Rev Genet* **3**, 176-188, doi:10.1038/nrg751 (2002).

3 Reeve, E. C. R. & Black, I. *Encyclopedia of genetics*. (Fitzroy Dearborn, 2001).

4 Adams, M. D. *et al.* The genome sequence of *Drosophila melanogaster*. *Science* **287**, 2185-2195 (2000).

5 Fortini, M. E., Skupski, M. P., Boguski, M. S. & Hariharan, I. K. A survey of human disease gene counterparts in the *Drosophila* genome. *J Cell Biol* **150**, F23-30 (2000).

6 Pandey, U. B. & Nichols, C. D. Human disease models in *Drosophila melanogaster* and the role of the fly in therapeutic drug discovery. *Pharmacol Rev* **63**, 411-436, doi:10.1124/pr.110.003293 (2011).

7 Friedman, R. & Hughes, A. L. Pattern and timing of gene duplication in animal genomes. *Genome Res* **11**, 1842-1847, doi:10.1101/gr.200601 (2001).

8 Drysdale, R. & Consortium, F. FlyBase : a database for the *Drosophila* research community. *Methods Mol Biol* **420**, 45-59, doi:10.1007/978-1-59745-583-1_3 (2008).

9 Initial sequencing and analysis of the human genome. *Nature* **409**, 860-921, doi:10.1038/35057062 (2001).

10 Allard, J. & Duan, C. Comparative Endocrinology of Aging and Longevity Regulation. *Front Endocrinol* **2**, 75 (2011).

11 Putri, S. P. *et al.* Current metabolomics: practical applications. *J Biosci Bioeng* **115**, 579-589, doi:10.1016/j.jbiosc.2012.12.007 (2013).

12 Fiehn, O. Metabolomics--the link between genotypes and phenotypes. *Plant Mol Biol* **48**, 155-171 (2002).

13 Silva, L. P. & Northen, T. R. Exometabolomics and MSI: deconstructing how cells interact to transform their small molecule environment. *Curr Opin Biotechnol* **34**, 209-216, doi:10.1016/j.copbio.2015.03.015 (2015).

14 Stringer, K. A. *et al.* Whole Blood Reveals More Metabolic Detail of the Human Metabolome than Serum as Measured by 1H-NMR Spectroscopy: Implications for Sepsis Metabolomics. *Shock* **44**, 200-208, doi:10.1097/SHK.0000000000000406 (2015).

15 Overmyer, K. A., Thonusin, C., Qi, N. R., Burant, C. F. & Evans, C. R. Impact of anesthesia and euthanasia on metabolomics of mammalian tissues: studies in a C57BL/6J mouse model. *PLoS One* **10**, e0117232, doi:10.1371/journal.pone.0117232 (2015).

16 Dunn, W. B., Wilson, I. D., Nicholls, A. W. & Broadhurst, D. The importance of

experimental design and QC samples in large-scale and MS-driven untargeted metabolomic studies of humans. *Bioanalysis* **4**, 2249-2264, doi:10.4155/bio.12.204 (2012).

17 Alonso, A., Marsal, S. & Julià, A. Analytical methods in untargeted metabolomics: state of the art in 2015. *Front Bioeng Biotechnol* **3**, 23, doi:10.3389/fbioe.2015.00023 (2015).

18 Bothwell, J. H. & Griffin, J. L. An introduction to biological nuclear magnetic resonance spectroscopy. *Biol Rev Camb Philos Soc* **86**, 493-510, doi:10.1111/j.1469-185X.2010.00157.x (2011).

19 Reo, N. V. NMR-based metabolomics. *Drug Chem Toxicol* **25**, 375-382, doi:10.1081/DCT-120014789 (2002).

20 Milne, S. B., Mathews, T. P., Myers, D. S., Ivanova, P. T. & Brown, H. A. Sum of the parts: mass spectrometry-based metabolomics. *Biochemistry* **52**, 3829-3840, doi:10.1021/bi400060e (2013).

21 Emwas, A.-H. M., Salek, R. M., Griffin, J. L. & Merzaban, J. NMR-based metabolomics in human disease diagnosis: applications, limitations, and recommendations. *Metabolomics* **9**, 1048-1072, doi:10.1007/s11306-013-0524-y (2013).

22 Madsen, R., Lundstedt, T. & Trygg, J. Chemometrics in metabolomics--a review in human disease diagnosis. *Anal Chim Acta* **659**, 23-33, doi:10.1016/j.aca.2009.11.042 (2010).

23 Dettmer, K., Aronov, P. A. & Hammock, B. D. Mass spectrometry-based metabolomics. *Mass Spectrom Rev* **26**, 51-78, doi:10.1002/mas.20108 (2007).

24 Kanehisa, M., Goto, S., Sato, Y., Furumichi, M. & Tanabe, M. KEGG for integration and interpretation of large-scale molecular data sets. *Nucleic Acids Res* **40**, D109-114, doi:10.1093/nar/gkr988 (2012).

25 Jewison, T. *et al.* SMPDB 2.0: big improvements to the Small Molecule Pathway Database. *Nucleic Acids Res* **42**, D478-484, doi:10.1093/nar/gkt1067 (2014).

26 Ma, H. *et al.* The Edinburgh human metabolic network reconstruction and its functional analysis. *Mol Syst Biol* **3**, 135, doi:10.1038/msb4100177 (2007).

27 Kelder, T. *et al.* WikiPathways: building research communities on biological pathways. *Nucleic Acids Res* **40**, D1301-1307, doi:10.1093/nar/gkr1074 (2012).

28 Caspi, R. *et al.* The MetaCyc Database of metabolic pathways and enzymes and the BioCyc collection of Pathway/Genome Databases. *Nucleic Acids Res* **36**, D623-631, doi:10.1093/nar/gkm900 (2008).

29 Wishart, D. S. *et al.* HMDB 3.0--The Human Metabolome Database in 2013. *Nucleic Acids Res* **41**, D801-807, doi:10.1093/nar/gks1065 (2013).

30 Sud, M. *et al.* LMSD: LIPID MAPS structure database. *Nucleic Acids Res* **35**, D527-532, doi:10.1093/nar/gkl838 (2007).

31 Tautenhahn, R. *et al.* An accelerated workflow for untargeted metabolomics using the METLIN database. *Nat Biotechnol* **30**, 826-828, doi:10.1038/nbt.2348 (2012).

32 Simón-Manso, Y. *et al.* Metabolite Profiling of a NIST Standard Reference Material for Human Plasma (SRM 1950): GC-MS, LC-MS, NMR, and Clinical Laboratory Analyses, Libraries, and Web-Based Resources. *Anal Chem* **85**, 11725-11731, doi:10.1021/ac402503m (2013).

33 Babushok, V. I. *et al.* Development of a database of gas chromatographic retention properties of organic compounds. *J Chromatogr A* **1157**, 414-421, doi:10.1016/j.chroma.2007.05.044 (2007).

34 Robinette, S. L., Zhang, F., Brüschweiler-Li, L. & Brüschweiler, R. Web server based complex mixture analysis by NMR. *Anal Chem* **80**, 3606-3611, doi:10.1021/ac702530t (2008).

35 Bingol, K. *et al.* Unified and isomer-specific NMR metabolomics database for the accurate analysis of (13)C-(1)H HSQC spectra. *ACS Chem Biol* **10**, 452-459, doi:10.1021/cb5006382 (2015).

36 Bingol, K., Bruschweiler-Li, L., Li, D. W. & Brüschweiler, R. Customized metabolomics database for the analysis of NMR ^{1}H-^{1}H TOCSY and ^{13}C-^{1}H HSQC-TOCSY spectra of complex mixtures. *Anal Chem* **86**, 5494-5501, doi:10.1021/ac500979g (2014).

37 Bingol, K., Zhang, F., Bruschweiler-Li, L. & Brüschweiler, R. TOCCATA: a customized carbon total correlation spectroscopy NMR metabolomics database. *Anal Chem* **84**, 9395-9401, doi:10.1021/ac302197e (2012).

38 Horai, H. *et al.* MassBank: a public repository for sharing mass spectral data for life sciences. *J Mass Spectrom* **45**, 703-714, doi:10.1002/jms.1777 (2010).

39 Hummel, M., Meister, R. & Mansmann, U. GlobalANCOVA: exploration and assessment of gene group effects. *Bioinformatics* **24**, 78-85, doi:10.1093/bioinformatics/btm531 (2008).

40 Ulrich, E. L. *et al.* BioMagResBank. *Nucleic Acids Res* **36**, D402-408, doi:10.1093/nar/gkm957 (2008).

41 Cui, Q. *et al.* Metabolite identification via the Madison Metabolomics Consortium Database. *Nat Biotechnol* **26**, 162-164, doi:10.1038/nbt0208-162 (2008).

42 Steinbeck, C., Krause, S. & Kuhn, S. NMRShiftDB-constructing a free chemical information system with open-source components. *J Chem Inf Comput Sci* **43**, 1733-1739, doi:10.1021/ci0341363 (2003).

43 Akiyama, K. *et al.* PRIMe: a Web site that assembles tools for metabolomics and transcriptomics. *In Silico Biol* **8**, 339-345 (2008).

44 Sakurai, T. *et al.* PRIMe Update: innovative content for plant metabolomics and integration of gene expression and metabolite accumulation. *Plant Cell Physiol* **54**, e5,

doi:10.1093/pcp/pcs184 (2013).

45 Ludwig, C. *et al.* Birmingham Metabolite Library: a publicly accessible database of 1-D ^{1}H and 2-D ^{1}H J-resolved NMR spectra of authentic metabolite standards (BML-NMR). *Metabolomics* **8**, 8-18, doi:10.1007/s11306-011-0347-7 (2012).

46 Graveley, B. R. *et al.* The developmental transcriptome of *Drosophila melanogaster*. *Nature* **471**, 473-479 (2011).

47 Brown, J. B. *et al.* Diversity and dynamics of the *Drosophila* transcriptome. *Nature* **512**, 393-399, doi:10.1038/nature12962 (2014).

48 Kostal, V. *et al.* Long-term cold acclimation extends survival time at 0 degrees C and modifies the metabolomic profiles of the larvae of the fruit fly *Drosophila melanogaster*. *PloS one* **6**, e25025, doi:10.1371/journal.pone.0025025 (2011).

49 Kostal, V., Simek, P., Zahradnickova, H., Cimlova, J. & Stetina, T. Conversion of the chill susceptible fruit fly larva (*Drosophila melanogaster*) to a freeze tolerant organism. *Proc Natl Acad Sci U S A* **109**, 3270-3274, doi:10.1073/pnas.1119986109 (2012).

50 Malmendal, A. *et al.* Metabolomic profiling of heat stress: hardening and recovery of homeostasis in *Drosophila*. *American journal of physiology. Regulatory, integrative and comparative physiology* **291**, R205-212, doi:10.1152/ajpregu.00867.2005 (2006).

51 Overgaard, J. *et al.* Metabolomic profiling of rapid cold hardening and cold shock in *Drosophila melanogaster*. *J Insect Physiol* **53**, 1218-1232, doi:10.1016/j.jinsphys.2007.06.012 (2007).

52 Pedersen, K. S. *et al.* Metabolomic signatures of inbreeding at benign and stressful temperatures in *Drosophila melanogaster*. *Genetics* **180**, 1233-1243, doi:10.1534/genetics.108.089144 (2008).

53 Colinet, H., Larvor, V., Laparie, M. & Renault, D. Exploring the plastic response to cold acclimation through metabolomics. *Funct Ecol* **26**, 711-722, doi:10.1111/j.1365-2435.2012.01985.x (2012).

54 Feala, J. D., Coquin, L., Paternostro, G. & McCulloch, A. D. Integrating metabolomics and phenomics with systems models of cardiac hypoxia. *Prog Biophys Mol Biol* **96**, 209-225, doi:10.1016/j.pbiomolbio.2007.07.014 (2008).

55 Al Bratty, M., Hobani, Y., Dow, J. A. T. & Watson, D. G. Metabolomic profiling of the effects of allopurinol on *Drosophila melanogaster*. *Metabolomics* **7**, 542-548, doi:10.1007/s11306-011-0275-6 (2011).

56 Sarup, P., Pedersen, S. M., Nielsen, N. C., Malmendal, A. & Loeschcke, V. The metabolic profile of long-lived *Drosophila melanogaster*. *PLoS One* **7**, e47461, doi:10.1371/journal.pone.0047461 (2012).

57 Heinrichsen, E. T. *et al.* Metabolic and transcriptional response to a high-fat diet in *Drosophila melanogaster*. *Mol Metab* **3**, 42-54, doi:10.1016/j.molmet.2013.10.003 (2014).

58 Chambers, M. C., Song, K. H. & Schneider, D. S. *Listeria monocytogenes* infection causes metabolic shifts in *Drosophila melanogaster*. *PLoS One* **7**, e50679, doi:10.1371/journal.pone.0050679 (2012).

59 Yang, B. *et al.* Metabolomic study of insomnia and intervention effects of Suanzaoren decoction using ultra-performance liquid-chromatography/electrospray-ionization synapt high-definition mass spectrometry. *J Pharm Biomed Anal* **58**, 113-124, doi:DOI 10.1016/j.jpba.2011.09.033 (2012).

60 Teets, N. M. *et al.* Combined transcriptomic and metabolomic approach uncovers molecular mechanisms of cold tolerance in a temperate flesh fly. *Physiol Genomics* **44**, 764-777, doi:10.1152/physiolgenomics.00042.2012 (2012).

61 MacMillan, H. A. *et al.* Cold acclimation wholly reorganizes the *Drosophila melanogaster* transcriptome and metabolome. *Sci Rep* **6**, 28999, doi:10.1038/srep28999 (2016).

62 Colinet, H., Larvor, V., Bical, R. & Renault, D. Dietary sugars affect cold tolerance of *Drosophila melanogaster*. *Metabolomics* **9**, 608-622, doi:10.1007/s11306-012-0471-z (2013).

63 Olsson, T. *et al.* Hemolymph metabolites and osmolality are tightly linked to cold tolerance of *Drosophila* species: a comparative study. *The Journal of Experimental Biology* **219**, 2504 (2016).

64 Hariharan, R. *et al.* Invariance and plasticity in the *Drosophila melanogaster* metabolomic network in response to temperature. *BMC Syst Biol* **8**, 139, doi:10.1186/s12918-014-0139-6 (2014).

65 Colinet, H. *et al.* Uncovering the benefits of fluctuating thermal regimes on cold tolerance of *Drosophila* flies by combined metabolomic and lipidomic approach. *Biochimica et Biophysica Acta (BBA) - Molecular and Cell Biology of Lipids* **1861**, 1736-1745, doi:10.1016/j.bbalip.2016.08.008 (2016).

66 Sarup, P., Petersen, S. M. M., Nielsen, N. C., Loeschcke, V. & Malmendal, A. Mild heat treatments induce long-term changes in metabolites associated with energy metabolism in *Drosophila melanogaster*. *Biogerontology* **17**, 873-882, doi:10.1007/s10522-016-9657-5 (2016).

67 Feala, J. D., Coquin, L., McCulloch, A. D. & Paternostro, G. Flexibility in energy metabolism supports hypoxia tolerance in *Drosophila* flight muscle: metabolomic and computational systems analysis. *Mol Syst Biol* **3**, 99, doi:10.1038/msb4100139 (2007).

68 Coquin, L., Feala, J. D., McCulloch, A. D. & Paternostro, G. Metabolomic and flux-balance analysis of age-related decline of hypoxia tolerance in *Drosophila* muscle tissue. *Mol Syst Biol* **4**, 233-n/a, doi:10.1038/msb.2008.71 (2008).

69 Knee, J. M., Rzezniczak, T. Z., Barsch, A., Guo, K. Z. & Merritt, T. J. A novel ion pairing LC/MS metabolomics protocol for study of a variety of biologically relevant

polar metabolites. *J Chromatogr B Analyt Technol Biomed Life Sci* **936**, 63-73, doi:10.1016/j.jchromb.2013.07.027 (2013).

70 Bakalov, V. *et al.* Metabolomics with Nuclear Magnetic Resonance Spectroscopy in a *Drosophila melanogaster* Model of Surviving Sepsis. *Metabolites* **6**, doi:10.3390/metabo6040047 (2016).

71 Li, H. M. *et al.* Bowman-Birk inhibitor affects pathways associated with energy metabolism in *Drosophila melanogaster*. *Insect Mol Biol* **19**, 303-313, doi:10.1111/j.1365-2583.2009.00984.x (2010).

72 Colinet, H. & Renault, D. Metabolic effects of CO_2 anaesthesia in *Drosophila melanogaster*. *Biol Lett* **8**, 1050 (2012).

73 Tennessen, J. M. *et al.* Coordinated metabolic transitions during *Drosophila* embryogenesis and the onset of aerobic glycolysis. *G3 (Bethesda)* **4**, 839-850, doi:10.1534/g3.114.010652 (2014).

74 Chintapalli, V. R., Al Bratty, M., Korzekwa, D., Watson, D. G. & Dow, J. A. Mapping an atlas of tissue-specific *Drosophila melanogaster* metabolomes by high resolution mass spectrometry. *PLoS One* **8**, e78066, doi:10.1371/journal.pone.0078066 (2013).

75 Gogna, N., Singh, V. J., Sheeba, V. & Dorai, K. NMR-based investigation of the *Drosophila melanogaster* metabolome under the influence of daily cycles of light and temperature. *Mol Biosyst* **11**, 3305-3315, doi:10.1039/c5mb00386e (2015).

76 Kamleh, M. A., Hobani, Y., Dow, J. A. T. & Watson, D. G. Metabolomic profiling of *Drosophila* using liquid chromatography Fourier transform mass spectrometry. *FEBS Lett* **582**, 2916-2922, doi:10.1016/j.febslet.2008.07.029 (2008).

77 Bratty, M. A., Chintapalli, V. R., Dow, J. A. T., Zhang, T. & Watson, D. G. Metabolomic profiling reveals that *Drosophila melanogaster* larvae with the y mutation have altered lysine metabolism. *FEBS Open Bio* **2**, 217-221, doi:10.1016/j.fob.2012.07.007 (2012).

78 Tennessen, J. M., Baker, K. D., Lam, G., Evans, J. & Thummel, C. S. The *Drosophila* estrogen-related receptor directs a metabolic switch that supports developmental growth. *Cell Metab* **13**, 139-148, doi:10.1016/j.cmet.2011.01.005 (2011).

79 Kamleh, M. A., Hobani, Y., Dow, J. A., Zheng, L. & Watson, D. G. Towards a platform for the metabonomic profiling of different strains of *Drosophila melanogaster* using liquid chromatography-Fourier transform mass spectrometry. *FEBS J* **276**, 6798-6809, doi:10.1111/j.1742-4658.2009.07397.x (2009).

80 Reed, L. K. *et al.* Systems genomics of metabolic phenotypes in wild-type *Drosophila melanogaster*. *Genetics* **197**, 781-793, doi:10.1534/genetics.114.163857 (2014).

81 Hoffman, J. M. *et al.* Effects of age, sex, and genotype on high-sensitivity metabolomic profiles in the fruit fly, *Drosophila melanogaster*. *Aging Cell* **13**, 596-604, doi:10.1111/acel.12215 (2014).

82 Laye, M. J., Tran, V., Jones, D. P., Kapahi, P. & Promislow, D. E. The effects of age and

dietary restriction on the tissue-specific metabolome of *Drosophila*. *Aging Cell* **14**, 797-808, doi:10.1111/acel.12358 (2015).

83 Parkhitko, A. A. *et al.* Tissue-specific down-regulation of S-adenosyl-homocysteine via suppression of dAhcyL1/dAhcyL2 extends health span and life span in *Drosophila*. *Genes Dev* **30**, 1409-1422, doi:10.1101/gad.282277.116 (2016).

84 López del Amo, V. *et al.* A *Drosophila* model of GDAP1 function reveals the involvement of insulin signalling in the mitochondria-dependent neuromuscular degeneration. *Biochimica et Biophysica Acta (BBA) - Molecular Basis of Disease* **1863**, 801-809, doi:10.1016/j.bbadis.2017.01.003 (2017).

85 Palanker Musselman, L., Fink, J. L. & Baranski, T. J. CoA protects against the deleterious effects of caloric overload in *Drosophila*. *J Lipid Res* **57**, 380-387, doi:10.1194/jlr.M062976 (2016).

86 Cheng, Z., Tsuda, M., Kishita, Y., Sato, Y. & Aigaki, T. Impaired energy metabolism in a *Drosophila* model of mitochondrial aconitase deficiency. *Biochem Biophys Res Commun* **433**, 145-150, doi:10.1016/j.bbrc.2013.02.040 (2013).

87 Ott, S., Vishnivetskaya, A., Malmendal, A. & Crowther, D. C. Metabolic changes may precede proteostatic dysfunction in a *Drosophila* model of amyloid beta peptide toxicity. *Neurobiol Aging* **41**, 39-52, doi:10.1016/j.neurobiolaging.2016.01.009 (2016).

88 Shukla, A. K. *et al.* Metabolomic Analysis Provides Insights on Paraquat-Induced Parkinson-Like Symptoms in *Drosophila melanogaster*. *Mol Neurobiol* **53**, 254-269, doi:10.1007/s12035-014-9003-3 (2016).

89 Lee, J.-E., Kim, Y., Kim, K. H., Lee, D. Y. & Lee, Y. Contribution of *Drosophila* TRPA1 to Metabolism. *PloS One* **11**, e0152935, doi:10.1371/journal.pone.0152935 (2016).

90 Carvalho, M. *et al.* Effects of diet and development on the *Drosophila* lipidome. *Mol Syst Biol* **8**, 600-n/a, doi:10.1038/msb.2012.29 (2012).

91 Reed, L. K., Baer, C. F. & Edison, A. S. Considerations when choosing a genetic model organism for metabolomics studies. *Curr Opin Chem Biol* **36**, 7-14, doi:10.1016/j.cbpa.2016.12.005 (2017).

92 Artal-Martinez de Narvajas, A. *et al.* Epigenetic regulation of autophagy by the methyltransferase G9a. *Mol Cell Biol* **33**, 3983-3993, doi:10.1128/MCB.00813-13 (2013).

93 Jumhawan, U. *et al.* Selection of Discriminant Markers for Authentication of Asian Palm Civet Coffee (Kopi Luwak): A Metabolomics Approach. *J Agric Food Chem* **61**, 7994-8001, doi:10.1021/jf401819s (2013).

94 Dempo, Y., Ohta, E., Nakayama, Y., Bamba, T. & Fukusaki, E. Molar-based targeted metabolic profiling of cyanobacterial strains with potential for biological production. *Metabolites* **4**, 499-516, doi:10.3390/metabo4020499 (2014).

95 Hashim, Z., Mukai, Y., Bamba, T. & Fukusaki, E. Metabolic profiling of retrograde

pathway transcription factors rtg1 and rtg3 knockout yeast. *Metabolites* **4**, 580-598, doi:10.3390/metabo4030580 (2014).

96 Meier, P., Finch, A. & Evan, G. Apoptosis in development. *Nature* **407**, 796-801, doi:10.1038/35037734 (2000).

97 Zhu, L. & Skoultchi, A. I. Coordinating cell proliferation and differentiation. *Curr Opin Genet Dev* **11**, 91-97 (2001).

98 Yi, H. *et al.* Gene expression atlas for human embryogenesis. *FASEB J* **24**, 3341-3350, doi:10.1096/fj.10-158782 (2010).

99 Arbeitman, M. N. *et al.* Gene expression during the life cycle of *Drosophila melanogaster*. *Science* **297**, 2270-2275, doi:10.1126/science.1072152 (2002).

100 Hill, A. A., Hunter, C. P., Tsung, B. T., Tucker-Kellogg, G. & Brown, E. L. Genomic analysis of gene expression in *C. elegans*. *Science* **290**, 809-812 (2000).

101 Gilbert, S. Early *Drosophila* Development. *Dev Biol* **6th edition** (2000).

102 Tram, U., Riggs, B. & Sullivan, W. in *eLS* (John Wiley & Sons, Ltd, 2001).

103 Church, R. B. & Robertson, F. W. Biochemical analysis of genetic differences in the growth of *Drosophila*. *Genet Res* **7**, 383-407 (1966).

104 Aguila, J. R., Suszko, J., Gibbs, A. G. & Hoshizaki, D. K. The role of larval fat cells in adult *Drosophila melanogaster*. *J Exp Biol* **210**, 956-963, doi:10.1242/jeb.001586 (2007).

105 Baehrecke, E. H. Ecdysone signaling cascade and regulation of *Drosophila* metamorphosis. *Arch Insect Biochem Physiol* **33**, 231-244, doi:10.1002/(SICI)1520-6327(1996)33:3/4<231::AID-ARCH5>3.0.CO;2-V (1996).

106 Rideout, E. J., Narsaiya, M. S. & Grewal, S. S. The Sex Determination Gene transformer Regulates Male-Female Differences in *Drosophila* Body Size. *PLoS Genet* **11**, e1005683, doi:10.1371/journal.pgen.1005683 (2016).

107 Parisi, M., Li, R. & Oliver, B. Lipid profiles of female and male *Drosophila*. *BMC Research Notes* **4**, 198, doi:10.1186/1756-0500-4-198 (2011).

108 Siera, S. G. & Cline, T. W. Sexual Back Talk With Evolutionary Implications: Stimulation of the *Drosophila* Sex-Determination Gene *Sex-lethal* by Its Target *transformer*. *Genetics* **180**, 1963 (2008).

109 Hayashi, S. *et al.* A novel application of metabolomics in vertebrate development. *Biochem Biophys Res Commun* **386**, 268-272, doi:10.1016/j.bbrc.2009.06.041 (2009).

110 Yoshida, R. *et al.* Metabolomics-based systematic prediction of yeast lifespan and its application for semi-rational screening of ageing-related mutants. *Aging Cell* **9**, 616-625, doi:10.1111/j.1474-9726.2010.00590.x (2010).

111 Vastag, L. *et al.* Remodeling of the metabolome during early frog development. *PLoS One* **6**, e16881, doi:10.1371/journal.pone.0016881 (2011).

112 Yamaguchi, M., Date, T. & Matsukage, A. Distribution of PCNA in *Drosophila* embryo

during nuclear division cycles. *J Cell Sci* **100 (Pt 4)**, 729-733 (1991).

113 Yamaguchi, M., Hirose, F., Nishida, Y. & Matsukage, A. Repression of the *Drosophila* proliferating-cell nuclear antigen gene promoter by zerknullt protein. *Mol Cell Biol* **11**, 4909-4917 (1991).

114 Bainbridge, S. P. & Bownes, M. Staging the metamorphosis of *Drosophila melanogaster*. *J Embryol Exp Morphol* **66**, 57-80 (1981).

115 Lommen, A. MetAlign: interface-driven, versatile metabolomics tool for hyphenated full-scan mass spectrometry data preprocessing. *Anal Chem* **81**, 3079-3086, doi:10.1021/ac900036d (2009).

116 Lommen, A. *et al.* An untargeted metabolomics approach to contaminant analysis: pinpointing potential unknown compounds. *Anal Chim Acta* **584**, 43-49, doi:10.1016/j.aca.2006.11.018 (2007).

117 Tsugawa, H., Tsujimoto, Y., Arita, M., Bamba, T. & Fukusaki, E. GC/MS based metabolomics: development of a data mining system for metabolite identification by using soft independent modeling of class analogy (SIMCA). *BMC Bioinformatics* **12**, 131, doi:10.1186/1471-2105-12-131 (2011).

118 Kawase, N., Tsugawa, H., Bamba, T. & Fukusaki, E. Different-batch metabolome analysis of *Saccharomyces cerevisiae* based on gas chromatography/mass spectrometry. *J Biosci Bioeng* **117**, 248-255, doi:10.1016/j.jbiosc.2013.07.008 (2014).

119 Eriksson, L. *et al.* Methods for reliability and uncertainty assessment and for applicability evaluations of classification- and regression-based QSARs. *Environ Health Perspect* **111**, 1361-1375 (2003).

120 Howe, E. *et al.* in *Biomedical Informatics for Cancer Research* (eds Michael F. Ochs, John T. Casagrande, & Ramana V. Davuluri) Ch. 15, 267-277 (Springer US, 2010).

121 Xia, J., Sinelnikov, I. V., Han, B. & Wishart, D. S. MetaboAnalyst 3.0—making metabolomics more meaningful. *Nucleic Acids Res* **43**, W251-W257 (2015).

122 Leptin, M. Gastrulation in *Drosophila*: the logic and the cellular mechanisms. *EMBO J* **18**, 3187-3192, doi:10.1093/emboj/18.12.3187 (1999).

123 Kubinyi, H. *3D QSAR in Drug Design: Volume 1: Theory Methods and Applications*. 523-550 (Springer, 1993).

124 Elbein, A. D., Pan, Y. T., Pastuszak, I. & Carroll, D. New insights on trehalose: a multifunctional molecule. *Glycobiology* **13**, 17R-27R, doi:10.1093/glycob/cwg047 (2003).

125 Chen, Q. & Haddad, G. G. Role of trehalose phosphate synthase and trehalose during hypoxia: from flies to mammals. *J Exp Biol* **207**, 3125-3129, doi:10.1242/jeb.01133 (2004).

126 Fisher, B. *et al. BDGP insitu homepage*. (2012).

127 Tram, U., Riggs, B. & Sullivan, W. *Cleavage and Gastrulation in Drosophila*

EmbryosCleavage and Gastrulation in Drosophila Embryos. (John Wiley & Sons, Ltd, 2001).

128 Bender, D. A. *Amino Acid Metabolism*. (Wiley, 2012).

129 Nation, J. L. *Insect Physiology and Biochemistry, Second Edition*. (CRC Press, 2008).

130 Chiang, H. C. Tactic Reactions of Young Adults of *Drosophila melanogaster*. *Am Midl Nat* **70**, 329-338, doi:10.2307/2423061 (1963).

131 Gilbert, L. I. & Schneiderman, H. A. Some Biochemical Aspects of Insect Metamorphosis. *Am Zool* **1**, 11-51, doi:10.2307/3881189 (1961).

132 Wigglesworth, V. B. *The Principles of Insect Physiology*. 425 (Springer Netherlands, 2012).

133 Wheelock, Å. & Wheelock, C. E. Trials and tribulations of 'omics data analysis: assessing quality of SIMCA-based multivariate models using examples from pulmonary medicine. *Mol Biosyst* **9**, 2589-2596, doi:10.1039/c3mb70194h (2013).

134 Scheitz, C. J. F., Guo, Y., Early, A. M., Harshman, L. G. & Clark, A. G. Heritability and Inter-Population Differences in Lipid Profiles of *Drosophila melanogaster*. *PloS One* **8**, e72726, doi:10.1371/journal.pone.0072726 (2013).

135 Parisi, M. *et al.* A survey of ovary-, testis-, and soma-biased gene expression in *Drosophila melanogaster* adults. *Genome Biol* **5**, doi:10.1186/gb-2004-5-6-r40 (2004).

136 Rong, Z., Tong, Z., Dominika, K., Shadi, A.-J. & Julian, A. T. D. a. D. G. W. A Comparison of the Metabolome of Male and Female *Drosophila melanogaster*. *Curr Metabolomics* **2**, 174-183, doi:10.2174/2213235X03666150108233830 (2014).

137 Neckameyer, W. S. & Matsuo, H. Distinct neural circuits reflect sex, sexual maturity, and reproductive status in response to stress in *Drosophila melanogaster*. *Neuroscience* **156**, 841-856, doi:10.1016/j.neuroscience.2008.08.020 (2008).

138 Taylor, K. & Kimbrell, D. A. Host immune response and differential survival of the sexes in *Drosophila*. *Fly (Austin)* **1**, 197-204 (2007).

139 Magwere, T., Chapman, T. & Partridge, L. Sex differences in the effect of dietary restriction on life span and mortality rates in female and male *Drosophila melanogaster*. *J Gerontol A Biol Sci Med Sci* **59**, 3-9 (2004).

140 Theodosiou, N. A. & Xu, T. Use of FLP/FRT system to study *Drosophila* development. *Methods* **14**, 355-365, doi:10.1006/meth.1998.0591 (1998).

141 Duffy, J. B. GAL4 system in *Drosophila*: a fly geneticist's Swiss army knife. *Genesis* **34**, 1-15, doi:10.1002/gene.10150 (2002).

142 Linford, N. J., Bilgir, C., Ro, J. & Pletcher, S. D. Measurement of lifespan in *Drosophila melanogaster*. *J Vis Exp*, doi:10.3791/50068 (2013).

143 Lee, Y. & Montell, C. *Drosophila* TRPA1 functions in temperature control of circadian rhythm in pacemaker neurons. *J Neurosci* **33**, 6716-6725, doi:10.1523/JNEUROSCI.4237-12.2013 (2013).

144 Lindsley, D. L., Grell, E. H. & Bridges, C. B. *Genetic variations of Drosophila melanogaster*. (Carnegie institution of Washington, 1972).

145 Salmon, A. B., Marx, D. B. & Harshman, L. G. A cost of reproduction in *Drosophila melanogaster*: stress susceptibility. *Evolution* **55**, 1600-1608 (2001).

146 Rajamohan, A. & Sinclair, B. J. Hardening trumps acclimation in improving cold tolerance of *Drosophila melanogaster* larvae. *Physiol Entomol* **34**, 217-223, doi:10.1111/j.1365-3032.2009.00677.x (2009).

147 Vaiserman, A. M., Zabuga, O. G., Kolyada, A. K., Pisaruk, A. V. & Kozeretska, I. A. Reciprocal cross differences in *Drosophila melanogaster* longevity: an evidence for non-genomic effects in heterosis phenomenon? *Biogerontology* **14**, 153-163, doi:10.1007/s10522-013-9419-6 (2013).

148 Mitchell, C. L. *et al.* Long-Term Resistance of *Drosophila melanogaster* to the Mushroom Toxin Alpha-Amanitin. *PLoS One* **10**, e0127569, doi:10.1371/journal.pone.0127569 (2015).

149 Williams, S. *et al.* Metabolomic and Gene Expression Profiles Exhibit Modular Genetic and Dietary Structure Linking Metabolic Syndrome Phenotypes in *Drosophila*. *G3 (Bethesda)* **5**, 2817-2829, doi:10.1534/g3.115.023564 (2015).

150 Scott Chialvo, C. H., Che, R., Reif, D., Motsinger-Reif, A. & Reed, L. K. Eigenvector metabolite analysis reveals dietary effects on the association among metabolite correlation patterns, gene expression, and phenotypes. *Metabolomics* **12**, 167, doi:10.1007/s11306-016-1117-3 (2016).

151 Tortoriello, G. *et al.* Targeted lipidomics in *Drosophila melanogaster* identifies novel 2-monoacylglycerols and N-acyl amides. *PLoS One* **8**, e67865, doi:10.1371/journal.pone.0067865 (2013).

152 Van Handel, E. Estimation of glycogen in small amounts of tissue. *Anal Biochem* **11**, 256-265 (1965).

153 Van Handel, E. Rapid determination of total lipids in mosquitoes. *J Am Mosq Control Assoc* **1**, 302-304 (1985).

154 Van Handel, E. & Day, J. F. Assay of lipids, glycogen and sugars in individual mosquitoes: correlations with wing length in field-collected Aedes vexans. *J Am Mosq Control Assoc* **4**, 549-550 (1988).

155 Kaufmann, C. & Brown, M. R. Regulation of carbohydrate metabolism and flight performance by a hypertrehalosaemic hormone in the mosquito *Anopheles gambiae*. *J Insect Physiol* **54**, 367-377, doi:10.1016/j.jinsphys.2007.10.007 (2008).

156 Davis, M. B. & Li, T. Genomic analysis of the ecdysone steroid signal at metamorphosis onset using ecdysoneless and *EcRnull Drosophila melanogaster* mutants. *Genes Genomics* **35**, 21-46, doi:10.1007/s13258-013-0061-0 (2013).

157 Warren, J. T. *et al.* Discrete pulses of molting hormone, 20-hydroxyecdysone, during

late larval development of *Drosophila melanogaster*: correlations with changes in gene activity. *Dev Dyn* **235**, 315-326, doi:10.1002/dvdy.20626 (2006).

158 Andres, A. J., Fletcher, J. C., Karim, F. D. & Thummel, C. S. Molecular analysis of the initiation of insect metamorphosis: a comparative study of *Drosophila* ecdysteroid-regulated transcription. *Dev Biol* **160**, 388-404, doi:10.1006/dbio.1993.1315 (1993).

159 Kaelin, W. G. & McKnight, S. L. Influence of metabolism on epigenetics and disease. *Cell* **153**, 56-69, doi:10.1016/j.cell.2013.03.004 (2013).

160 Lu, C. & Thompson, C. B. Metabolic regulation of epigenetics. *Cell Metab* **16**, 9-17, doi:10.1016/j.cmet.2012.06.001 (2012).

161 Jorge, T. F. *et al.* Mass spectrometry-based plant metabolomics: Metabolite responses to abiotic stress. *Mass Spectrom Rev*, doi:10.1002/mas.21449 (2015).

162 Alreshidi, M. M. *et al.* Metabolomic and proteomic responses of *Staphylococcus aureus* to prolonged cold stress. *Journal of Proteomics* **121**, 44-55, doi:10.1016/j.jprot.2015.03.010 (2015).

163 Heijmans, B. T. *et al.* Persistent epigenetic differences associated with prenatal exposure to famine in humans. *Proc Natl Acad Sci U S A* **105**, 17046-17049, doi:10.1073/pnas.0806560105 (2008).

164 Fulco, M. *et al.* Sir2 regulates skeletal muscle differentiation as a potential sensor of the redox state. *Mol Cell* **12**, 51-62 (2003).

165 Slade, J. D. & Staveley, B. E. Extended longevity and survivorship during amino-acid starvation in a Drosophila Sir2 mutant heterozygote. *Genome* **59**, 311-318, doi:10.1139/gen-2015-0213 (2016).

166 He, C. & Klionsky, D. J. Regulation mechanisms and signaling pathways of autophagy. *Annu Rev Genet* **43**, 67-93, doi:10.1146/annurev-genet-102808-114910 (2009).

167 Tachibana, M., Sugimoto, K., Fukushima, T. & Shinkai, Y. Set domain-containing protein, G9a, is a novel lysine-preferring mammalian histone methyltransferase with hyperactivity and specific selectivity to lysines 9 and 27 of histone H3. *J Biol Chem* **276**, 25309-25317, doi:10.1074/jbc.M101914200 (2001).

168 Collins, R. E. *et al.* In vitro and in vivo analyses of a Phe/Tyr switch controlling product specificity of histone lysine methyltransferases. *J Biol Chem* **280**, 5563-5570, doi:10.1074/jbc.M410483200 (2005).

169 Tachibana, M. *et al.* Histone methyltransferases G9a and GLP form heteromeric complexes and are both crucial for methylation of euchromatin at H3-K9. *Genes Dev* **19**, 815-826, doi:10.1101/gad.1284005 (2005).

170 Patnaik, D. *et al.* Substrate specificity and kinetic mechanism of mammalian G9a histone H3 methyltransferase. *J Biol Chem* **279**, 53248-53258, doi:10.1074/jbc.M409604200 (2004).

171 Kubicek, S. *et al.* Reversal of H3K9me2 by a small-molecule inhibitor for the G9a

histone methyltransferase. *Mol Cell* **25**, 473-481, doi:10.1016/j.molcel.2007.01.017 (2007).

172 Tachibana, M. *et al.* G9a histone methyltransferase plays a dominant role in euchromatic histone H3 lysine 9 methylation and is essential for early embryogenesis. *Genes Dev* **16**, 1779-1791, doi:10.1101/gad.989402 (2002).

173 Feldman, N. *et al.* G9a-mediated irreversible epigenetic inactivation of Oct-3/4 during early embryogenesis. *Nat Cell Biol* **8**, 188-194, doi:10.1038/ncb1353 (2006).

174 Epsztejn-Litman, S. *et al.* De novo DNA methylation promoted by G9a prevents reprogramming of embryonically silenced genes. *Nat Struct Mol Biol* **15**, 1176-1183, doi:10.1038/nsmb.1476 (2008).

175 Zylicz, J. J. *et al.* Chromatin dynamics and the role of G9a in gene regulation and enhancer silencing during early mouse development. *Elife* **4**, doi:10.7554/eLife.09571 (2015).

176 Chen, H., Yan, Y., Davidson, T. L., Shinkai, Y. & Costa, M. Hypoxic stress induces dimethylated histone H3 lysine 9 through histone methyltransferase G9a in mammalian cells. *Cancer Res* **66**, 9009-9016, doi:10.1158/0008-5472.CAN-06-0101 (2006).

177 Xin, Z. *et al.* Role of histone methyltransferase G9a in CpG methylation of the Prader-Willi syndrome imprinting center. *J Biol Chem* **278**, 14996-15000, doi:10.1074/jbc.M211753200 (2003).

178 Ikegami, K. *et al.* Genome-wide and locus-specific DNA hypomethylation in G9a deficient mouse embryonic stem cells. *Genes Cells* **12**, 1-11, doi:10.1111/j.1365-2443.2006.01029.x (2007).

179 Estève, P. O. *et al.* Direct interaction between DNMT1 and G9a coordinates DNA and histone methylation during replication. *Genes Dev* **20**, 3089-3103, doi:10.1101/gad.1463706 (2006).

180 Chin, H. G. *et al.* Automethylation of G9a and its implication in wider substrate specificity and HP1 binding. *Nucleic Acids Res* **35**, 7313-7323, doi:10.1093/nar/gkm726 (2007).

181 Lee, J. S. *et al.* Negative regulation of hypoxic responses via induced Reptin methylation. *Mol Cell* **39**, 71-85, doi:10.1016/j.molcel.2010.06.008 (2010).

182 Lee, J. S. *et al.* Hypoxia-induced methylation of a pontin chromatin remodeling factor. *Proc Natl Acad Sci U S A* **108**, 13510-13515, doi:10.1073/pnas.1106106108 (2011).

183 Huang, J. *et al.* G9a and Glp methylate lysine 373 in the tumor suppressor p53. *J Biol Chem* **285**, 9636-9641, doi:10.1074/jbc.M109.062588 (2010).

184 Jin, W. *et al.* Involvement of MyoD and c-myb in regulation of basal and estrogen-induced transcription activity of the BRCA1 gene. *Breast Cancer Res Treat* **125**, 699-713, doi:10.1007/s10549-010-0876-1 (2011).

185 Rathert, P. *et al.* Protein lysine methyltransferase G9a acts on non-histone targets. *Nat*

Chem Biol **4**, 344-346, doi:10.1038/nchembio.88 (2008).

186 Kondo, Y. *et al.* Downregulation of histone H3 lysine 9 methyltransferase G9a induces centrosome disruption and chromosome instability in cancer cells. *PLoS One* **3**, e2037, doi:10.1371/journal.pone.0002037 (2008).

187 Chen, M. W. *et al.* H3K9 histone methyltransferase G9a promotes lung cancer invasion and metastasis by silencing the cell adhesion molecule Ep-CAM. *Cancer Res* **70**, 7830-7840, doi:10.1158/0008-5472.CAN-10-0833 (2010).

188 Dong, C. *et al.* G9a interacts with Snail and is critical for Snail-mediated E-cadherin repression in human breast cancer. *J Clin Invest* **122**, 1469-1486, doi:10.1172/JCI57349 (2012).

189 Hua, K. T. *et al.* The H3K9 methyltransferase G9a is a marker of aggressive ovarian cancer that promotes peritoneal metastasis. *Mol Cancer* **13**, 189, doi:10.1186/1476-4598-13-189 (2014).

190 Shinkai, Y. & Tachibana, M. H3K9 methyltransferase G9a and the related molecule GLP. *Genes Dev* **25**, 781-788, doi:10.1101/gad.2027411 (2011).

191 Cho, H. S. *et al.* Enhanced expression of EHMT2 is involved in the proliferation of cancer cells through negative regulation of SIAH1. *Neoplasia* **13**, 676-684 (2011).

192 Ren, A., Qiu, Y., Cui, H. & Fu, G. Inhibition of H3K9 methyltransferase G9a induces autophagy and apoptosis in oral squamous cell carcinoma. *Biochem Biophys Res Commun* **459**, 10-17, doi:10.1016/j.bbrc.2015.01.068 (2015).

193 Casciello, F., Windloch, K., Gannon, F. & Lee, J. S. Functional Role of G9a Histone Methyltransferase in Cancer. *Front Immunol* **6**, 487, doi:10.3389/fimmu.2015.00487 (2015).

194 Stabell, M. *et al.* The *Drosophila* G9a gene encodes a multi-catalytic histone methyltransferase required for normal development. *Nucleic Acids Res* **34**, 4609-4621, doi:10.1093/nar/gkl640 (2006).

195 Seum, C., Bontron, S., Reo, E., Delattre, M. & Spierer, P. *Drosophila* G9a is a nonessential gene. *Genetics* **177**, 1955-1957, doi:10.1534/genetics.107.078220 (2007).

196 Kato, Y., Kato, M., Tachibana, M., Shinkai, Y. & Yamaguchi, M. Characterization of *Drosophila* G9a in vivo and identification of genetic interactants. *Genes Cells* **13**, 703-722, doi:10.1111/j.1365-2443.2008.01199.x (2008).

197 Hinton, T., Noyes, D. T. & Ellis, J. Amino Acids and Growth Factors in a Chemi-Cally Defined Medium for *Drosophila*. *Physiol Zool* **24**, 335-353, doi:10.2307/30152141 (1951).

198 Seglen, P. O., Gordon, P. B. & Poli, A. Amino acid inhibition of the autophagic/lysosomal pathway of protein degradation in isolated rat hepatocytes. *Biochim Biophys Acta* **630**, 103-118 (1980).

199 Nicklin, P. *et al.* Bidirectional transport of amino acids regulates mTOR and autophagy.

Cell **136**, 521-534, doi:10.1016/j.cell.2008.11.044 (2009).

200 Mizushima, N., Ohsumi, Y. & Yoshimori, T. Autophagosome formation in mammalian cells. *Cell Struct Funct* **27**, 421-429 (2002).

201 Huang, H. *et al.* Bulk RNA degradation by nitrogen starvation-induced autophagy in yeast. *EMBO J* **34**, 154-168, doi:10.15252/embj.201489083 (2015).

202 Reyes-DelaTorre, A., Riesgo-Escovar, J. R. & Peña-Rangel, M. T. *Carbohydrate Metabolism in Drosophila: Reliance on the Disaccharide Trehalose.* (INTECH Open Access Publisher, 2012).

203 Slobodkin, M. R. & Elazar, Z. The Atg8 family: multifunctional ubiquitin-like key regulators of autophagy. *Essays Biochem* **55**, 51-64, doi:10.1042/bse0550051 (2013).

204 Bittencourt, D. *et al.* G9a functions as a molecular scaffold for assembly of transcriptional coactivators on a subset of glucocorticoid receptor target genes. *Proc Natl Acad Sci U S A* **109**, 19673-19678, doi:10.1073/pnas.1211803109 (2012).

205 Shimaji, K. *et al.* Genomewide identification of target genes of histone methyltransferase dG9a during *Drosophila* embryogenesis. *Genes Cells* **20**, 902-914, doi:10.1111/gtc.12281 (2015).

206 Tracy, K. & Baehrecke, E. H. The role of autophagy in *Drosophila* metamorphosis. *Curr Top Dev Biol* **103**, 101-125, doi:10.1016/B978-0-12-385979-2.00004-6 (2013).

207 Rabinowitz, J. D. & White, E. Autophagy and metabolism. *Science* **330**, 1344-1348, doi:10.1126/science.1193497 (2010).

208 Eng, C. H. & Abraham, R. T. The autophagy conundrum in cancer: influence of tumorigenic metabolic reprogramming. *Oncogene* **30**, 4687-4696, doi:10.1038/onc.2011.220 (2011).

Appendices

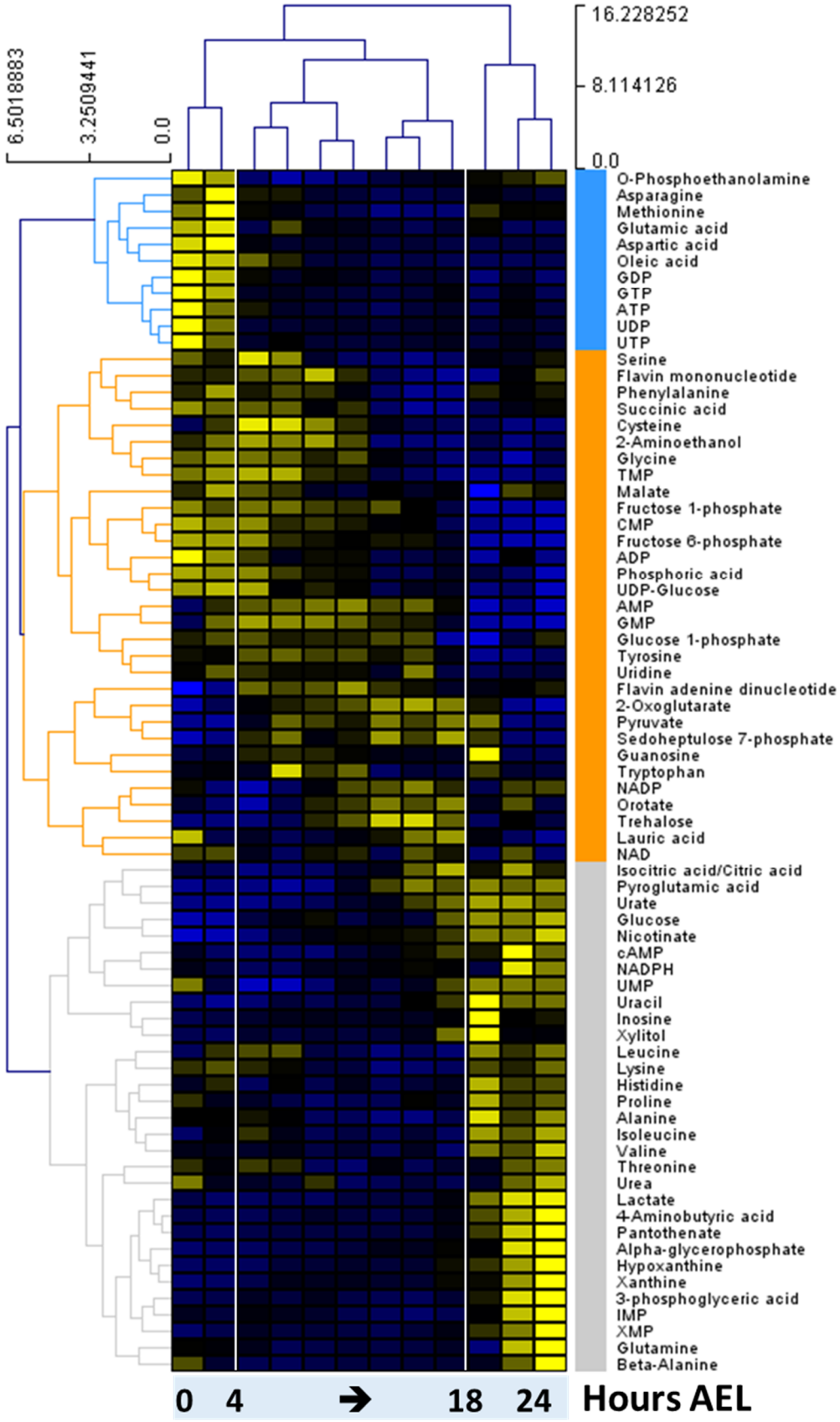

Figure S2-1: Metabolic profiles of CS during embryogenesis. The color scale, showing the relative levels of each metabolite to its average value, is plotted at the top of the figure.

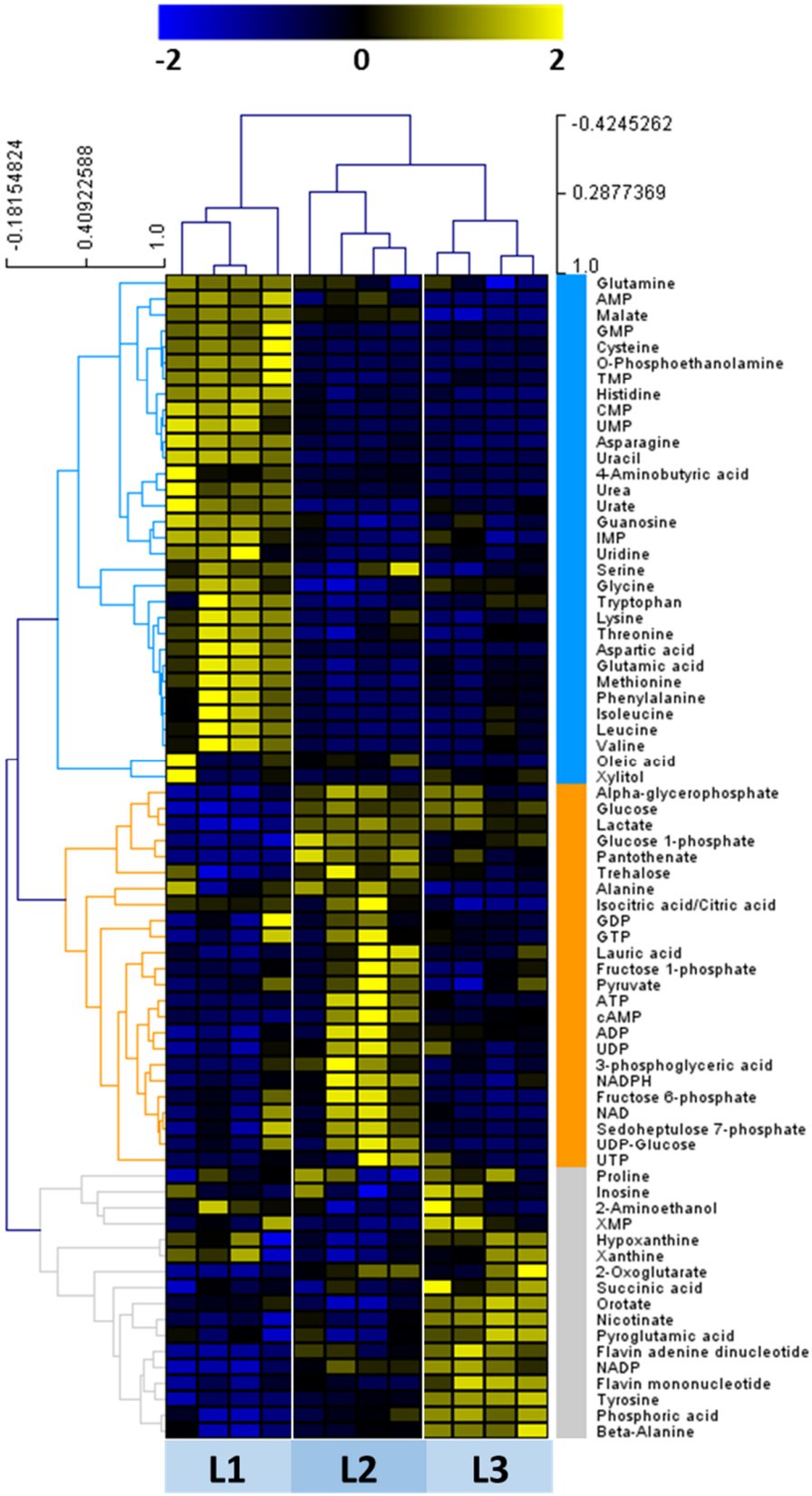

Figure S2-2: Metabolic profiles of CS during larval stages. The color scale, showing the relative levels of each metabolite to its average value, is plotted at the top of the figure. . L1: first instar larvae; L2: second instar larvae; L3: third instar larvae

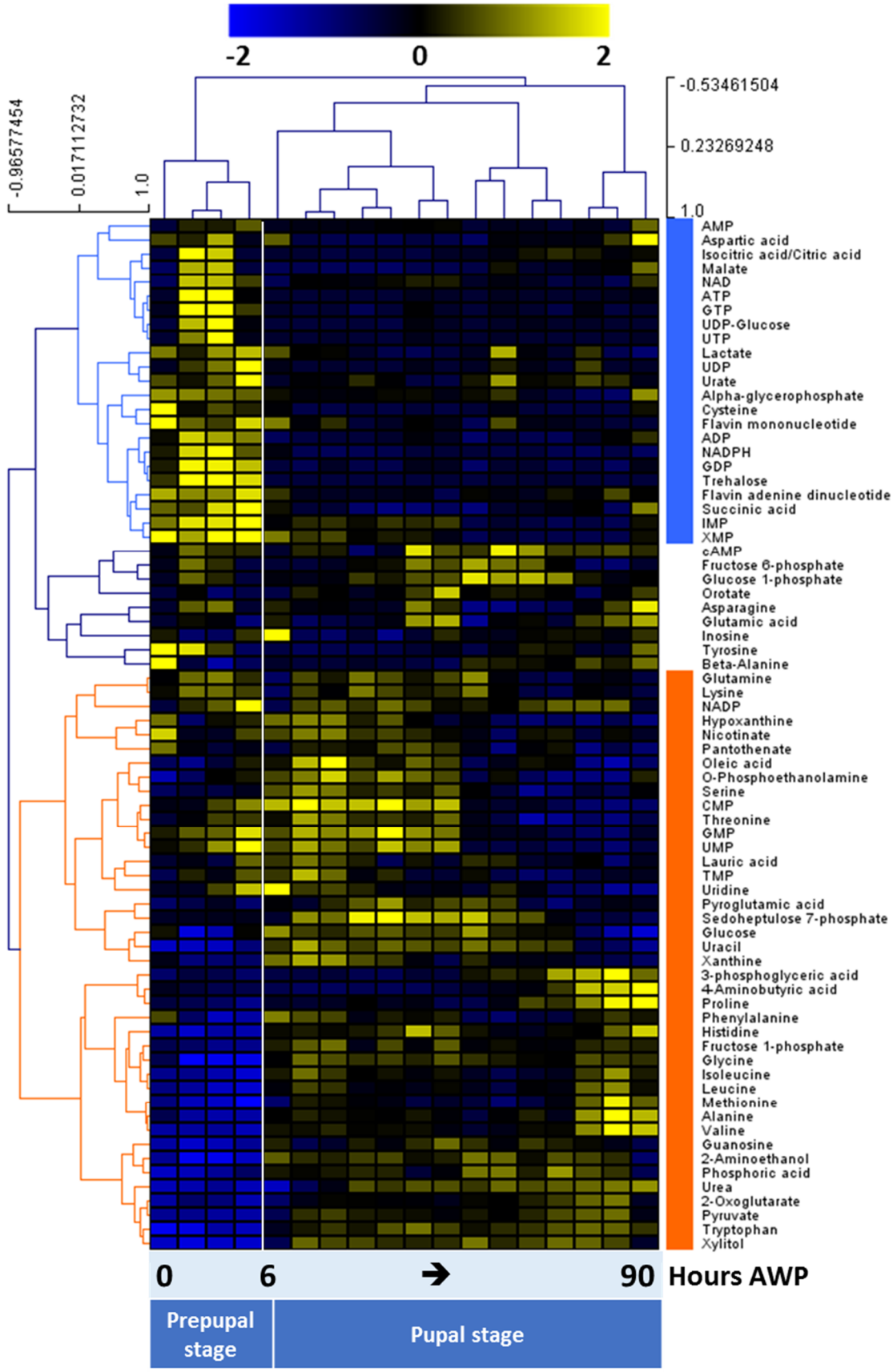

Figure S2-3: Metabolic profiles of CS during metamorphosis. The color scale, showing the relative levels of each metabolite to its average value, is plotted at the top of the figure.

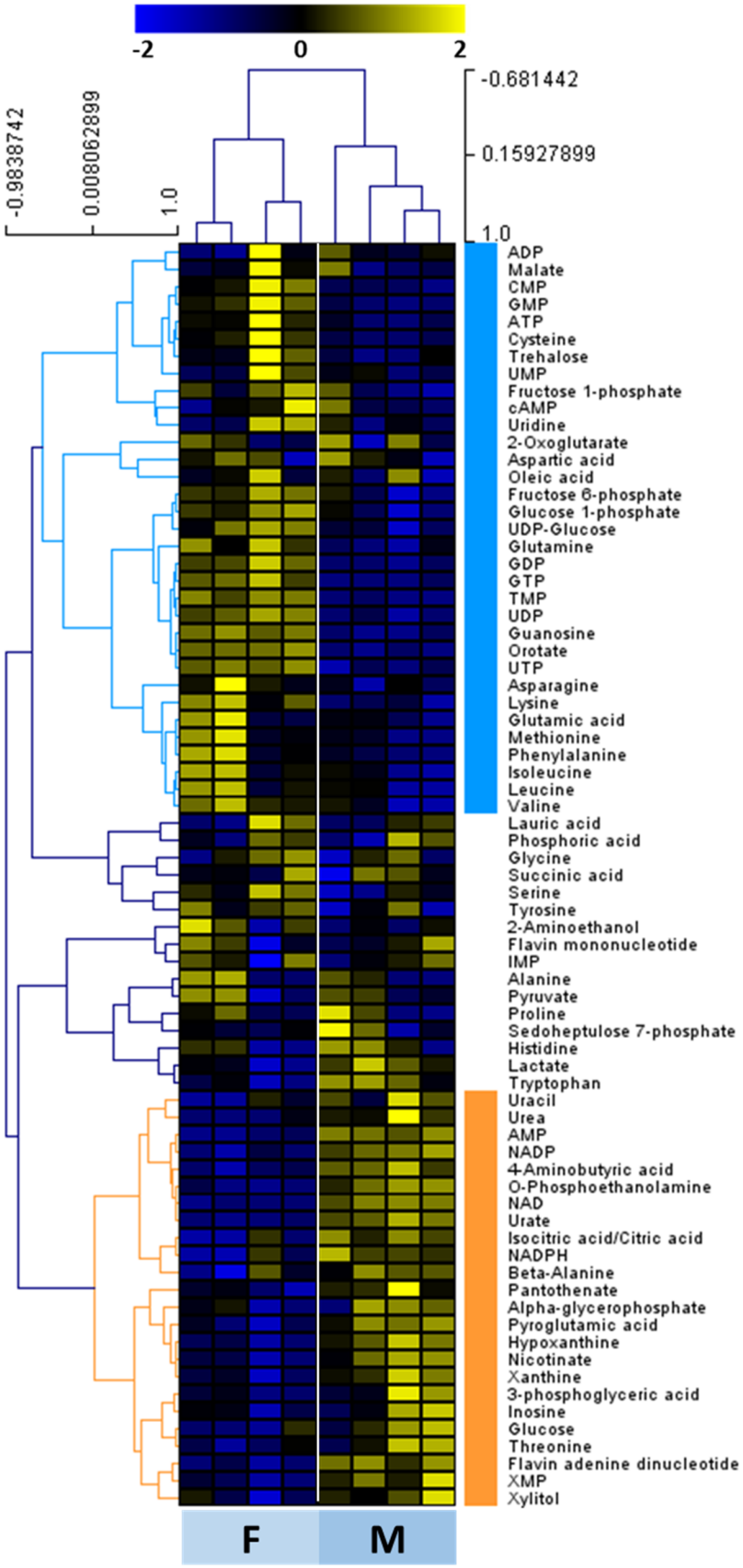

Figure S2-: Metabolic profiles of 5-day-old male and female CS. The color scale, showing the relative levels of each metabolite to its average value, is plotted at the top of the figure.

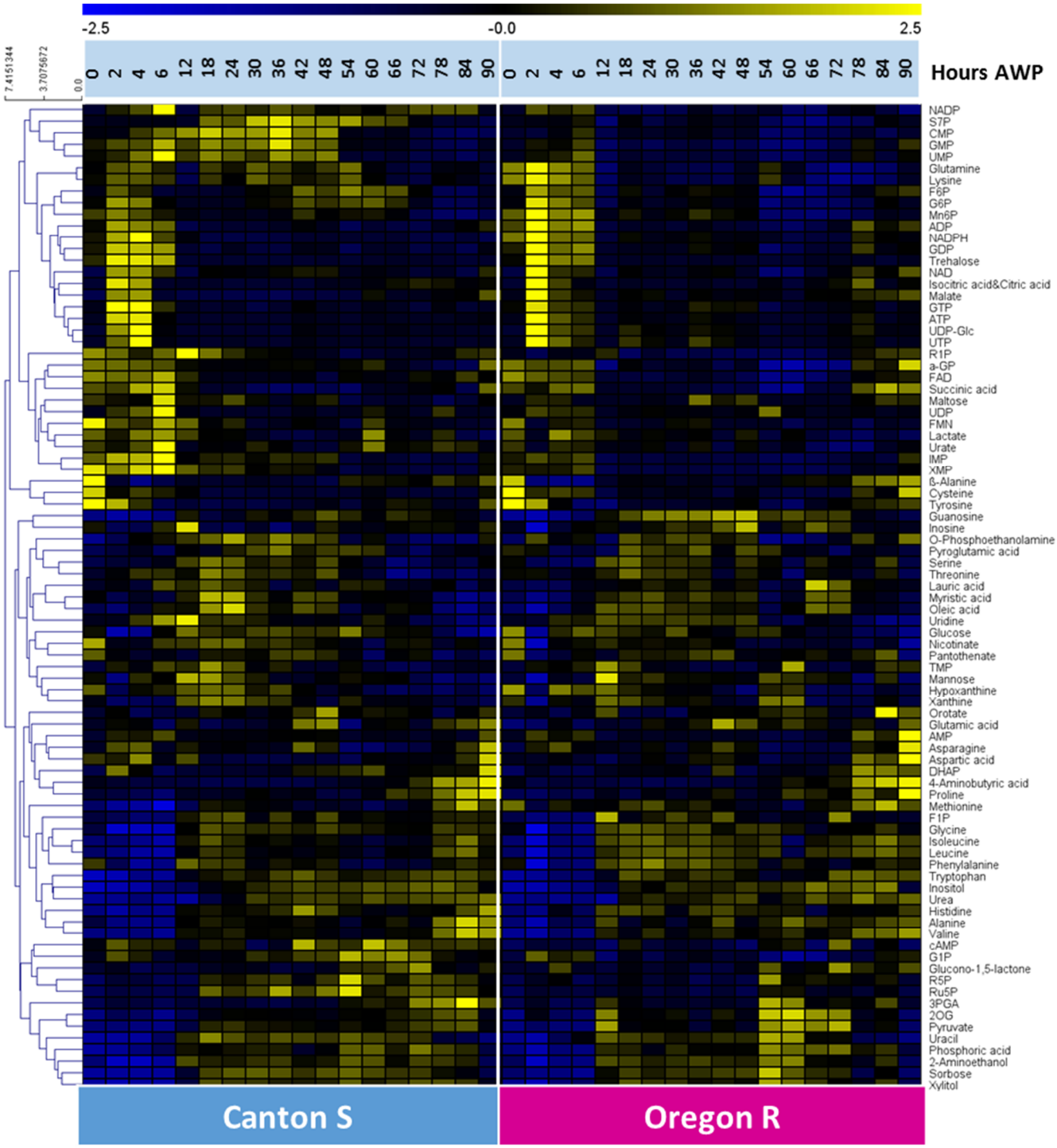

Figure S3-1: Metabolic profiles of CS and Oregon R during metamorphosis. The color scale, showing the relative levels of each metabolite to its average value, is plotted at the top of the figure.

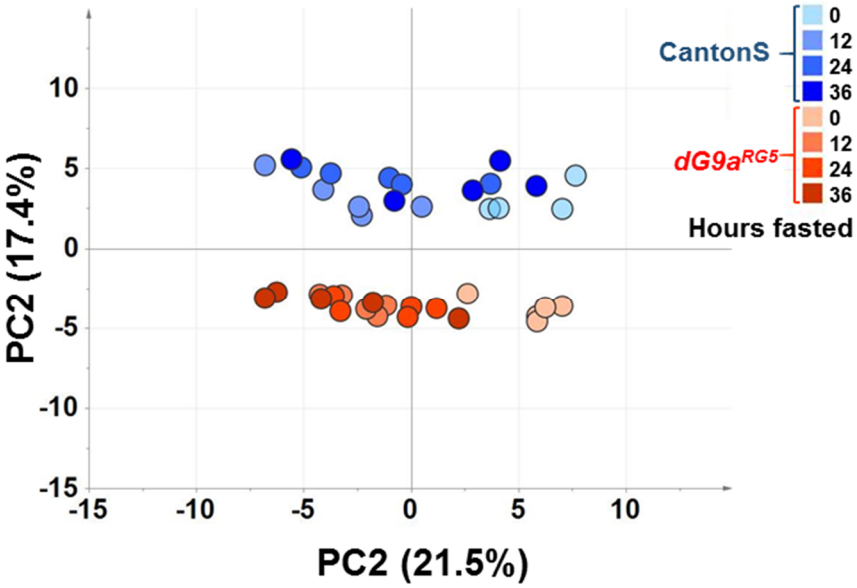

Figure S4-1: Comparison of the metabolic profiles between wild type and *dG9a*^{RG5} mutant flies under starvation using PCA. PCA score plot constructed by PC1 (21.5%) and PC2 (17.4%)

Table S1: Optimized multiple reaction monitoring (MRM) parameters and retention time for each metabolite measured by LC-MS/MS.

Name	Retention Time (min)	Product Ion (*m/z*)	Reference Ion (*m/z*)
Arginine	1.216	173.05>131.05	173.05>156.05
Histidine	1.243	154.05>93.00	154.05>137.05
4-Aminobutyrate	1.512	162.05>102.00	
Serine	1.668	104.05>74.10	164.05>104.00
Asparagine	1.672	131.05>113.05	131.05>114.05
Lysine	1.718	145.10>97.05	145.10>99.05
Glutamine	1.719	145.10>127.05	145.10>42.05
Threonine	1.741	118.05>74.05	178.05>118.00
Hydroxyproline	1.753	190.05>130.05	261.05>130.05 130.05>84.00
Hexose	1.781	179.05>89.00	239.05>179.00
Cysteine	1.848	239.05>120.10	120.05>33.00
2-Aminobutyrate	1.858	162.05>102.00	
Proline	2.028	174.05>114.00	114.05>68.00
Trehalose	2.045	341.05>89.10	401.10>341.10
Sucrose	2.294	341.05>89.10	401.10>341.10
Valine	2.379	176.05>116.05	116.05>45.00
Cytidine	2.791	302.05>242.00	242.05>109.00
Methionine	2.998	148.05>47.05	148.05>100.00
Pyridoxamine-5 Phosphate	3.001	247.05>230.00	247.05>79.05
Isoleucine	3.915	190.05>130.05	261.10>130.05 130.05>84.00
Leucine	4.225	190.05>130.05	261.10>130.05 130.05>84.00
Guanine	4.458	150.05>133.05	150.05>66.00
Tyrosine	4.497	180.05>163.05	180.05>119.05
Glutamate	4.506	146.05>102.05	146.05>128.05
Aspartate	4.649	132.05>88.05	132.05>115.00
Adenine	4.653	134.10>107.05	134.10>92.00
Uridine	4.681	243.05>110.05	303.05>243.00
Xanthine	4.729	151.05>108.05	151.05>80.05
Hypoxanthine	4.851	135.05>92.00	135.05>65.00
Inosine	5.036	267.05>135.05	267.05>108.00

Thymine	5.037	125.05>42.00	185.05>125.05
Guanosine	5.156	282.10>150.05	282.10>133.05
Shikimate	5.314	173.05>93.00	173.05>111.00
Glycerate	5.681	105.05>75.05	105.05>87.05
Urate	5.722	167.10>124.05	167.10>96.00
Phenylalanine	5.741	164.05>147.05	164.05>103.00
Thymidine	5.903	301.10>241.00	241.05>42.00
Glycolate	5.915	75.05>47.05	135.05>75.00
Adenosine	6.096	266.10>134.05	266.10>107.05
Glucose 6-phosphate	6.708	259.05>97.00	259.05>79.05
Disaccharide- phosphate	6.829	421.10>79.05	421.10>241.05
Glyoxylate	6.985	73.00>73.00	73.00>45.00
Mannose 6-phosphate	6.999	259.05>97.00	259.05>79.05
Sorbose 6-phosphate	7.008	261.05>97.00	261.05>79.05
Ribose 5-phosphate	7.211	229.05>97.00	229.05>79.05 229.05>139.05
S7P	7.247	289.10>97.00	289.10>79.05 289.05>199.05
F6P	7.268	259.05>97.00	259.05>79.05
Pyroglutamate	7.301	188.05>128.00	128.05>84.05
Tryptophan	7.363	203.10>116.05	203.10>74.00
Lactate	7.407	89.05>43.00	89.05>45.05
Arabinose 5-Phosphate	7.442	229.05>97.00	229.05>79.05 229.05>139.00
G1P	7.492	259.05>79.05	259.05>97.00 259.05>241.10
a-GP	7.556	171.05>79.05	171.05>97.00
Glyceraldehyde 3-phosphate	7.775	169.05>97.00	169.05>79.05
NAD	7.782	662.10>540.10	662.10>159.00
Ribulose 5-phosphate	7.908	229.05>97.00	229.05>79.05 229.05>139.05
Orotate	7.935	155.05>111.05	155.05>42.00
CMP	8.056	322.10>79.05	322.10>97.00
F1P	8.058	259.05>97.00	259.05>79.05
2-C-methylerythritol 4-phosphate	8.099	215.05>79.05	431.10>215.00
R1P	8.265	229.05>79.05	229.05>211.05
Pyruvate	8.272	87.05>43.00	147.05>87.00
UMP	8.507	323.10>79.05	323.10>97.00

DHAP	8.565	169.05>97.00	169.05>79.05
AICAR	8.574	337.10>79.05	337.10>125.05
GMP	8.575	362.10>79.05	362.10>97.00
IMP	8.609	347.05>79.05	347.05>135.00
TMP	9.141	321.10>195.05	321.10>79.05
AMP	9.214	346.10>79.05	346.10>97.00
Pantothenate	9.242	218.05>88.00	218.05>146.05
Nicotinate	9.333	122.05>78.00	122.05>51.00
cAMP	9.697	328.10>134.05	328.10>79.05
Glutathione	9.792	306.05>143.05	613.10>306.05
Succinate	9.958	117.05>73.00	117.05>99.05
Carbamoyl-P	10.139	140.05>79.05	140.05>97.00
UDP-Glucose	10.148	565.05>323.05	565.05>97.00
Malate	10.158	133.05>115.00	133.05>71.05
XMP	10.308	363.10>211.05	363.10>151.05
2-Oxoglutarate	10.316	145.05>101.05	145.05>57.00
ADP-Glucose	10.328	588.05>346.05	588.05>241.05
CDP	10.348	402.10>79.05	402.10>159.05
Acetyl-phosphate	10.385	139.00>79.05	279.05>139.00
Fumarate	10.412	115.05>71.00	175.05>115.00
GDP	10.419	442.10>79.05	442.10>159.05
UDP	10.451	403.10>159.00	403.10>79.05
3-phosphoglycerate	10.477	185.05>97.00	185.05>79.05
Shikimate 3-phosphate	10.517	253.05>97.00	253.05>235.05
KDPG	10.526	257.05>97.00	257.05>141.05
NADH	10.546	664.10>79.05	664.10>346.10
NADP	10.584	742.10>620.10	742.10>159.05
ADP	10.631	426.10>79.05	426.10>134.05
Phophoglycolate	10.651	155.00>79.05	155.00>97.00
Phosphoenolpyruvate	10.693	167.05>79.05	335.10>167.05
Citrate	10.698	191.05>87.00	191.05>111.05
Ribulose bisphosphate	10.751	309.05>97.00	309.05>79.05
Isocitrate	10.782	191.05>73.00	191.05>111.05
4-Hydroxy-3-methyl-but-2-enyl pyrophosphate	10.793	261.05>79.05	261.05>243.00
2-Isopropylmalate	10.829	175.05>115.05	175.05>113.05
Flavin mononucleotide	10.912	455.10>97.00	455.10>79.05
GTP	10.964	522.10>159.00	522.10>424.05

CTP	10.965	482.10>159.00	482.10>79.05
UTP	10.992	483.10>159.00	483.10>79.05
ATP	11.018	506.10>159.00	506.10>408.10
Phosphoribosyl pyrophosphate	11.026	389.10>177.05	389.10>291.05
Bisphosphoglyceric acid	11.031	265.05>167.05	265.05>79.05
NADPH	11.044	744.10>159.05	744.10>408.10
FAD	11.071	784.10>346.10	784.10>97.00
Malonyl CoA	11.133	852.10>808.10	852.10>408.10
CoA	11.142	766.10>408.10	766.10>79.05
3-Hydroxybutyryl-CoA	11.143	852.10>772.10	852.10>408.10
3- Hydroxyl-3-methylglutaryl CoA	11.147	910.10>408.10	910.10>426.05
Succinyl CoA	11.151	866.10>408.10	866.10>786.10
Acetyl CoA	11.169	808.10>408.10	808.10>159.05
(+)-10-Camphorsulfonate	11.183	231.10>80.00	
Isopentenyl pyrophosphate **Dimethylallyl pyrophosphate**	11.205	245.05>79.05	245.05>227.05
Crotonyl CoA	11.269	834.10>408.10	834.10>159.00
Butyryl CoA	11.311	836.10>408.10	836.10>159.00

List of Publications

Original papers

Phan Nguyen Thuy An, Masamitsu Yamaguchi, Takeshi Bamba, Eiichiro Fukusaki (2014). "Metabolome analysis of *Drosophila melanogaster* during embryogenesis." PLoS One **9**(8): e99519. doi:10.1371/journal.pone.0099519

Phan Nguyen Thuy An, Masamitsu Yamaguchi, Eiichiro Fukusaki (2017). "Metabolic profiling of *Drosophila melanogaster* metamorphosis: A new insight into the central metabolic pathways" Metabolomics **13**, 29. doi: 10.1007/s11306-017-1167-1

Phan Nguyen Thuy An, Kouhei Shimaji, Hideki Yoshida, Hiroshi Kimura, Eiichiro Fukusaki, and Masamitsu Yamaguchi (2017). "Epigenetic regulation of starvation-induced autophagy in *Drosophila* by histone methyltransferase G9a" Scientific reports (under review)

Conferences

Phan Nguyen Thuy An, Masamitsu Yamaguchi, Shuichi Shimma, Eiichiro Fukusaki. Metabolic profiling of *Drosophila melanogaster* metamorphosis: a new insight into the metabolic pathway (Oral and poster, 2016). *International Biological Mass Spectrometry Symposium 2016, Tokyo, Japan.*

Phan Nguyen Thuy An, Masamitsu Yamaguchi, Shuichi Shimma, Eiichiro Fukusaki. Metabolic profiling of *Drosophila melanogaster* metamorphosis: a new insight into the metabolic pathway (Oral, 2016). *Seminar on Asia Insect and Biomedical Research 2016, Chiangmai, Thailand.*

Phan Nguyen Thuy An, Masamitsu Yamaguchi, Takeshi Bamba, Eiichiro Fukusaki. Metanolic Profiling of *Drosophila melanogaster* Metamorphosis (Poster 1P-118, 2015). *67th Annual Meeting of the Society for Biotechnology Japan , Kagoshima, Japan.*

Phan Nguyen Thuy An, Masamitsu Yamaguchi, Takeshi Bamba, Eiichiro Fukusaki. Metanolic Profiling of *Drosophila melanogaster* Metamorphosis (Oral, 2015). *Aachen-Osaka Joint Symposium "Biological and Chemical Methods for Selective Catalysis" , RWTH Aachen, Germany.*

Phan Nguyen Thuy An, Masamitsu Yamaguchi, Takeshi Bamba, Eiichiro Fukusaki. Metabolic Profiling of *Drosophila melanogaster* Metamorphosis (Oral, 2015). *JSPS Core-to-Core Program Seminar on Asia Insect Biomedical Research, Ho Chi Minh University of Science, Ho Chi Minh, Vietnam.*

Phan Nguyen Thuy An, Masamitsu Yamaguchi, Takeshi Bamba, Eiichiro Fukusaki. Metabolic Profiling of *Drosophila melanogaster* Metamorphosis (Poster P468, 2015). *11th International Conference of the Metabolomics Society（Metabolomics2015）, Hyatt Regency San Francisco Airport, San Francisco Bay Area, California, USA*

Phan Nguyen Thuy An, Masamitsu Yamaguchi, Takeshi Bamba, Eiichiro Fukusaki. Metabolome Analysis of *Drosophila melanogaster* during Embryogenesis (Oral, 2014). *JSPS Core-to-Core Program Seminar on Asia Insect Biomedical Research, Kyoto Institute of Technology, Kyoto, Japan.*

Phan Nguyen Thuy An, Masamitsu Yamaguchi, Takeshi Bamba, Eiichiro Fukusaki. Metabolome Analysis of *Drosophila melanogaster* during Embryogenesis (Oral 3A-M8, 2014). *10th International Conference of the Metabolomics Society（Metabolomics2014）, Tsuruoka, Japan.*

Phan Nguyen Thuy An, Masamitsu Yamaguchi, Takeshi Bamba, Eiichiro Fukusaki. Developing an application of Metabolomics in *Drosophila melanogaster* embryogenesis (Poster 3P-022, 2013). *65th Annual Meeting of the Society for Biotechnology Japan , Hiroshima, Japan.*

Acknowledgment

First of all, I would like to express my great gratitude to my supervisor Prof. Eiichiro Fukusaki. His valuable and constructive suggestions helped me come up with the thesis topic and guided me over these years to achieve the final goals. During the most difficult times, he gave me the moral support and the freedom I needed to move on.

I also would like to give special appreciation to Prof. Masamitsu Yamaguchi for his patient guidance, encouragement and useful critiques. The joy and enthusiasm he has for science was contagious and motivational for me, even during tough times in the Ph.D. pursuit.

Besides my supervisors, I would like to thank the rest of my thesis committee: Prof. Kazuhito Fujiyama and Prof. Hajime Watanabe for their insightful comments which incented me to improve my presentation from various perspectives.

I would also like to thank MEXT and JSPS for financial support throughout my study.

Dozens of people have helped and taught me immensely at Osaka University. Many thanks to Prof. Takeshi Bamba, Assist. Prof. Hisayo Ono and Assist. Prof. Sastia P. Putri for their invaluable comments and constructive recommendations. I also wish to thank to all Fukusaki Lab members especially to my beloved friends Udi, Shao, Zanaria, Yang, Risako, Teruko, HangHang, Mitsunaga, Dempo, Mega, Sana and Wisman for your supports not only in my research but also in my life here. My gratitude also goes to my Vietnamese friends for their warm friendship. All of you are my second family here in Japan.

Finally, I would like to thank my family for their endless love, support and encouragement in my whole life. Words cannot express how grateful I am. Special thanks to Daniel Sauer for always standing by my side, I can’t thank you enough for encouraging me throughout this experience.

March, 2017